



G2027

SYNTHESIS AND PHOTOPHYSICAL STUDIES OF SOME SWITCHABLE HEMICYANINE SYSTEMS

THESIS SUBMITTED TO
THE UNIVERSITY OF KERALA
IN FULFILMENT OF THE REQUIREMENTS
FOR THE DEGREE OF
DOCTOR OF PHILOSOPHY
IN CHEMISTRY
UNDER THE FACULTY OF SCIENCE

BY
S. ZEENA

PHOTOCHEMISTRY RESEARCH UNIT
REGIONAL RESEARCH LABORATORY (CSIR)
TRIVANDRUM-695 019, KERALA, INDIA

MAY 2001

R
541.14
:043

P12

SYNTHESIS AND PHOTOPHYSICAL STUDIES OF SOME SWITCHABLE HEMICYANINE SYSTEMS

**THESIS SUBMITTED TO
THE UNIVERSITY OF KERALA
IN FULFILMENT OF THE REQUIREMENTS
FOR THE DEGREE OF
DOCTOR OF PHILOSOPHY
IN CHEMISTRY
UNDER THE FACULTY OF SCIENCE**

**BY
S. ZEENA**

**PHOTOCHEMISTRY RESEARCH UNIT
REGIONAL RESEARCH LABORATORY (CSIR)
TRIVANDRUM-695 019, KERALA, INDIA**

MAY 2001

To my Parents

STATEMENT

I hereby declare that the matter embodied in this thesis is the result of investigations carried out by me at the Photochemistry Research Unit of the Regional Research Laboratory (CSIR), Trivandrum, under the guidance of Dr. K. George Thomas and the same has not been submitted elsewhere for a degree.

In keeping with the general practice of reporting scientific observations, due acknowledgement has been made wherever the work described is based on the findings of other investigators.



S. Zeena



Dr. K. GEORGE THOMAS
SCIENTIST


PHOTOCHEMISTRY RESEARCH UNIT
REGIONAL RESEARCH LABORATORY (CSIR)
TRIVANDRUM-695 019, INDIA

Telephone: 91-471-515318 Fax: 91-471-490186
e. Mail: georgetk@md3.vsnl.nct.in.

May 25, 2001

CERTIFICATE

Certified that the work embodied in this thesis entitled: **“Synthesis and Photophysical Studies of Some Switchable Hemicyanine Systems”** has been carried out by Miss. S. Zeena under my supervision and the same has not been submitted elsewhere for a degree.


K. George Thomas
(Thesis Supervisor)

ACKNOWLEDGEMENTS

It is with great pleasure that I place on record my deep sense of gratitude to Dr. K. George Thomas, my research supervisor, for suggesting the research problem and for his guidance and encouragement, leading to the successful completion of this work.

I would like to express my sincere thanks to Professor M. V. George for his constant encouragement and help throughout the tenure of this work. I wish to thank Dr. G. Vijay Nair, Director, Regional Research Laboratory, Trivandrum for providing me the necessary facilities for carrying out this work.

I express my thanks to Dr. Suresh Das, Dr. A. Ajayaghosh, Dr. K. R. Gopidas, Dr. D. Ramaiah and other members of the Photochemistry Research Unit for their suggestions and support.

I would also like to thank Professor P. Natarajan and Dr. P. Ramamurthy, National Centre for Ultrafast Processes, University of Madras for allowing access to the Picosecond Time Correlated Single Photon Counting and Laser Flash Photolysis facilities and Dr. (Mrs.) M. Lalithambika, for the help rendered to me in carrying out the viscosity measurements reported in this thesis.

I acknowledge Mr. P. K. Sudeep, Mr. Robert Philip and all my friends in the various sections of the Regional Research Laboratory for the help rendered to me during various stages of my work. I express my sincere thanks to Mrs. Sarada Nair for her secretarial help in various stages of my work. I would like to thank all my teachers who have motivated me at different stages of my education

Financial assistance from CSIR, New Delhi is gratefully acknowledged.

Finally, I am deeply indebted to all the members of my family for their invaluable support and encouragement.

Trivandrum

May 25, 2001



S. Zeena

CONTENTS

	Page
Statement	ii
Certificate	iii
Acknowledgements	iv
Preface	viii
Chapter 1. A Brief Review on Molecular Switching Devices	
1.1. Molecular Devices	1
1.2. Organic Molecules as Components of Molecular Devices	2
1.3. Molecular Switching Devices	3
1.4. Applications of Molecular Switching Devices	4
1.5. Electrochemical Switching of Emission	5
1.6. Molecular Switches Based on Photochromics	8
1.7. Photochemically Induced Conformational Switching	11
1.8. References	13
Chapter 2. Singlet Excited State Dynamics of Hemicyanine Dyes	
2.1. Abstract	17
2.2. Introduction	17
2.3. Results and Discussion	26
2.4. Conclusions	58
2.5. Experimental Section	58
2.6. References	61

Chapter 3. Conformational Switching and Exciton Interactions in Hemicyanine Based Bichromophores

3.1. Abstract	65
3.2. Introduction	66
3.3. Results and Discussion	78
3.4. Conclusion	102
3.5. Experimental Section	102
3.6. References	109

Chapter 4. Photophysical Processes in Pyrene Based Conjugated Donor-Acceptor Systems

4.1. Abstract	113
4.2. Introduction	114
4.3. Results and Discussion	116
4.4. Conclusions	131
4.5. Experimental Section	132
4.6. References	135

PREFACE

Design and study of switching devices is an emerging and rapidly expanding branch of molecular and supramolecular chemistry. The development in this area is of importance for a variety of photonic applications such as information processing and storage, molecular recognition and controlled release devices. A brief review on molecular switching devices, with special emphasis on photo- and electrochemical switching devices, is presented in Chapter 1 of the thesis. The overall objective of the present investigation is to examine the photophysical and switching behaviour of some hemicyanine chromophores and bichromophores.

Polymethine dyes with heterocyclic acceptor and non-heterocyclic donor groups in terminal position are referred to as hemicyanines. The Chapter 2 of the thesis deals with the photophysical studies, particularly the singlet excited state dynamics of a few hemicyanine chromophores (Chart 2.4). The donor-acceptor properties of hemicyanines were varied by linking 4-(N,N-dimethyl)aminostyryl donor group to acceptors of varying strength. A systematic study of the effect of the environment (polarity and viscosity) on the singlet excited state dynamics of hemicyanines was carried out. The excited singlet state properties of hemicyanines were found to depend mainly on the viscosity of the environment. A substantial increase in the fluorescence quantum yields as well as singlet lifetimes, with increase in viscosity of the medium, suggested restricted bond twisting in the

singlet excited state. Activation parameters (diffusive and thermally activated intrinsic barriers) for the nonradiative deactivation from the excited singlet state were estimated. In hemicyanines, diffusive barrier was found to have substantial contribution and attributed to the bond twisting in the singlet excited state

Bichromophores are molecular systems containing two chromophoric units, linked together by a bridging units and in the present case hemicyanine units are connected by poly(oxoethylene) linkers. Chapter 3 of the thesis describes the synthesis, photophysical studies and switching behaviour of a few hemicyanine based bichromophoric systems (Chart 3.11). The bichromophores prefer a well-defined folded conformation (intramolecular aggregates of H-type) in low polar media and at lower temperatures. The polarity dependent conformational changes of the bridging unit and the solvophobicity of the dye in nonpolar medium, drives the folding of the bichromophores. On increasing the temperature or polarity of the medium they adopt an extended conformation. The photophysical and excited state properties of both the forms are quite different and investigated, in detail. Unfolding of the folded form was also brought about by laser excitation. Thus, the conformational changes of the bichromophore were tuned by varying the solvent polarity, temperature as well as through irradiation.

The host-guest binding properties in a supramolecular assembly can be modulated by the reversible interconversion of one of its unit. Chapter 4 of the thesis deals with the synthesis and photophysical studies of a pyrene based conjugated donor-acceptor system and the corresponding bichromophore (Chart 4.1).

Both the compounds absorb around 400 nm in dichloromethane and sensitive to micromolar quantities of copper ions. The steady state and time resolved fluorescence properties in the absence and presence of copper ions were investigated. The photophysical properties of the uncomplexed and complexed forms were quite different and the later one can be converted into uncomplexed ligand by chemical reduction.

The chart numbers listed in this Preface refer to those given in different Chapters in the thesis.

CHAPTER 1

A Brief Review on Molecular Switching Devices

1.1. Molecular Devices

Macroscopic devices possess extensive applications in our day to day life. Such devices can be considered as assemblies of several macroscopic components designed to achieve specific functions. The extension of this concept to the molecular level forms the basis of molecular devices.¹ A molecular device can be defined as an assembly of molecular components designed to achieve specific functions. The idea of “molecular electronics” was first suggested by Carter in a “Molecular Electronics Devices Workshop” held in Washington DC in 1981.¹ Carter hypothesized that a single molecule or a few molecules could be used for switching and memory functions. A variety of models for molecular switches and functionalized molecular circuits, as molecular devices, have been proposed later by Balzani and co-workers.² Lehn and co-workers³ have made substantial contributions to the conceptual development of molecular and supramolecular devices. Several molecular systems of varying complexity, which can perform specific functions, have been synthesized in recent years.⁴⁻⁸ These include molecular devices such as sensors, logic gates (for computing)⁹⁻¹³ and information storage systems.¹⁴ By extending the concept of information storage from macroscopic devices to molecular level, the amount of information stored could be

increased by several orders of magnitude. Design of most of these molecular systems, capable of performing specific functions are based on organic materials.

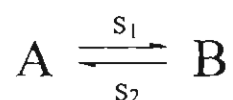
1.2. Organic Molecules as Components of Molecular Devices

Limitations of inorganic solids in their scope, flexibility in synthesis and predictability of the desired properties have directed research activities towards the development of materials based on organic molecules.¹⁵ Organic molecules are now widely accepted as useful synthetic building blocks in non-linear optics,¹⁶ liquid crystals in modern displays,¹⁷ superconductors,¹⁸ ferromagnets,¹⁹⁻²² optical sensors²³ and supramolecular devices (ordered molecular assemblies based on molecular recognition and self-organization).^{24, 25} There are several advantages in using organic materials for such applications. The photophysical properties of organic materials can be fine-tuned by small structural variations and also it can be easily processed to the desired structures by molecular engineering. Recent studies have shown that the disadvantages associated with the stability and fatigue resistance of organic compounds can be resolved by structural modifications.²⁶ The necessary ordering of organic molecules into larger macroscopic structures can be achieved by Langmuir-Blodgett techniques,²⁷⁻³⁰ the aggregation of surfactant molecules into micelles and vesicles,³¹ doping in polymer matrices or by self-assembly through molecular recognition processes.^{24,25,32} The flexibility in the synthetic pathways allows the introduction of functional groups for attachment or incorporation into the polymers, thereby it is possible to drastically improve the

material properties. The typical properties of polymers, like the ease of processibility, mechanical strength, long-term stability etc, combined with the above mentioned advantages of organic molecules may form the basis of future use of these materials for molecular switching devices.³³

1.3. Molecular Switching Devices

The basic requirement for a switching device is bistability, i.e., a molecular species (or supramolecular system) capable of reversible interconversion between two thermally stable states with the aid of an external stimulus.^{1,3} Any molecular system having two stable states with reversible switching ability can in principle be used as a memory element (binary logic) in a digital computer. The working principle of such a device is illustrated in Scheme 1.1, where 'A' and 'B' represent



Scheme 1.1

two different states of a bistable system. The substrate in the 'A' state carries information in the form of a signal such as color, luminescence, conductivity, nonlinear optical signal, phase transition etc. The form 'A' can be interconverted to 'B' by an external stimulus 'S₁' (photochemical or electrochemical) and as a consequence some of the properties such as redox activity, energy and electron transfer behavior are modified. With the aid of a different stimulus 'S₂', form 'B' can be switched back to 'A'. The interconversion between the two forms should be

efficient and proceed with good reversibility and with resistance to fatigue. The switching devices consist of two main components - a stimulus (an external trigger) and a substrate (the species undergoing switching). A whole set of molecular switches based on substrate-stimulus pairs, for e.g., opto-photo, opto-electro, electro-photo switches etc., have been demonstrated. If the stimulus to which the device responds is optical in nature and if it alters the optical properties of the molecule (i.e., the signal generated is optical in nature), then it is referred to as an opto-photo switch. Similarly, when the optical signal tunes the electric properties of the molecule, then it is referred to as an opto-electro switch. The chemistry of signal generation, processing, transfer, conversion and detection is referred to as semiochemistry.³ Development in this area is important for a variety of photonic applications such as information processing and storage, molecular recognition and controlled release devices.³

1.4. Applications of Molecular Switching Devices

Among the various phototriggered natural processes, vision and plant gene expression adopt switching mechanisms for performing their functions. Several pertinent reviews,³⁴ which reveal the basic aspects of these natural systems, are available. Fundamental understanding of these light activated reversible isomerization processes reveals the potential for development of artificial photochemical switching systems and optical data storage devices.³⁵⁻⁵³ Photochemical and electrochemical switching have been utilized for specific

binding, release and transport of metal cations and organic molecules.³⁵ The design of photoswitchable compounds covalently linked to electrode surfaces is yet another step in the development of reversible sensing devices.³⁶ Stimuli responsive self-organized systems, such as photoswitchable micelle and vesicle, have applications as controlled release devices in medicine and agriculture.³⁷ Earlier investigations on switching devices were reviewed in two comprehensive articles: (i) on artificial photobiological switching systems and their application in sensing biomaterials and biomodel compounds by Willner and Willner³⁵ and (ii) on the design of reversible optical storage of organic materials by Feringa and co-workers.³⁸ An extensive compilation of the fluorescent signaling systems, with special reference to molecular switches and molecular sensors, is available in a 1997 review, by de Silva and co-workers.⁴³ More recently, Balzani, Stoddart and co-workers have reviewed the photochemically and electrochemically induced changes in interlocked molecules (catenanes and rotaxanes) as well as in coordination and supramolecular complexes.³⁹ A few representative examples of the photochemical and electrochemical switching devices, relevant to the present investigation, are presented here.

1.5. Electrochemical Switching of Emission

A two component device combining a luminescent centre and an electroactive unit may function as a photo-electroswitch in which the emission properties are modulated by redox interconversion *via* energy or electron transfer

quenching. Electrochemical switching of the emission was first demonstrated by Lehn and co-workers by linking tris-bipyridine ruthenium(II) centre to quinone (**1**, Chart 1.1).⁴⁰ This quinone-hydroquinone redox couple fulfils the requirements of a bistable electro-photoswitch; reduced form is luminescent, whereas the emission of the oxidized form is totally quenched.

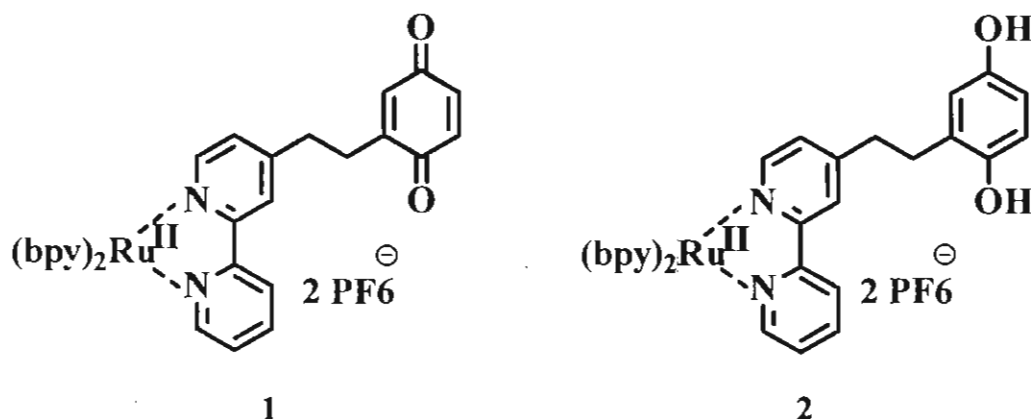


Chart 1.1

Interconversion between the redox-couple allows reversible switching of luminescence *via* a photoinduced electron transfer (PET) from the metal centre to the acceptor unit (quinone). Later, Daub and co-workers⁴¹ have demonstrated dual mode switching of luminescence by electrochemically reducing a benzodifurane-quinone system (**3** in Chart 1.2). The parent molecule and its anion are nonfluorescent

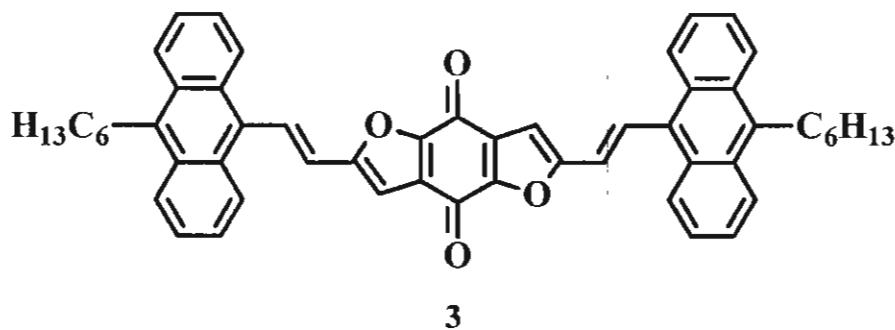


Chart 1.2

whereas the dianion of **3** is strongly fluorescent. An electro-photoswitch (**4** in Chart 1.3) working on the same principle was demonstrated by Arounagiri and Maiya.⁴²

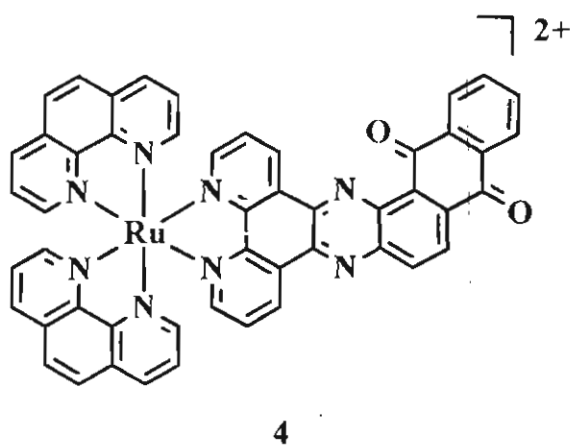
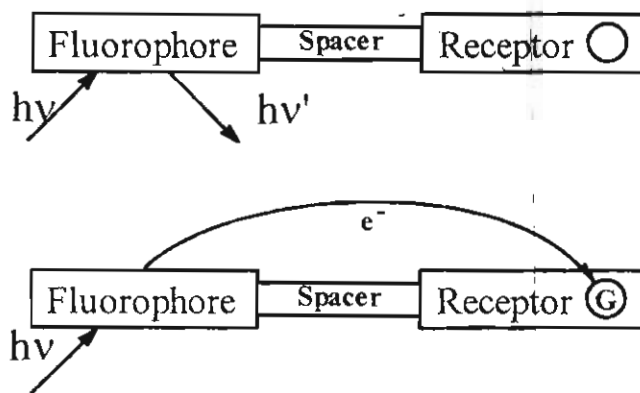


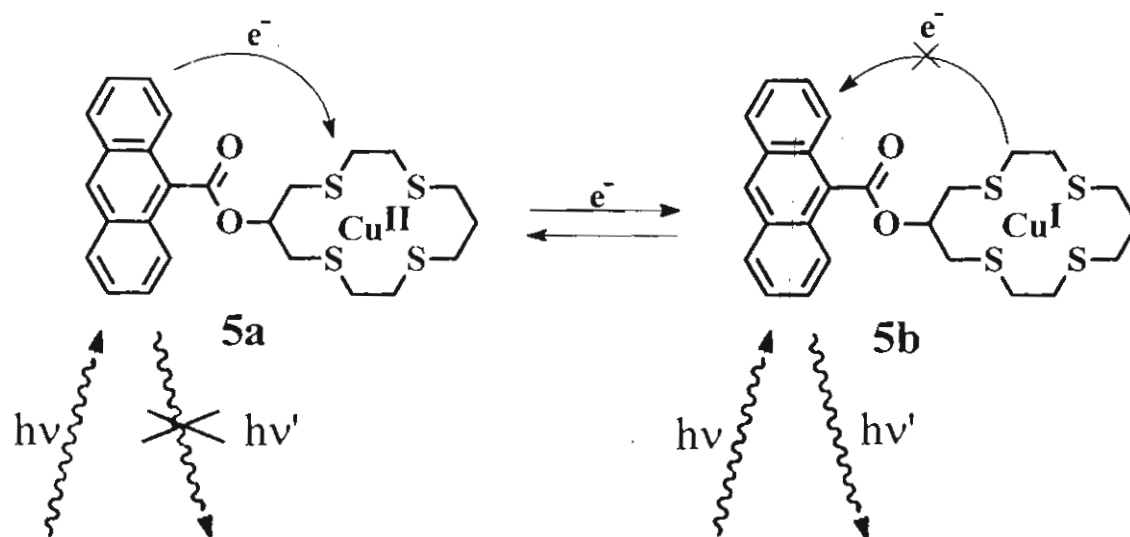
Chart 1.3

Another type of electrophotoswitch was suggested by de Silva which utilizes the intrinsic redox activities of guest molecules i.e., redox interconversion of metal ions between their various oxidation states and a schematic representation of its working is shown in Scheme 1.2.⁴³ On excitation, P \ddot{E} T occurs between the metal ion (G), complexed in the receptor and the fluorophore, depending upon their



Scheme 1.2

redox potential. A molecular system working on this concept is shown in Scheme 1.3. In this system, the anthracene fluorescence was switched 'on' and 'off', through the redox interconversion of Cu^{II}/Cu^I couple.



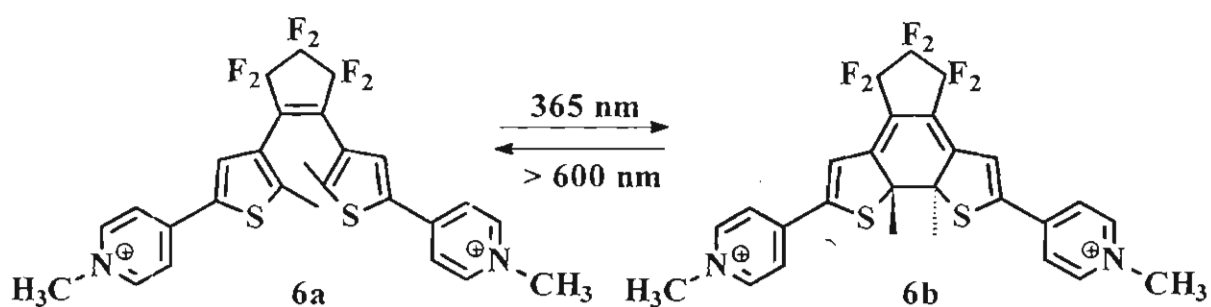
Scheme 1.3

1.6. Molecular Switches Based on Photochromics

The principle of information storage process involves, writing, reading and erasing of information in a binary format provided by two distinct photochemical forms. Three-dimensional optical data storage of memory, using a photochromic material, has been earlier reported by Parthenopoulos and Rentzepis.⁴⁴ On irradiation, photochromic molecules normally form colored products, which revert back to the colorless (or less colored) state, either thermally or on irradiation with light of another frequency. Photochromic reactions are accompanied by bond rearrangements and several systems have been extensively investigated, which

includes *cis-trans* isomerization (indigos, azo compounds), cleavage (spiropyrans) and electrocyclic processes (fulgides). Extensive reviews and books on photochromic molecules are available in the literature.⁴⁵⁻⁵¹ In most of the above-mentioned systems, the low fatigue resistance (the undesirable photoreactions restrict the number of reversible transformations) and thermal reversibility, limit their use in devices. A new class of thermally stable photochromic system, diarylethenes, was developed by Irie which possess most of the desirable properties as materials for optical storage and switching.²⁶ A brief description of diarylethene based molecular switches are presented below.

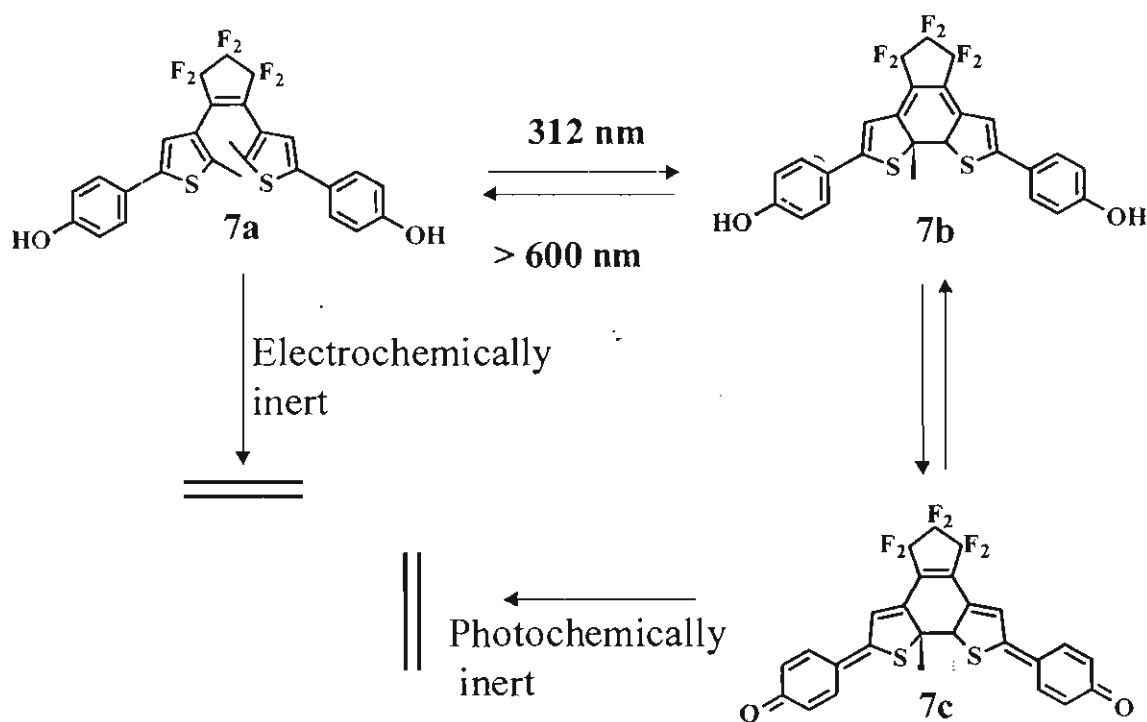
Diarylethenes (an example is shown in Scheme 1.4) can undergo thermally irreversible and fatigue-resistant photochromic reactions. They are well suited as



Scheme 1.4

optical switching units, since irradiation with light of well separated wavelengths can interconvert them between isomers (conjugated closed state or nonconjugated open state) with distinct physical properties. Most of the diarylethenes possessing benzothiophene ring undergo photochromic cycles more than 1.0×10^4 times and the absorption maximum of the closed-ring form extends to the near-infrared

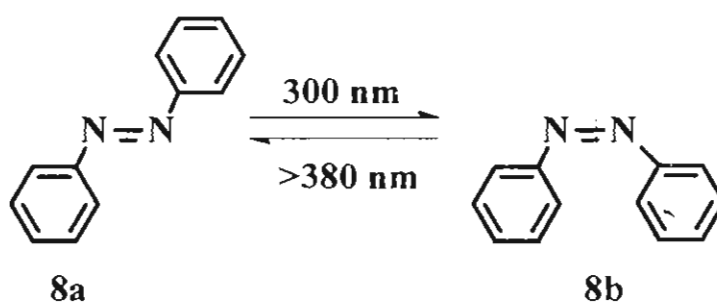
region depending on the substitution. The response time for the cyclization and ring opening reactions are less than 10 picosecond. These properties make them ideal candidates for switching and optical recording applications. However, non-destructive read-out capacity (i.e., reading with light, without destroying the memory) is lacking in these systems and this is one of the most challenging problems in the development of optical data storage systems. However, some progress has been made in this direction by making use of what is known as “gated photochemical systems”. The chemically gated photochromic devices so far reported⁵² are not ideal due to several practical reasons. Recently, Lehn and co-workers have designed photochromic systems, which can be gated electrochemically (Scheme 1.5).⁵³



Scheme 1.5

1.7. Photochemically Induced Conformational Switching

The photochemical isomerization of an olefinic bond is one of the fundamental processes in vision. The structural perturbations induced by the *cis-trans* isomerization of the retinal moiety (of rhodopsin), results in conformational changes in the protein molecule and through a cascade of reactions, neural pulse responsible for vision is generated. This principle has been “copied from nature” to design molecular systems which can undergo light induced structural changes for signaling applications. A number of artificial systems based on the azobenzene functionality were investigated based on this principle. Azobenzenes exist in two forms, *E* (*trans*) and *Z* (*cis*) forms, and their interconversions were induced by irradiation with appropriate wavelengths (Scheme 1.6).



Scheme 1.6

Upon photochemical excitation, structural changes occur in molecular systems having azobenzene functionality and such changes were utilized for modulating (i) the host-guest properties (for e.g., controlled metal binding)^{35,54,55} (ii) phase changes in liquid crystals^{56,57} (iii) photo-triggered reversible gel formation⁵⁸ and (iv) photoinduced switching of conductivity.^{59,60} However, the

unwanted thermal reactions prohibit the use of azobenzene based molecular systems from their use in information storage systems.

Chemically, photochemically and electrochemically controllable conformational motion of interlocked molecules such as catenanes, rotaxanes and pseudorotaxanes have been extensively investigated and reviewed.³⁹ The stimuli induced molecular motions in these systems may undoubtedly play a key role in development in the future optoelectronic devices. These aspects are not discussed here since they are beyond the scope of the thesis.

The main objective of the present investigation was to examine some hemicyanine systems, with particular reference to their photophysical properties as well as switching behaviour. Brief reviews pertaining to hemicyanines as well as bichromophores are presented in Sections 2.2 and 3.2, respectively.

1.8. References

- (1) Carter, F. L. in *Molecular Electronic Devices*, Marcel Dekker, New York, **1982**.
- (2) Balzani, V.; Maggi, L.; Scandola, F. in *Supramolecular Photochemistry*, Reidel, Holland, **1987**, 1.
- (3) Lehn, J. M. in *Supramolecular Chemistry: Concepts and Perspectives*, VCH, Weinheim, **1995**.
- (4) Balzani, V.; Gomez-Lopez, M.; Stoddart, J. P. *Acc. Chem. Res.* **1998**, *31*, 405.
- (5) Sauvage, J. P. *Acc. Chem. Res.* **1998**, *31*, 611.
- (6) Emmelius, M.; Pawlowski, G.; Vollmann, H. W. *Angew. Chem. Int. Ed. Engl.* **1989**, *28*, 1445.
- (7) Clayden, J.; Pink, J. H. *Angew. Chem. Int. Ed. Engl.* **1997**, *36*, 1866.
- (8) Ishow, E.; Credi, A.; Balzani, V.; Spadola, F.; Mandolini, L. *Chem. Eur. J.* **1999**, *5*, 984.
- (9) de Silva, A. P.; Gunaratne, H. Q. N.; Mc Coy, C. P. *Nature* **1993**, *364*, 42.
- (10) de Silva, A. P.; Gunaratne, H. Q. N.; Maguire, G. E. M. *Chem. Commun.* **1994**, 1213.
- (11) de Silva, A. P.; Gunaratne, H. Q. N.; Mc Coy, C. P. *J. Am. Chem. Soc.* **1997**, *119*, 7891.
- (12) de Silva, A. P.; Dixon, I. M.; Gunaratne, H. Q. N.; Gunnlaugsson, T.; Maxwell, P. R. S.; Rice, T. E. *J. Am. Chem. Soc.* **1999**, *121*, 1393.
- (13) de Silva, A. P.; McClenaghan, N. D. *J. Am. Chem. Soc.* **2000**, *122*, 3965.
- (14) Kawata, S.; Kawata, Y. *Chem. Rev.* **2000**, *100*, 1777.
- (15) Kampf, G.; Iazear, N.; Lower, H.; Siebourg, W. in *Polymers in Information Storage Technology*, New York, **1989**.
- (16) Harder, S. R.; Sohn, J. E.; Stucky, G. D. in *Material for Nonlinear Optics, Chemical Perspectives*, American Chemical Society, Washington, **1991**.

- (17) Escher, C.; Winger, R. *Adv. Mater.* **1992**, *4*, 189.
- (18) Ishiguro, T.; Yamaji, K. in *Organic Superconductors*, Springer Verlag, Berlin, **1990**.
- (19) Yoshida, Z.; Sugimoto, T. *Angew. Chem. Int. Ed. Engl.* **1988**, *27*, 1573.
- (20) Rajza, A. *J. Org. Chem.* **1991**, *56*, 2557.
- (21) Iwamura, H.; Fujita, I.; Itoh, K.; Izuoka, A.; Kinoshita, T.; Miko, F.; Sawaki, Y.; Sugawara, T.; Takai, T.; Teki, Y. *J. Am. Chem. Soc.* **1990**, *112*, 4074.
- (22) Miller, J. S.; Epstein, A. J.; Reitt, W. M. *Science* **1988**, *240*, 40.
- (23) Reinhoudt, D. N.; Sudholter, E. J. R. *Adv. Mater.* **1990**, *2*, 23.
- (24) Lehn, J. M. *Angew. Chem. Int. Ed. Engl.* **1990**, *29*, 1304.
- (25) Lehn, J. M. *Angew. Chem. Int. Ed. Engl.* **1988**, *27*, 89.
- (26) Irie, M. *Chem. Rev.* **2000**, *100*, 1685.
- (27) Ulman, A. in *An Introduction to Ultrathin Organic Films, from Langmuir-Blodgett to Self Assembly*, Academic Press, New York, **1991**.
- (28) Fuchs, H.; Ohst, H.; Prass, W. *Adv. Mater.* **1991**, *3*, 10.
- (29) Ulman, A. *Adv. Mater.* **1990**, *2*, 573.
- (30) Tieka, B. *Adv. Mater.* **1990**, *2*, 222.
- (31) Vogtle, F. in *Supramolecular Chemistry*, Wiley, New York, **1991**.
- (32) Schneider, H. J.; Durr, H. in *Frontiers in Supramolecular Organic Chemistry and Photochemistry*, VCH, Weinheim, **1990**.
- (33) Miller, J. S. *Adv. Mater.* **1990**, *2*, 601.
- (34) Liebman, P. A.; Parker, K. R.; Dratz, E. A., *Annu. Rev. Physiol* **1987**, *49*, 765.
- (35) Willner, I.; Willner, B. in (Ed.: H. Morrison), *Vol. 2*, Wiley, New York, pp 2-110, **1993**.
- (36) Wilner, I.; Rubin, S. *Angew. Chem. Int. Ed. Engl.* **1996**, *35*, 367.
- (37) Medina, J. C.; Goodnow, T. T.; Kaifer, A. E.; Gokel, G. W. in *Electrochemistry in Colloids and Dispersions*, (Eds.: R. A. Machay, J. Texter), VCH, New York, **1992**, 95.

- (38) Feringa, B. L.; Jager, W. F.; Lange, B. D. *Tetrahedron* **1993**, *49*, 8267.
- (39) Balzani, V.; Credi, A.; Raymo, F. M.; Stoddart, J. F. *Angew. Chem. Int. Ed.* **2000**, *39*, 3348.
- (40) Gouille, V.; Harriman, A.; Lehn, J. M. *J. Chem. Soc., Chem. Commun.* **1993**, 1034.
- (41) Daub, J.; Beck, M.; Knorr, A.; Spreitzer, H. *Pure & Appl. Chem.* **1996**, *68*, 1399.
- (42) Arounaguirri, S.; Maiya, B. G. *Inorg. Chem.* **1999**, *38*, 842.
- (43) de Silva, A. P.; Gunaratne, H. Q. N.; Gunnlaugsson, T.; Huxley, A. J. M.; McCoy, C. P.; Rademacher, J. T.; Rice, T. E. *Chem. Rev.* **1997**, *97*, 1515.
- (44) Parthenopoulos, D. M.; Rentzepis, P. M. *Science* **1989**, *245*, 843.
- (45) Tsujioka, T.; Tatzono, F.; Harada, T.; Kuroki, K.; Irie, M. *Jpn. J. Appl. Phys.* **1994**, *33*, 5788.
- (46) Tatzono, F.; Harada, T.; Shimizu, Y.; Ohara, M.; Irie, M. *Jpn. J. Appl. Phys.* **1993**, *32*, 3987.
- (47) Tsujioka, T.; Shimizu, Y.; Irie, M. *Jpn. J. Appl. Phys.* **1994**, *33*, 1914.
- (48) Tsujioka, T.; Kume, M.; Irie, M. *Jpn. J. Appl. Phys.* **1995**, *34*, 6439.
- (49) Tsujioka, T.; Harada, T.; Kume, M.; Kuroka, K.; Irie, M. *Jpn. J. Appl. Phys.* **1995**, *2*, 181.
- (50) Tsujioka, T.; Kume, M.; Irie, M. *Jpn. J. Appl. Phys.* **1996**, *35*, 4353.
- (51) Tsujioka, T.; Kume, M.; Horikawa, Y.; Ishikawa, A.; Irie, M. *Jpn. J. Appl. Phys.* **1997**, *36*, 526.
- (52) Irie, M.; Miyatake, O.; Uchida, K. *J. Am. Chem. Soc.* **1992**, *114*, 8715.
- (53) Yokoyama, Y.; Yamane, T.; Kurita, Y. *J. Chem. Soc., Chem. Commun.* **1991**, 1722.
- (54) Fabbrizzi, L.; Poggi, A. *Chem. Soc. Rev.* **1995**, 197.
- (55) Singewald, E. T.; Mirkin, C. A.; Stern, C. L. *Angew. Chem. Int. Ed. Engl.* **1995**, *34*, 1624.
- (56) Wilner, I.; Marx, S.; Eichen, Y. *Angew. Chem. Int. Ed. Engl.* **1992**, *31*, 1243.

- (57) Wurthner, F.; Rebek, J. *Angew. Chem. Int. Ed. Engl.* **1995**, *34*, 446.
- (58) Shinkai, S.; Aoki, M.; Ikeda, A.; Murata, K.; Nishi, T. *J. Chem. Soc. Chem. Commun.* **1991**, 1715.
- (59) Kimura, K.; Kaneshige, M.; Yamashita, T.; Yokoyama, M. *J. Org. Chem.* **1994**, *59*, 1251.
- (60) Tachibana, H.; Matsumoto, M. *Adv. Mater.* **1993**, *11*, 796.

CHAPTER 2

Singlet Excited State Dynamics of Hemicyanine Dyes

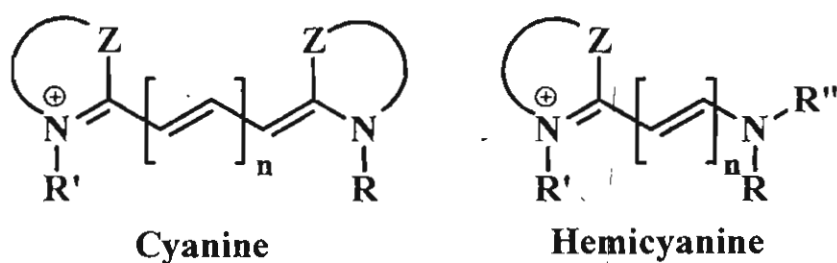
2.1. Abstract

The synthesis and photophysical properties of three hemicyanine dyes 4-6 (Chart 2.4) are reported. The donor-acceptor properties of hemicyanine dyes were varied by linking 4-(N,N-dimethyl)aminostyryl group to heterocyclic acceptors of varying strength. Photophysical properties of these dyes (4-6) were investigated in solvents of varying polarity and viscosity. Hemicyanines possess relatively low fluorescence quantum yields (≤ 0.01) in polar solvents. A significant increase in fluorescence quantum yield and lifetimes was observed with increase in viscosity of the solvent medium. The radiative as well as nonradiative decay channels from the singlet excited state were investigated by varying the viscosity of the medium. Various activation processes involved in the excited state bond twisting were investigated. The viscosity-dependent radiationless relaxation observed in hemicyanine dyes is suggestive of a restricted rotor motion in the singlet excited state.

2.2. Introduction

Interest in the design and studies of chromophoric systems has increased significantly in recent years, due to their potential applications in optoelectronic devices (for e.g. optical recording systems,¹⁴³ thermal writing

displays⁴ and laser printing systems⁵) and in biomedical procedures⁶⁻¹³ (in imaging and as probes for detection of cations, anions and organic molecules). Most of the chromophoric systems used for such applications contain strong electron donor-acceptor groups (for e.g. polymethine dyes) and exhibit solvent dependent emission properties resulting from an internal charge transfer process in their excited state. Polymethine dyes¹⁴ are characterized as donor-acceptor systems linked together by conjugated double bonds, with electron donating/accepting groups in the terminal positions. They are further classified as cyanines, hemicyanines etc. based on the type of electron donor and acceptor groups. If both the donor as well as acceptor groups are heterocyclic, then they are referred to as cyanines. Polymethine dyes with heterocyclic acceptor and non-heterocyclic donor groups in terminal positions are referred to as hemicyanines. General structure of cyanines and hemicyanines are shown in Chart 2.1.



n = no. of double bonds
 Z = heteroatom - S, N, O
 R, R', R'' = alkyl group

Chart 2.1. General structure of cyanines and hemicyanines¹⁴

2.2.1. Applications of Hemicyanines

The amphiphilic hemicyanines have been used as voltage sensitive fluorescence probes to record the fast changes in the electrical membrane potential (molecular voltmeter) in neurons.¹⁵⁻²⁰ A typical example of a hemicyanine dye, frequently used as fluorescent probe,²¹ is shown in Chart 2.2. An explicit knowledge on the photophysical properties of hemicyanine dyes is helpful in optimizing the design strategies of such probes for biological applications.

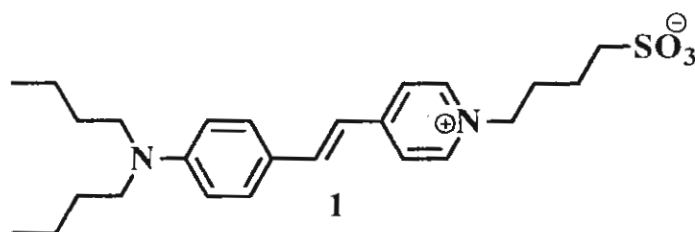


Chart 2.2. A voltage sensitive fluorescence probe
((Dibutylamino)stilbazolium butylsulfonate)²¹

Hemicyanines have also received attention as materials for nonlinear optics and molecular electronics.²²⁻²⁶ The viscosity dependent photophysical properties and the charge transfer nature of hemicyanines offer applications in polymer science and as sensors in analytical chemistry. Hemicyanine based chromoionophores **2** and **3** (Chart 2.3) have been recently synthesized and their metal sensing properties were investigated. Complexation of **2** as well as **3** with metal cations leads to dramatic changes in their absorption and emission properties, due to suppression of its intramolecular charge transfer.²⁷

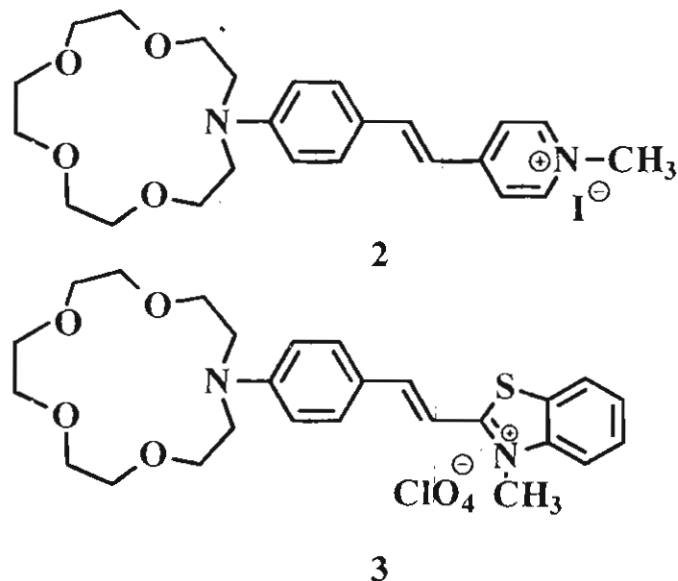
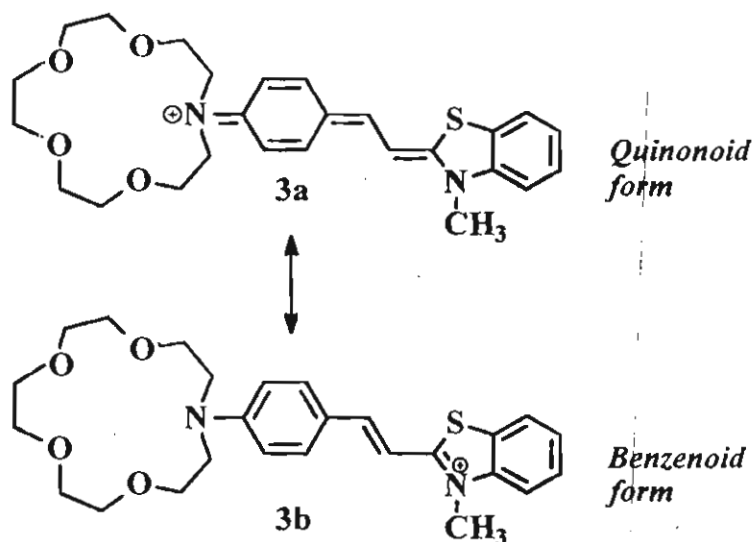


Chart 2.3. Hemicyanine chromoionophores^{27, 28}

2.2.2. Charge Transfer and Structure of Hemicyanines

The structure of hemicyanine dye **3** has been investigated in the crystalline state by X-ray diffraction (XRD) studies and in solution by ¹H NMR studies.²⁷ The hemicyanine part of the molecule possesses remarkably planar structure with an extensive π -conjugation throughout the chromophore. Based on these studies, it has been suggested that intramolecular charge transfer (ICT), from the anilinic nitrogen to the benzothiazolium nitrogen, occur through the involvement of resonance hybrids as shown in Scheme 2.1. Both the XRD, as well as NMR studies indicate that the crown moiety is puckered and is not considered here for discussion. In the present studies we have undertaken a detailed investigation of the photophysical properties of a



Scheme 2.1. Resonance hybrids of hemicyanines²⁷

series of hemicyanine dyes (Chart 2.4) by linking heterocyclic acceptor groups of varying strength to the 4-dimethylaminostyryl group.

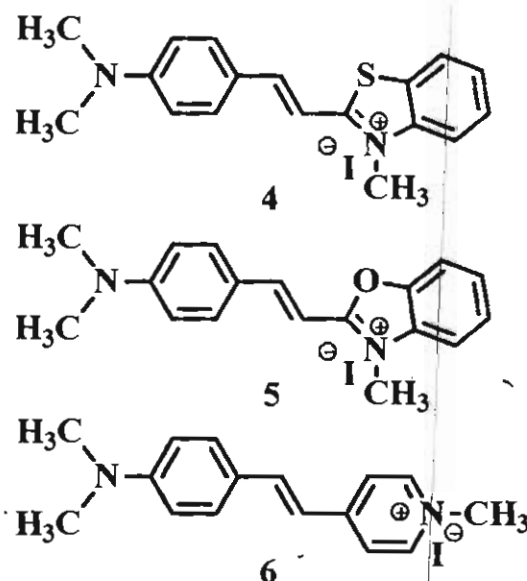


Chart 2.4. Hemicyanines under investigation

The photophysical studies of several hemicyanine dyes have been investigated, in homogenous as well as microheterogeneous systems. Among

these, the excited state dynamics of *trans*-4-[4-(dimethylaminophenyl)styryl]-1-methylpyridiniumiodide (**6** in Chart 2.4) was subjected to extensive investigation employing computer simulation as well as spectroscopic measurements.²⁹⁻³³ A brief summary of the excited singlet as well as triplet state properties of hemicyanines is presented in the following sections.

2.2.3. Photophysical Properties of Hemicyanines

Stilbazolium salts (the quaternary salts of styrylpyridine **7** or styryl quinoline **8**, Chart 2.5) possess interesting photochemical and photophysical

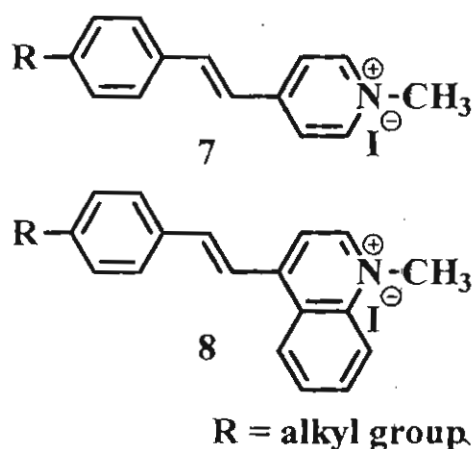


Chart 2.5. Stilbazolium salts

properties. Photochemical *trans-cis* isomerization of stilbazolium salts have been investigated by several groups³⁴⁻⁴² and it is concluded that the isomerization mechanism depend mainly on the substitution at the 4-position of the styryl ring. For example, the photoisomerization mechanism changes from singlet mediated to triplet mediated, when the substitution in the 4-position of the styryl ring (R= H, CH₃, OCH₃ or CN) is replaced by nitro

group.^{34,36} In an earlier study, Görner and Gruen have investigated various deactivation channels from the excited state of the quaternary salts of *trans*-1-alkyl-4-[4-dialkylaminostyryl]pyridinium and *trans*-1-alkyl-4-[4-dialkylaminostyryl]quinolinium (Chart 2.6) by laser flash photolysis and pulse radiolytic methods.²⁹

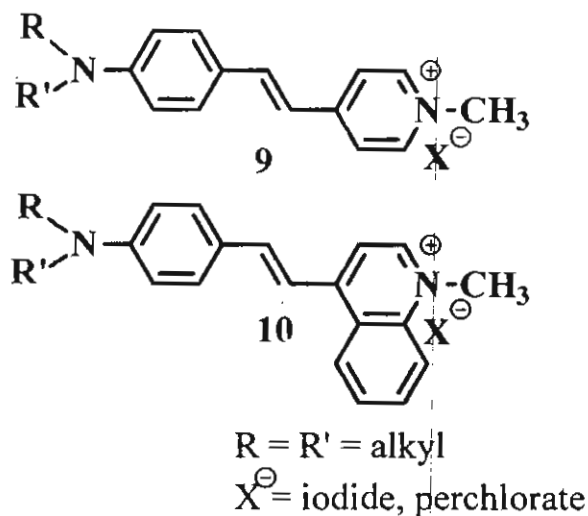


Chart 2.6

The introduction of dialkylamino group in the 4-position of the styryl ring markedly reduces the *trans-cis* isomerization yield ($\Phi_{t \rightarrow c} < 1\%$).³⁸ Also, these compounds exhibit a low intersystem crossing (ISC) in polar solvents. Based on these observations, it is concluded that in polar solvents the deactivation from the singlet excited state is mainly through an internal conversion (IC) channel.

Photoexcitation of hemicyanines result in internal twisting and a twisted intramolecular charge transfer (TICT) model was invoked by Fromherz and

Heilemann to explain the fluorescence behaviour of **6**.³⁰ In the present case no dual fluorescence was observed in the emission spectra and suggests that the twisted states are possibly nonemissive in nature, unlike other molecules having TICT states. There are several chemical bonds in hemicyanines, which can undergo excited state bond twisting (rotamerism) and it is difficult to suggest the exact deactivation path on the basis of spectroscopic results. For e.g., hemicyanine **6** (Chart 2.7) has three single bonds (Φ_1 , Φ_2 and Φ_3) which can undergo twisting in the excited state.⁴³ It is also possible that the TICT states of one or more bonds may be involved in the excited state deactivation.

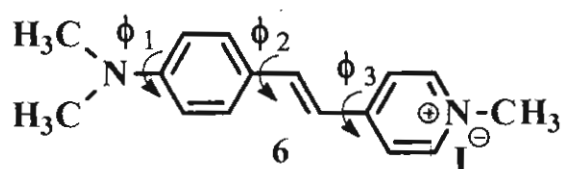
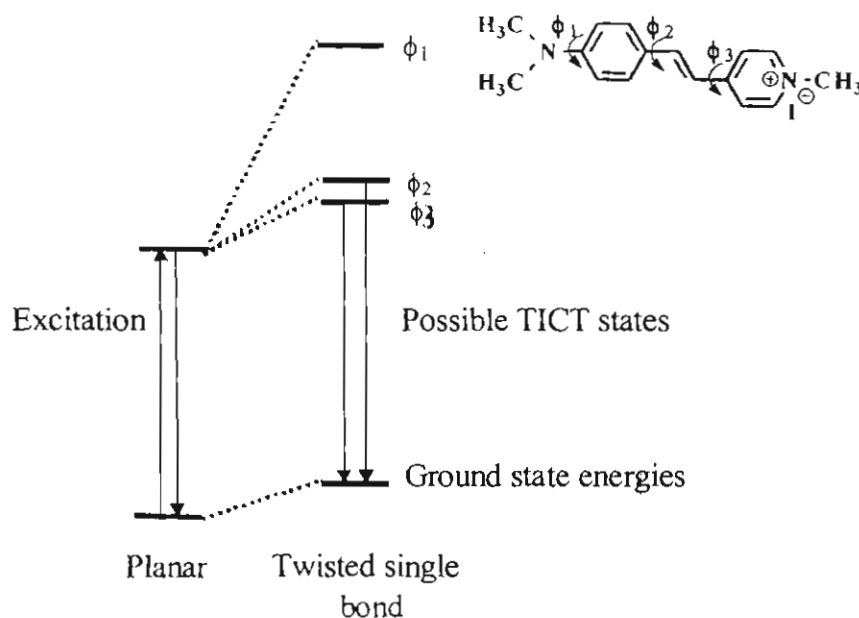


Chart 2.7. Internal twisting channels in hemicyanines⁴³

Spectroscopic studies have shown that hemicyanine **6** possess a low photoisomerization yield (in most solvents $\Phi_{t \rightarrow c} < 1\%$) and poor intersystem crossing efficiency (in polar solvents) and hence these deactivation channels are not considered in the present discussion.²⁹ Rettig and co-workers have performed quantum chemical investigations³¹ of various TICT conformations of **6** (Chart 2.7) and the model suggested is shown in Scheme 2.2. The possible deactivation channel through the twisting of diamino group (Φ_1) can be completely neglected since the corresponding CT state formed is ~ 1.5 eV

higher in energy than the Franck-Condon (FC) state. The twist of the single bonds adjacent to central double bond (Φ_2 and Φ_3) also results in CT states, comparable in energy to that of FC state (Scheme 2.2). By incorporating the solvent effects in the theoretical model, Cao et al.⁴³ have pointed out that the excited state twisting of the anilinic ring (Φ_2) becomes barrierless in polar



Scheme 2.2. Calculated energies of the twisted conformations of **6**^{29,41}

solvents. However, the rotation around the pyridyl-ethylene bond (Φ_3) is not so much influenced by solvation effects. In conclusion, these theoretical studies indicate that the torsion of the aniline moiety is mainly responsible for the singlet state deactivation through a nonradiative channel. These theoretical observations were further supported by photophysical investigations of hemicyanines in various matrices such as amylose, reverse micelle and in

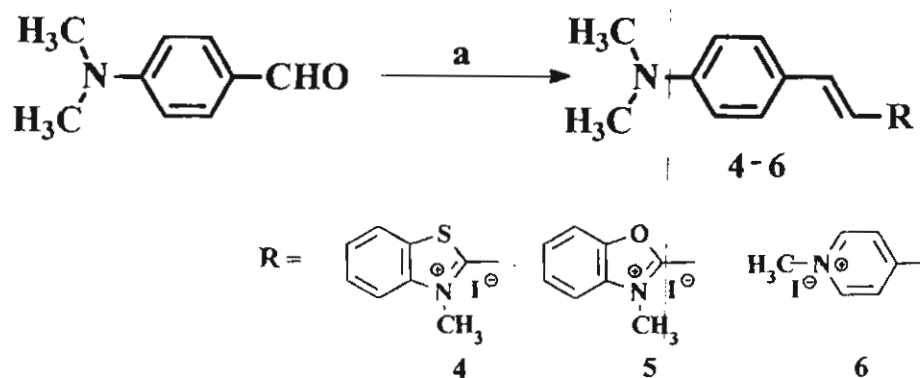
optically transparent mica layers.⁴⁴⁻⁴⁹ The quantum yield of hemicyanine was found to increase substantially when encapsulated in constrained media such as mica.⁵⁰ A longer lifetime was observed for **6** when it was solvated by nanosized water pools formed in reverse micelles.³³ The enhancement of singlet quantum yields and lifetimes can be attributed to the slowing down of the internal twisting in rigid matrices. The above studies indicate that the excited state bond twisting of hemicyanine dyes are extremely sensitive to the environment. The environmental effects were related to a radiationless deactivation process influenced by two macroscopic parameters, solvent polarity and viscosity.²⁹ In this Chapter, we have examined the contributions of these factors (polarity as well as viscosity) on the internal twisting dynamics of hemicyanines **4-6**. Singlet excited state deactivation processes of **4-6** were investigated by varying (i) the viscosity of the medium, keeping the polarity factor more or less constant and (ii) the polarity of the medium, keeping the viscosity factor constant.

2.3. Results and Discussion

Both the steady state and time resolved spectroscopic techniques were employed to investigate the ground as well as excited state properties of hemicyanines **4-6**. The absorption and emission maxima, fluorescence quantum yields and fluorescence lifetimes were measured under various conditions.

2.3.1. Synthesis and Characterization.

Syntheses of the hemicyanines **4-6** were carried out as per a reported procedure (Scheme 2.3).⁵¹ The compounds were fully characterized on the basis of analytical results and spectral data. The experimental procedures for the synthesis, purification and characterization of the hemicyanines are given in Section 2.5.



Scheme 2.3. Synthesis of hemicyanines a) quaternary salt of the corresponding heteroaromatic compound, piperidine, dry methanol (the salts used for **4**, 2-methylbenzothiazolium methiodide; **5**, 2-methylbenzoxazolium methiodide; **6**, 2-methylpyridinium methiodide).

2.3.2. Absorption and Emission Spectra

The absorption spectrum of hemicyanine dye **4** in dichloromethane shows a maximum around 551 nm (trace a, Figure 2.1). The corresponding emission spectrum has a maximum at around 597 nm. A large hypsochromic shift in absorption maximum was observed on increasing the polarity of the solvent, for all the hemicyanines under investigation. For example, the absorption spectrum of **4** in a polar solvent such as acetonitrile was shifted to

520 nm (trace a, Figure 2.1). The absorption spectral properties of **6** were earlier investigated by several groups.^{29-31,43,52} It has been suggested that the ground state of **6** has its positive charge concentrated on the pyridyl ring while the excited state has even charge distribution particularly in polar solvents, due to efficient charge transfer.⁴³ The excited state molecule is thus less polar in polar solvents than the ground state and hence the absorption spectrum shifts to blue with increasing polarity.⁵³ The photophysical, NMR and X-ray diffraction studies have indicated that the broad absorption band observed in the case of **6** is due to a charge transfer transition originating from the electron rich dimethylaminostyryl group to the electron deficient pyridine moiety.^{27,28}

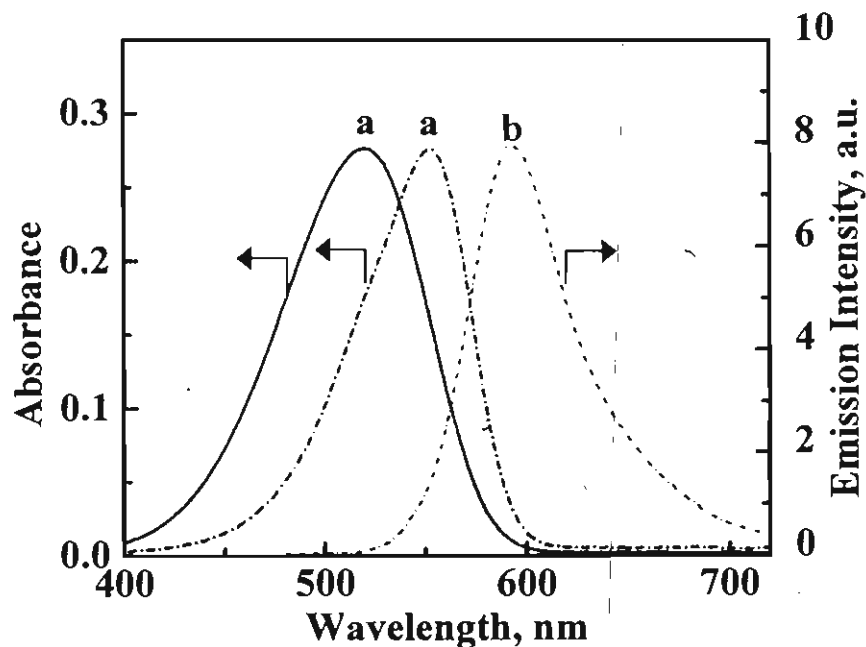


Figure 2.1. Absorption (a) and emission (b) spectra of hemicyanine **4** in acetonitrile (—) and dichloromethane (----)

Also a spectral broadening was observed for **6** in polar solvents.³² The torsional motions in **6**, coupled with the solvent reorganization, result in the spectral broadening.

The charge transfer (CT) in hemicyanines **4** and **5** was confirmed by examining the effect of perchloric acid on the absorption spectral features (Figure 2.2). Addition of perchloric acid protonates the amino moiety, leading to the disappearance of the long wavelength band. This is accompanied by the formation of a new blue shifted band centered at 350 nm. A decrease in emission intensity was also observed on protonation. These studies suggest that the origin of the long wavelength absorption band, observed in **4** and **5**, is due to a charge transfer transition.

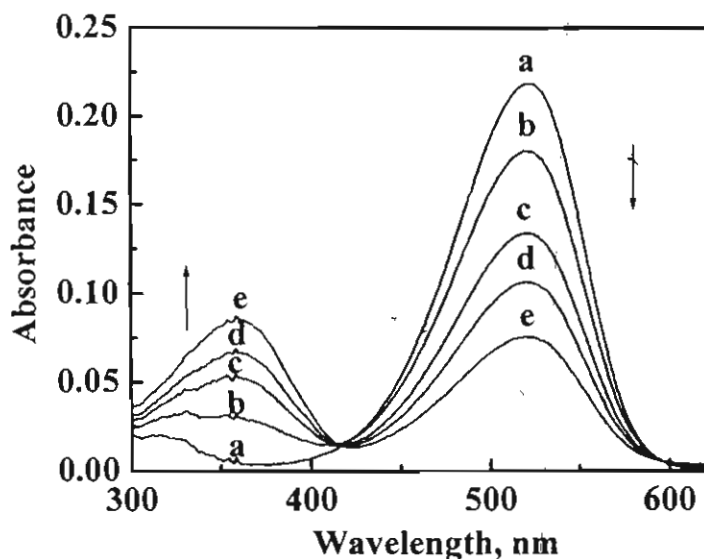


Figure 2.2. Effect of perchloric acid on the absorption spectra of **4** in CH_2Cl_2 : $[\text{HClO}_4]$ (a) 0, (b) 3.2, (c) 6.5, (d) 9.8 and (e) 13.1 μM .

The absorption and emission spectra of **4-6** were measured in a series of straight chain alcohols of varying polarity and the results are presented in Tables 2.1-2.3. The solvent molecules influence the photophysical properties of the chromophoric systems through solute-solvent interactions, depending on the functional groups present. In the present investigation, the photophysical studies are restricted to alcoholic solvents in order to minimize such complications. In general, a bathochromic shift in the absorption spectra was observed for **4-6** in straight chain alcohols, with increase in polarity, whereas the emission maxima remained unaffected. The absorption maxima of **4-6** were

Table 2.1. Correlation of absorption and emission maxima^a of **4 with solvent polarity functions^{b,c}**

Solvent	λ_{\max} , nm ^a		$(\nu_a - \nu_f)$ ^d cm ⁻¹	E_T^N ^b	Δf ^c
	abs.	em.			
Methanol	523	594	2285.4	0.762	0.309
Propan-1-ol	529	593	2054.4	0.617	0.275
Butan-1-ol	532	594	1961.9	0.586	0.264
Pentan-1-ol	532	594	1947.8	0.586	0.250
Hexan-1-ol	531	593	1954.8	0.559	0.248

^a Absorption and emission maxima; ^b E_T^N , Reichardt's solvent polarity parameter⁵⁴; ^c Δf , Lippert's solvent polarity function⁵⁵; ^d $(\nu_a - \nu_f)$, Stokes shift.

Table 2.2. Correlation of absorption and emission maxima^a of 5 with solvent polarity functions^{b,c}

Solvent	λ_{\max} , nm ^a		$(\nu_a - \nu_f)$ ^d cm ⁻¹	E_T^N ^b	Δf ^c
	abs.	em.			
Methanol	494	555	2224.9	0.762	0.309
Propan-1-ol	500	555	1981.9	0.617	0.275
Butan-1-ol	502	555	1902.3	0.586	0.264
Pentan-1-ol	502	555	1918.2	0.586	0.250
Hexan-1-ol	503	555	1878.5	0.559	0.248

^a Absorption and emission maxima; ^b E_T^N , Reichardt's solvent polarity parameter⁵⁴; ^c Δf , Lippert's solvent polarity function⁵⁵; ^d $(\nu_a - \nu_f)$, Stokes shift.

Table 2.3. Correlation of absorption and emission maxima^a of 6 with solvent polarity functions^{b,c}

Solvent	λ_{\max} , nm ^a		$(\nu_a - \nu_f)$ ^d cm ⁻¹	E_T^N ^b	Δf ^c
	abs.	em.			
Methanol	476	613	4695.2	0.762	0.309
Propan-1-ol	478	609	4482.6	0.617	0.275
Butan-1-ol	487	607	4059.4	0.586	0.264
Pentan-1-ol	485	610	4216.6	0.586	0.250
Hexan-1-ol	486	606	4066.0	0.559	0.248

^a Absorption and emission maxima; ^b E_T^N , Reichardt's solvent polarity parameter⁵⁴; ^c Δf , Lippert's solvent polarity function⁵⁵; ^d $(\nu_a - \nu_f)$, Stokes shift.

correlated with the Reichardt's solvent polarity parameter (E_T^N) and defined according to equation 2.1⁵⁴ as a dimensionless figure, using water and TMS (tetramethylsilane) as extreme polar and nonpolar reference solvents. The E_T^N scale ranges from 0 for TMS, the least polar solvent, to 1 for water, the most polar solvent. E_T is the molar electronic transition energy of 2,6-diphenyl-(2,4,6-triphenyl-1-pyridino)phenolate betaine dye measured in kcal/mol at 298 K and 1 bar pressure according to equation 2.2.⁵⁴

$$E_T^N = \frac{E_T(\text{solvent}) - E_T(\text{TMS})}{E_T(\text{water}) - E_T(\text{TMS})}$$

$$= \frac{E_T(\text{solvent}) - 30.7}{32.4} \quad (2.1)$$

$$E_T(30) \text{ (kcal/mol)} = \frac{28591}{\lambda_{\text{max}}(\text{nm})} \quad (2.2)$$

A higher E_T^N value indicates a higher solvent polarity. For hemicyanines **4** and **5** a good correlation was observed, whereas for **6** the correlation was not satisfactory. The square of the correlation coefficient (r^2) of E_T^N versus λ_{max} for hemicyanines is presented in Figure 2.3.

The Stokes shift ($\Delta\nu_{\text{st}}$) of hemicyanines **4-6** in straight chain alcohols were estimated from the absorption and emission maxima (Tables 2.1-2.3). The $\Delta\nu_{\text{st}}$ values were correlated with (i) Reichardts' parameter (Figure 2.4) and (ii) solvent polarity function, Δf (Figure 2.5). For hemicyanine dyes **4** and **5**,

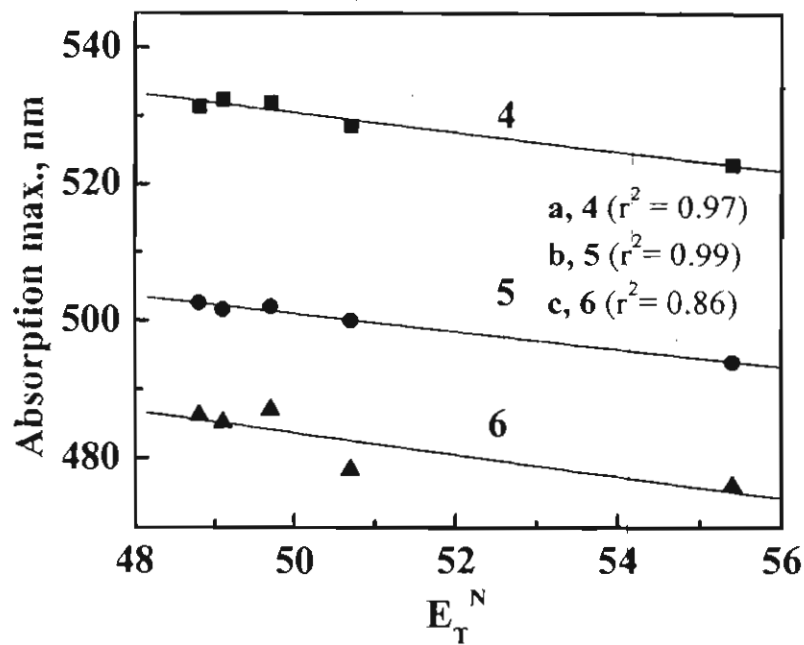


Figure 2.3. Plots of Reichardt's parameter (E_T^N) vs absorption maxima (nm) of hemicyanines 4-6 in straight chain alcohols.

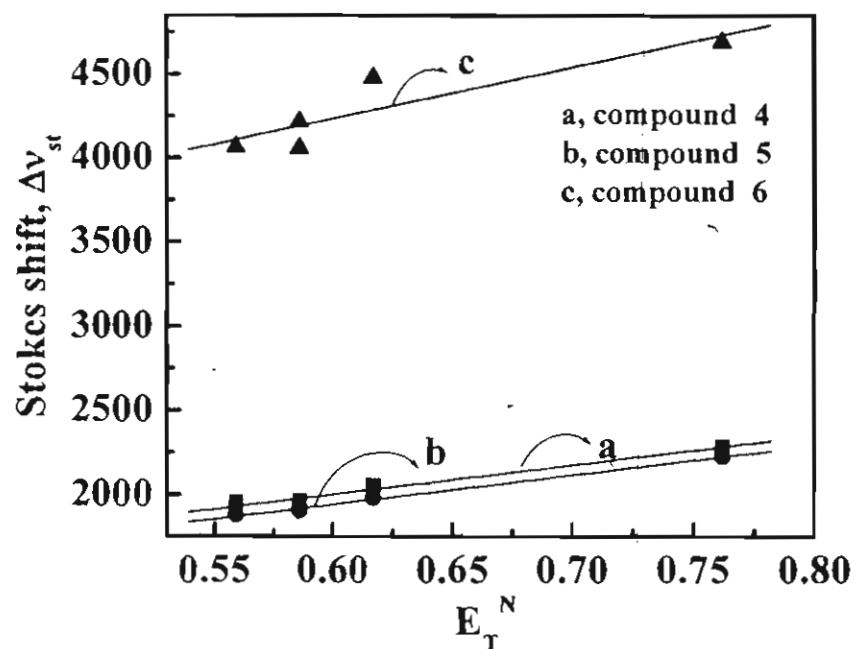


Figure 2.4. Plots of Reichardt's parameter (E_T^N) vs Stokes shift ($\Delta\nu_{st}$) of 4-6 in straight chain alcohols.

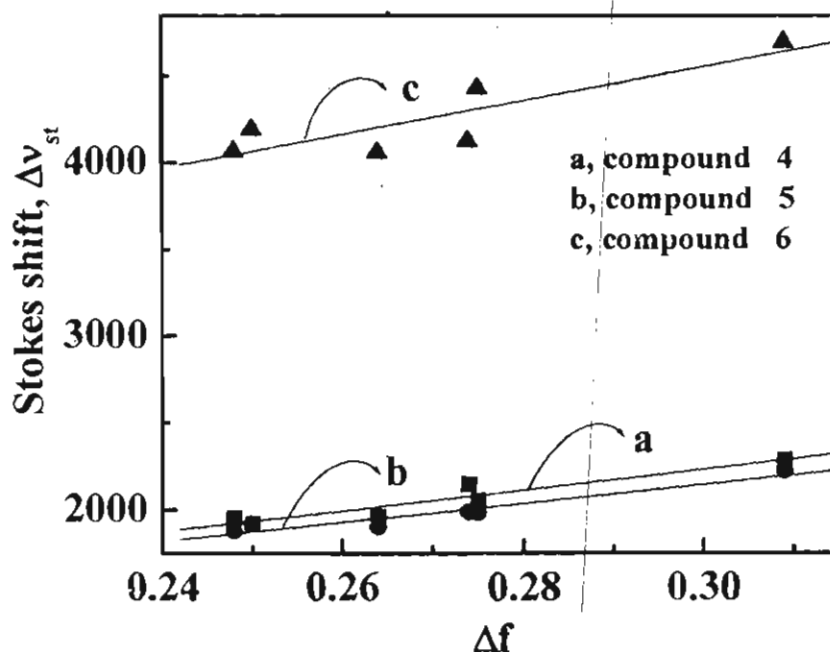


Figure 2.5. Plots of solvent polarity function (Δf) vs Stokes shift (Δv_{st}) for 4-6 in straight chain alcohols.

the Stokes shift increases linearly with E_T^N and Δf values. The data points of 6 were scattered in both the plots and hence these correlations were not further pursued. The increase in Δv_{st} values with solvent polarity indicates that the chromophores undergo a dipole moment change on photoexcitation. The difference in dipole moment, $\Delta\mu_{eg}$ between the excited and ground states of 4 and 5 were estimated from the Lippert-Mataga equation (equation 2.3),^{56,57}

$$\Delta v_{st} = \nu_{abs} - \nu_{em} = \frac{2\Delta\mu_{eg}^2 \Delta f}{hca^3} + \text{Constant} \quad (2.3)$$

where 'a' is the radius (\AA) of the spherical cavity in Onsager's theory of reaction field, 'h' is the Planck's constant ($\text{JK}^{-1}\text{mol}^{-1}$) and 'c' is the velocity of

light (ms^{-1}). The solvent polarity parameter Δf is related to the solvent refractive index (n) and dielectric constant (ϵ) as per equation 2.4.

$$\Delta f = \frac{(\epsilon - 1)}{2\epsilon + 1} - \frac{(n^2 - 1)}{2n^2 + 1} \quad (2.4)$$

The difference in dipole moment, $\Delta\mu_{eg}$ for hemicyanines **4** and **5** were estimated as 11.47 D and 10.76 D, respectively.

The emission spectra of **4**, recorded in a series of straight chain alcohols, of varying polarity, is shown in Figure 2.6. The quantum yield of fluorescence decreased by an order of magnitude by increasing the polarity of the solvent. For example, in hexanol ($E_T^N = 0.559$) the fluorescence yield (Φ_f) is estimated as 3.2×10^{-4} , whereas the Φ_f in methanol ($E_T^N = 0.762$) is 4×10^{-3} . The Φ_f values of **4-6** in straight chain alcohols are summarized in Table 2.4. As discussed in Section 2.2, the hemicyanine **6** prefers a twisted conformation in its excited state.³² An increase in solvent polarity stabilizes the twisted state leading to a decrease in quantum yield.²⁹ Apart from the solvent polarity, the viscosity of the medium may also influence the emission properties of hemicyanines. An increase in viscosity was observed for higher homologues of straight chain alcohols (Table 2.4) and this may also be responsible for the changes in the fluorescence yield. In order to obtain a better insight on the dependence of viscosity and polarity, emission properties of **4-6** were carried out in isoviscous solvents of varying polarity. Propan-1-ol at 265 K, butan-1-ol at 279 K, pentan-1-ol at 289 K and hexan-1-ol at 299 K possess almost the

same viscosity (5 cP) and the Φ_f of 4-6 were found to remain more or less constant in isoviscous solvents. These results are summarized in Table 2.5. In the present study, viscosities of solvent were maintained at 5 cP by keeping the solutions at different temperatures and the activation factors are not considered. These aspects are discussed in the following sections by investigating the viscosity dependent photophysical properties of hemicyanines by (i) varying the composition of glycerol/methanol at constant temperature and (ii) varying the temperature of the medium (glycerol). Temperature dependent studies can provide a better understanding of the intramolecular activated processes from the singlet excited state of hemicyanines.

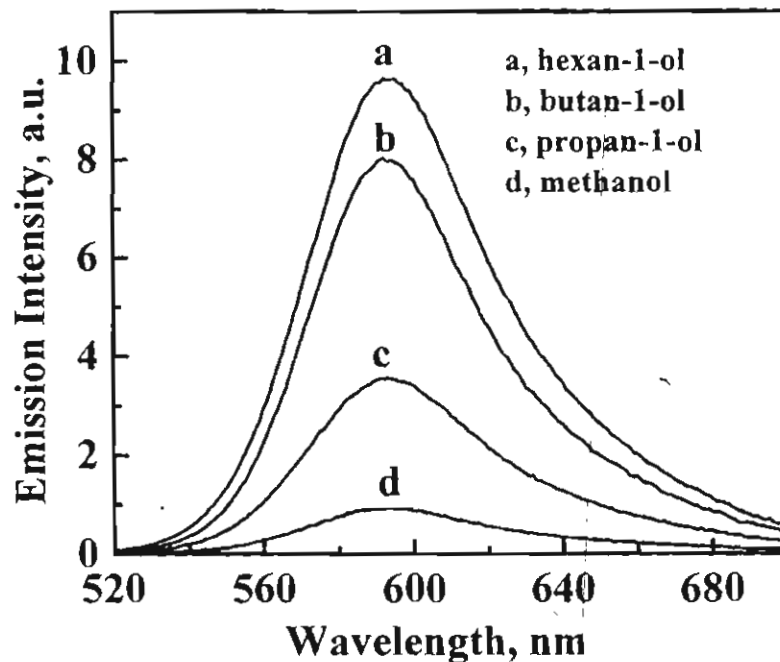


Figure 2.6. Emission spectra of hemicyanine 4 in straight chain alcohols.

Table 2.4. Fluorescence quantum yield of 4 and 6 in straight chain alcohols

Solvent	$E_T^N{}^a$	$\eta(\text{cP})^b$	Φ_f^c	
			4	6
Methanol	0.762	0.547	0.004	0.007
Propan-1-ol	0.617	1.947	0.012	0.018
Butan-1-ol	0.586	2.607	0.027	0.006
Pentan-1-ol	0.586	3.190	0.024	0.045
Hexan-1-ol	0.559	4.592	0.032	0.073

^a E_T^N , Reichardt's solvent polarity parameter⁵⁴;

^b η , viscosity at 298 K⁵⁸; ^c Φ_f , quantum yield of fluorescence, error limit $\pm 5\%$.

Table 2.5. Fluorescence quantum yields of 4-6 in isoviscous alcohols ($\eta = 5 \text{ cP}$)⁵⁹ of varying polarity

Solvent (temp.)	$E_T^N{}^a$	Φ_f^b		
		4	5	6
Propan-1-ol (265 K)	0.617	0.04	0.03	0.08
Butan-1-ol (279 K)	0.586	0.04	0.04	0.10
Pentan-1-ol (289 K)	0.586	0.05	0.03	0.11
Hexan-1-ol (299 K)	0.559	0.045	0.04	0.08

^a E_T^N , Reichardt's solvent polarity parameter⁵⁴; ^b Φ_f , quantum yield of fluorescence, error limit $\pm 5\%$.

2.3.3. Effect of Viscosity

The effect of viscosity (η) of the medium, on the fluorescence quantum yields (Φ_f) and lifetimes (τ_f) of hemicyanines were studied by varying the compositions of methanol and glycerol. Viscosity of glycerol/methanol mixtures were determined using Brookefield Viscometer. All the measurements were carried out at 293 K. Since both the solvents are highly polar in nature the polarity changes were neglected (dielectric constant of methanol and glycerol are 32.6 and 42.5, respectively).

The absorption spectral features of **4-6** remain unaffected in methanol/glycerol mixtures of varying viscosity and the viscosity dependent emission studies were carried out using optically matched solutions (OD at 440 nm = 0.1). The emission spectra of hemicyanine **4** in different glycerol/methanol mixtures are shown in Figure 2.7. Dramatic enhancement in the emission yields were observed for **4-6** with increase in viscosity of the medium. The emission yield of **4** in methanol ($\eta = 0.49$ cP) is very low ($(5 \pm 0.25) \times 10^{-2}$), whereas in glycerol ($\eta = 1490$ cP) it is 0.34 ± 0.03 . This can be attributed to the slowing down of excited state bond twisting in viscous medium. The fluorescence quantum yields of **4-6** in different glycerol/methanol compositions are summarized in Tables 2.6 - 2.8.

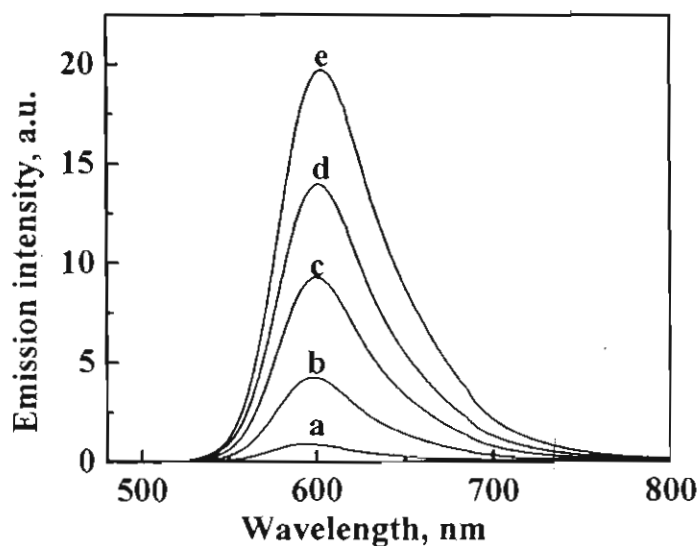


Figure 2.7. Effect of addition of glycerol on the fluorescence of **4** in methanol: Glycerol % (η , cP) (a) 0 (0.49), (b) 70% (80), (c) 80% (328), (d) 85% (448) and (e) 100 (1490).

The fluorescence decay profiles of **4-6** in methanol/glycerol mixtures were recorded by using the time correlated single-photon counting (TCSPC) system. Samples were excited at 440 nm and the emission were followed at 600 nm. All the fluorescence lifetimes were measured at 293 K. The decay curves in all the above cases were fitted to a monoexponential decay and the lifetime were extracted from the measured decay curves by deconvolution of the instrument response function. Figure 2.8 shows the fluorescence decay profile of **4** in methanol/glycerol mixture and an enhancement in lifetimes was observed with increase in viscosity for all the three compounds. For e.g., lifetimes of **4** in methanol ($\eta = 0.49$ cP) and glycerol ($\eta = 1490$ cP) are 0.1 and 1.4 ns, respectively (error limits < 5%). The lifetimes of **4-6** in methanol/glycerol mixtures are summarized in Tables 2.6-2.8.

Table 2.6. Fluorescence properties^a and singlet state deactivation rate constants^{b,c} of 4 in glycerol/methanol mixtures at 293 K

% Glycerol in Methanol	η , cP ^d	Φ_f ^a	τ_f , ns ^a	k_r , 10^9 s^{-1} ^b	k_{nr} , 10^9 s^{-1} ^c
0	0.49	0.005	0.10	0.050	9.950
70	80	0.078	0.22	0.355	4.191
75	198	0.107	0.31	0.345	2.881
80	328	0.136	0.47	0.289	1.838
85	448	0.185	0.47	0.393	1.734
95	1114	0.335	0.68	0.493	0.978
100	1490	0.344	1.39	0.248	0.472

^a Φ_f , quantum yield of fluorescence and τ_f , fluorescence lifetime (error limit $\pm 5\%$);

^b k_r , rate constant for radiative decay estimated as per equation 2.5; ^c k_{nr} , rate constant for nonradiative decay estimated as per equation 2.6; ^dviscosity of glycerol/methanol mixtures determined using Brookefield Viscometer.

Table 2.7. Fluorescence properties^a and singlet state deactivation rate constants^{b,c} of 5 in glycerol/methanol mixtures at 293 K

% Glycerol in Methanol	η , cP ^d	Φ_f ^a	τ_f , ns ^a	k_r , 10^9 s^{-1} ^b	k_{nr}^{tot} , 10^9 s^{-1} ^c
70	80	0.07	0.230	0.304	4.043
75	198	0.10	0.237	0.424	3.798
80	328	0.14	0.377	0.371	2.281
85	448	0.18	0.569	0.316	1.441
90	696	0.20	0.566	0.353	1.413
95	1114	0.25	0.784	0.319	0.957
100	1490	0.33	1.120	0.295	0.598

^a Φ_f , quantum yield of fluorescence and τ_f , fluorescence lifetime (error limit $\pm 5\%$); ^b k_r , rate constant for radiative decay estimated as per equation 2.5; ^c k_{nr} , rate constant for nonradiative decay estimated as per equation 2.6; ^d viscosity of glycerol/methanol mixtures determined using Brookfield Viscometer.

Table 2.8. Fluorescence properties^a and singlet state deactivation rate constants^{b,c} of 6 in glycerol/methanol mixtures at 293 K

% Glycerol - /Methanol	η , cP ^d	Φ_f ^a	τ_f , ns ^a	k_r , 10^9 s^{-1} ^b	k_{nr}^{tot} , 10^9 s^{-1} ^c
70	80	0.066	0.260	0.254	3.592
75	198	0.080	0.358	0.224	2.570
80	328	0.121	0.431	0.281	2.039
85	448	0.150	0.559	0.268	1.521
90	696	0.166	0.611	0.272	1.365
95	1114	0.216	0.781	0.277	1.004
100	1490	0.227	1.180	0.192	0.655

^a Φ_f , quantum yield of fluorescence and τ_f fluorescence lifetime (error limit $\pm 5\%$); ^b k_r , rate constant for radiative decay estimated as per equation 2.5; ^c k_{nr} , rate constant for nonradiative decay estimated as per equation 2.6; ^dviscosity of glycerol/methanol mixtures determined using Brookfield Viscometer.

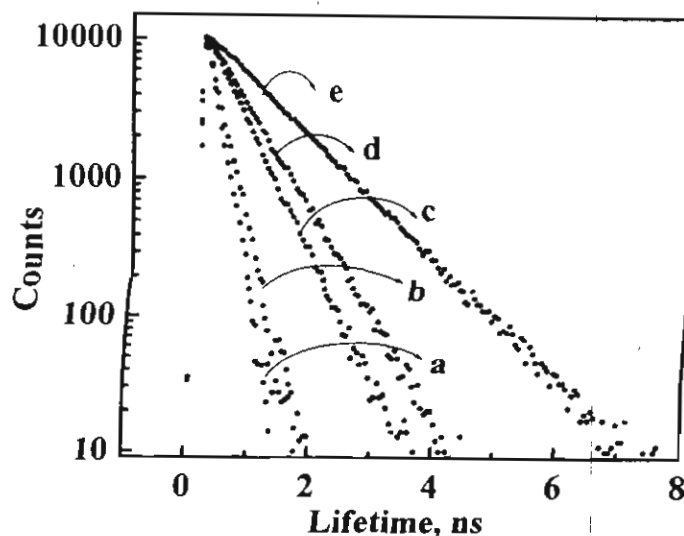


Figure 2.8. Effect of addition of glycerol on the fluorescence decay profile of **4** in methanol: Glycerol % (η , cP) (a) 70 (80), (b) 75% (198), (c) 80% (328), (d) 85% (448) and (e) 100 (1490).

The enhancement of lifetime with viscosity is attributed to the *rigidization of the molecule in the excited state, which retards the bond twisting* in viscous medium. The radiative rate constants (k_r) and the total nonradiative rate constants (k_{nr}^{tot}) from the singlet excited state of **4-6** in methanol/glycerol mixtures were estimated from the Φ_f and τ_f values, using equations 2.5 and 2.6 and they are summarized in Tables 2.6-2.8.

$$k_r = \frac{\phi_f}{\tau_f} \quad (2.5)$$

$$k_{nr}^{tot} = \frac{(1 - \phi_f)}{\tau_f} \quad (2.6)$$

Plots of the singlet state deactivation rate constants, k_r and k_{nr}^{tot} , as a function of viscosity for hemicyanines **4-6** are shown in Figures 2.9-2.11.

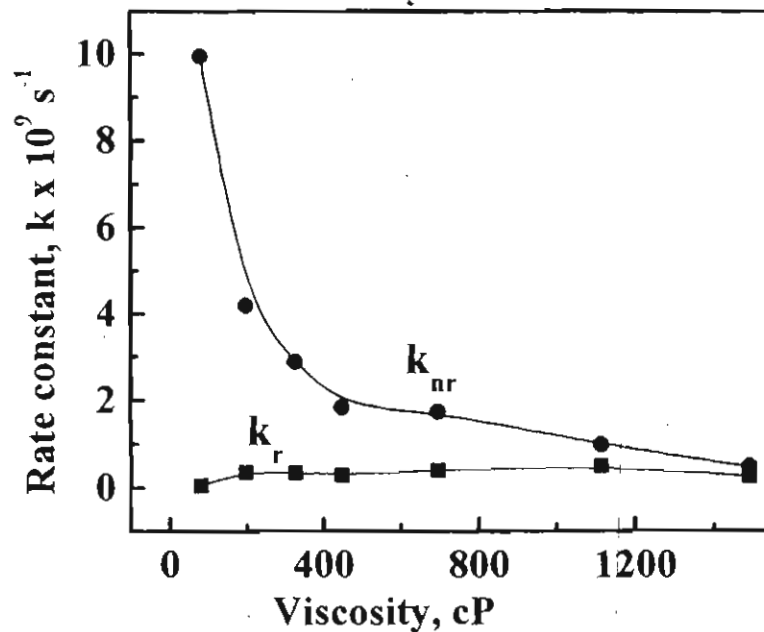


Figure 2.9. Plot of singlet state deactivation rate constants of 4 (k_r and k_{nr}) vs viscosity in different compositions of methanol/glycerol mixtures.

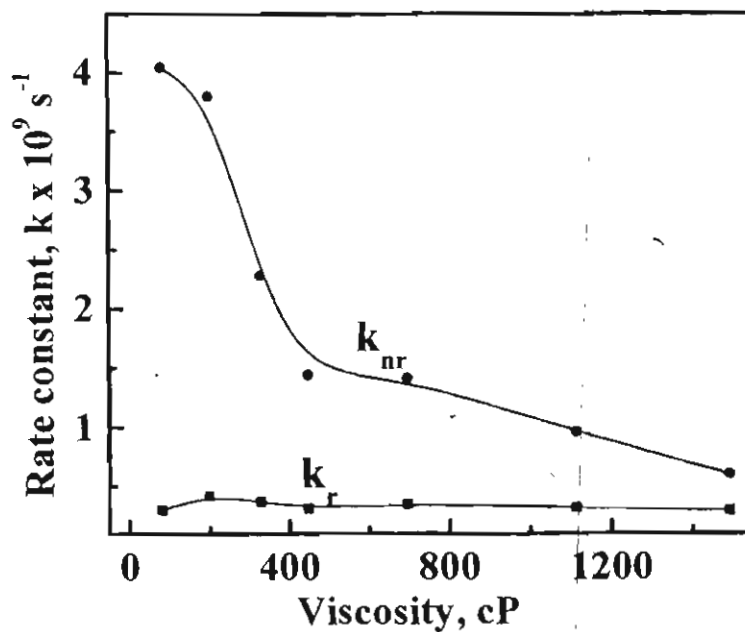


Figure 2.10. Plot of singlet state deactivation rate constants of 5 (k_r and k_{nr}) vs viscosity in different compositions of methanol/glycerol mixtures.

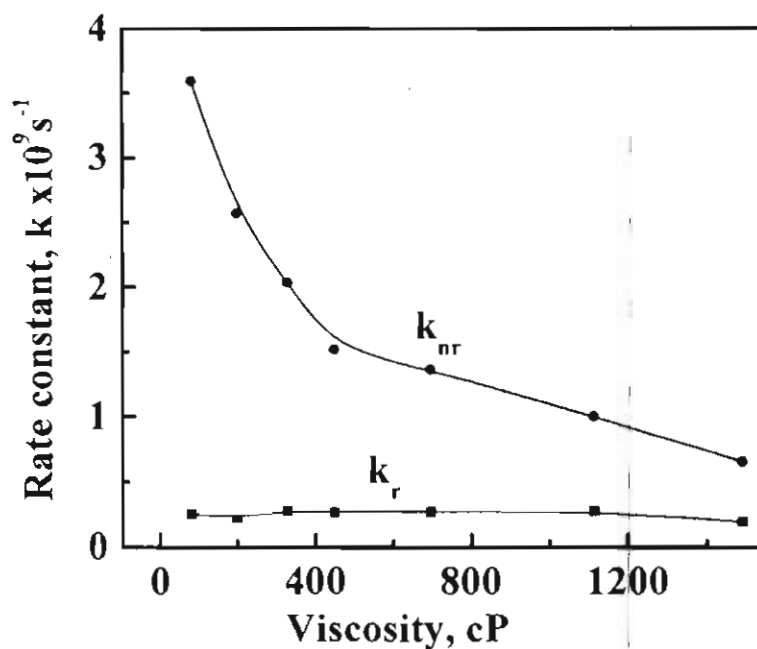


Figure 2.11. Plot of singlet state deactivation rate constants of **6** (k_r and k_{nr}) vs viscosity in different compositions of methanol/glycerol mixtures.

The rate constant of singlet state deactivation through radiative decay (k_r) remains more or less viscosity independent for all the three compounds, whereas a substantial decrease in the total nonradiative rate constant (k_{nr}^{tot}) was observed, with increase in the viscosity of the medium. The relaxation through nonradiative channel becomes less significant in highly viscous medium.

The relaxation rates of several triphenylmethane and polymethine dyes were investigated earlier⁶⁰ and the macroscopic shear viscosity (η) were related to k_{nr} using a linear relationship⁶¹ (equation 2.7)

$$k_{nr} \propto \eta^{-\alpha} \quad (2.7)$$

where, α is the viscosity dependent parameter, for radiationless relaxation. Earlier studies have shown that the value of α is not a constant for a particular dye molecule and depends more on the nature of the solvent system. The nonradiative rate constants (k_{nr}) of 4-6, summarized in Tables 2.6-2.8, are further related to η . A linear correlation was obtained between $\ln k_{nr}^{tot}$ and $\ln \eta$, in methanol/glycerol mixtures (Figures 2.12-2.14) and the values of α were determined from the slope. In the case of hemicyanines 4 as well as 6, the values of α were estimated as 0.5, whereas for 5 a higher value (0.77) was obtained. The values obtained for 4 and 6 were similar to that reported by Sundstrom and Gillbro⁶¹ for cyanines (~ 0.5) in methanol/glycerol and methanol/water mixtures.

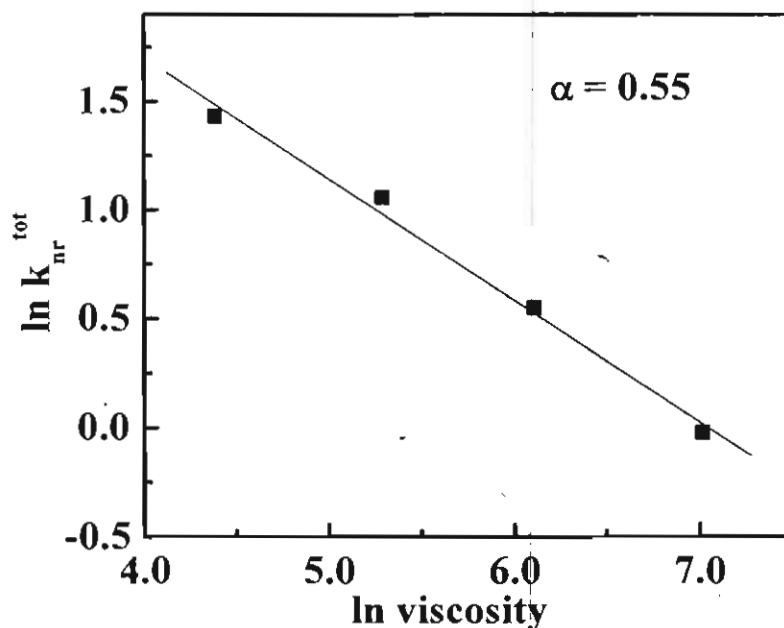


Figure 2.12. Plot of $\ln k_{nr}^{tot}$ vs \ln viscosity for 4 in different compositions of methanol/glycerol mixtures.

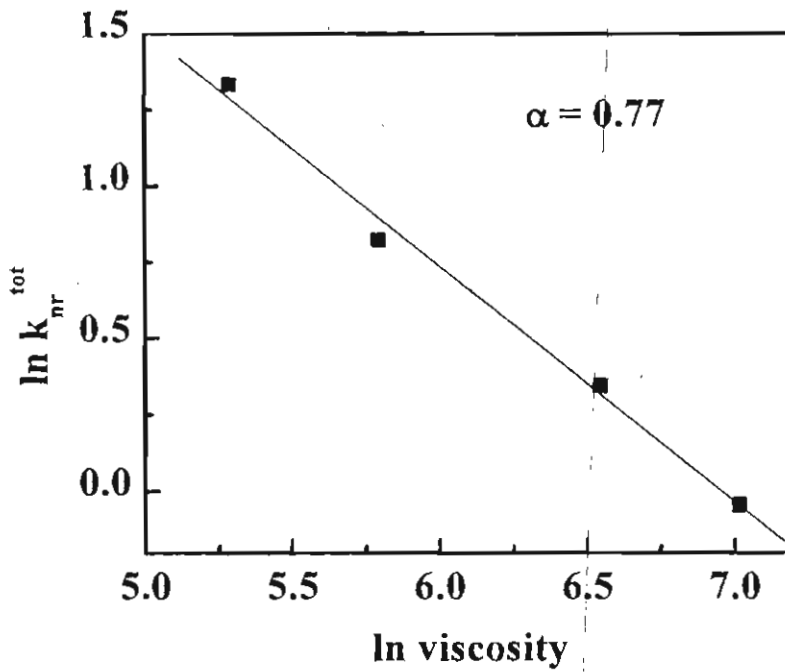


Figure 2.13. Plot of $\ln k_{nr}^{tot}$ vs \ln viscosity for 5 in different compositions of methanol/glycerol mixtures.

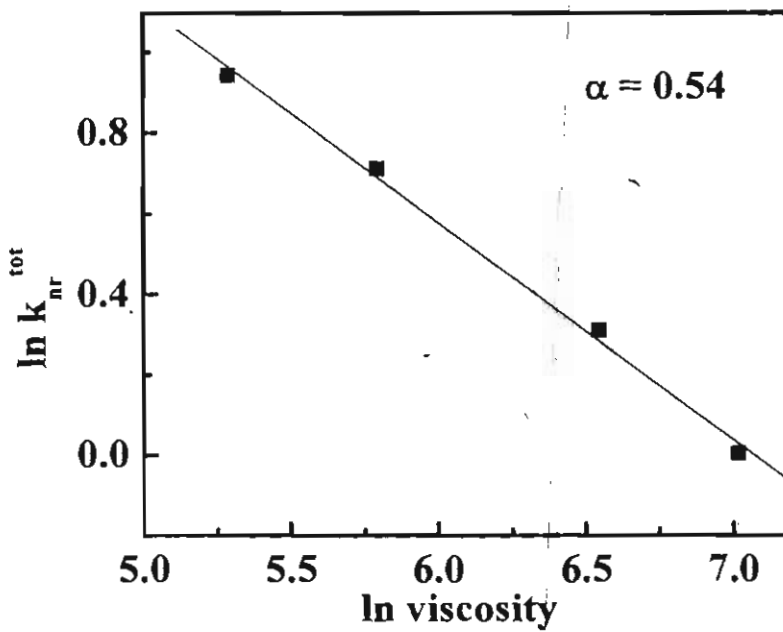


Figure 2.14. Plot of $\ln k_{nr}^{tot}$ vs \ln viscosity for 6 in different compositions of methanol/glycerol mixtures.

In the present case, the macroscopic viscosity of the medium was varied by changing the compositions of methanol and glycerol, at constant temperature. Since the solvent compositions are different in each case, the microscopic viscosity experienced by the chromophore may vary due to the size differences of methanol and glycerol. This problem can be addressed, to an extent, by using single solvent systems and by varying the viscosity by changing the temperature of the medium. Viscosity of glycerol in the temperatures, ranging from 253 K to 298 K, are presented in Table 2.9.⁵⁸ The viscosity of glycerol varied from 9.54×10^2 cP (298 K) to 1.38×10^5 cP (253 K) on decreasing the temperature of glycerol.

The emission spectra of **4** and **5** in glycerol were measured at different temperatures in the range of 253 K to 298 K. A representative example is shown in Figure 2.15. A dramatic enhancement in the emission intensity, with a hypsochromic shift in emission maximum was observed, on decreasing the temperature of the medium. Similar results were observed for hemicyanine **5**. The solutions were excited at 450 nm and the corrections for minor changes in absorbance at excitation wavelength, on decreasing the temperature, were accounted while calculating Φ_f . The Φ_f of **4** and **5** at different temperatures are presented in Table 2.9.

The fluorescence decay profiles of **4** and **5** in glycerol were investigated by varying the temperature (298-253 K) of the medium. A representative example is shown in Figure 2.16. The decay curves, in all cases, were fitted to

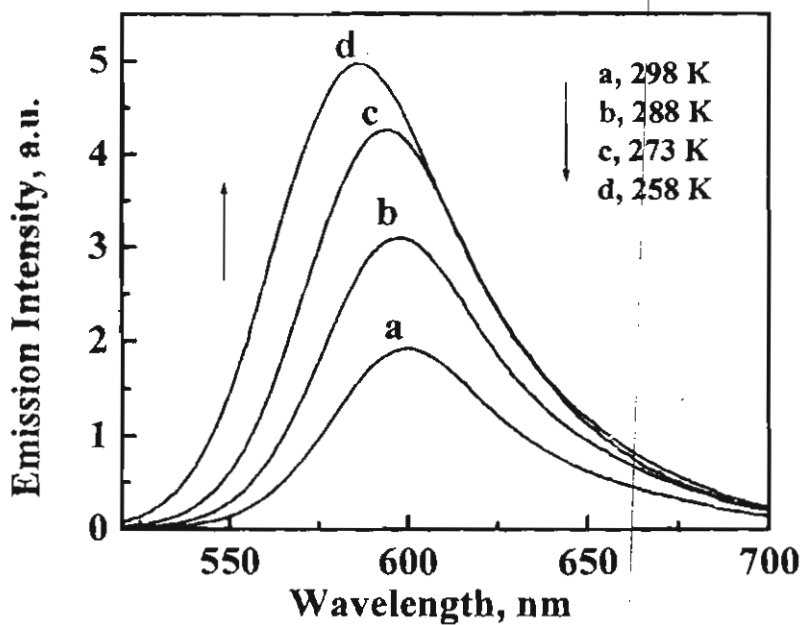


Figure 2.15. Emission spectra of 4 in glycerol at various temperatures.

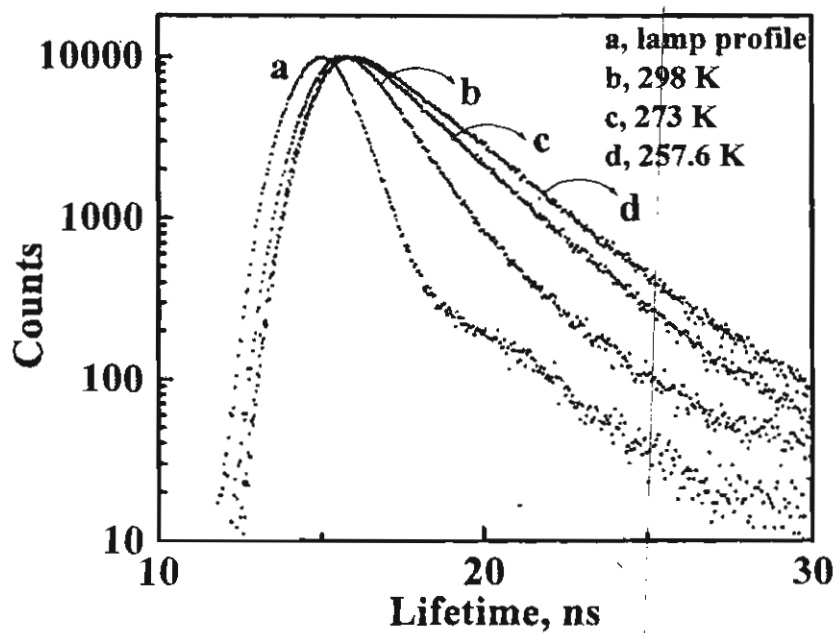


Figure 2.16. Fluorescence decay profiles of 4 in glycerol at various temperatures.

a monoexponential form and the τ_f values are summarized in Table 2.9. A gradual increase in fluorescence lifetime was observed with decrease in temperature and the τ_f at lower temperatures (below 275 K) remains more or less constant. The changes in τ_f values with temperature (i.e., viscosity) are shown in Figure 2.17. As is evident from the Figure 2.17, the curve assumes a plateau below 275 K and the corresponding lifetime is referred to as the limiting fluorescence lifetime (τ_{\max}). τ_{\max} of 4 and 5 in glycerol are 2.15 ns and 2.0 ns, respectively.

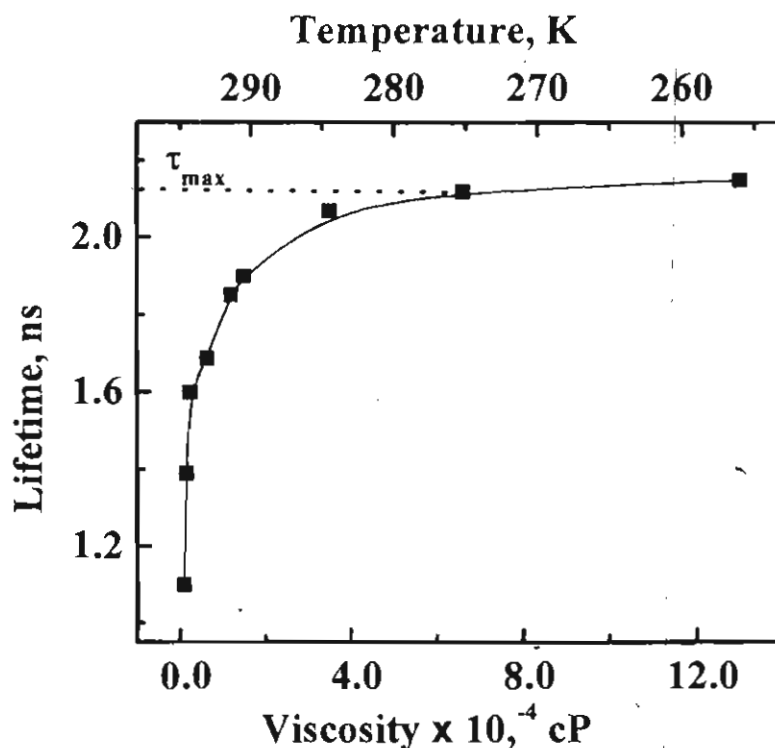


Figure 2.17. Plot of lifetime vs viscosity in glycerol for 4. The radiative rate constant (k_r) and the sum of rate constants of all the nonradiative processes (k_{nr}^{tot}) of 4 in glycerol, at different temperatures were determined from the Φ_f and τ_f values (Table 2.9) using equations 2.5 and 2.6.

k_r and k_{nr}^{tot} values are tabulated in Table 2.10. The radiative rate constant (k_r) remains more or less unchanged whereas a dramatic decrease in the total nonradiative rate constant (k_{nr}^{tot}) was observed with increase in viscosity of the medium, by decreasing the temperature of glycerol. Similar results were observed for 4-6, on varying the viscosity of the medium, by changing the compositions of methanol/glycerol mixtures (Figures 2.9-2.11).

Correlation of the natural logarithm of the total nonradiative rate constants for hemicyanines (obtained by varying the temperature of glycerol) and the natural logarithm of the viscosity of glycerol were further investigated. A linear plot (Figure 2.18) was obtained for both the compounds. The values

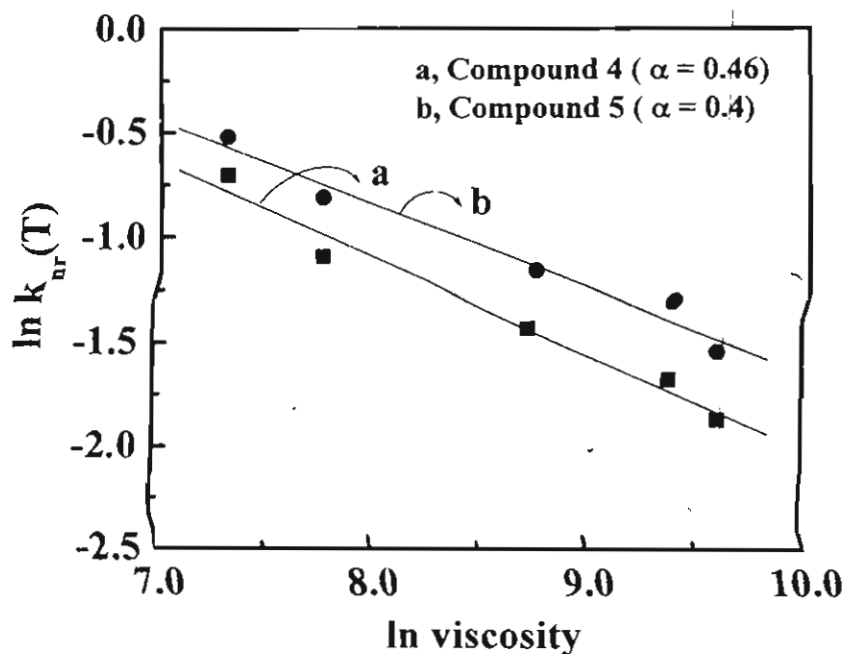


Figure 2.18. Plot of $\ln k_{nr}(T)$ vs $\ln \eta$ for 4 and 5 in glycerol at different temperatures.

Table 2.9. Emission properties of 4 and 5 in glycerol at different temperatures

Temp., K	η , cP ^a	4		5	
		Φ_f ^b	τ_f , ns ^c	Φ_f ^b	τ_f , ns ^c
248	---	0.798	2.20	0.594	2.00
253	130000	0.774	2.15	0.578	1.98
257.6	66000	0.766	2.12	0.567	2.11
262.2	35000	0.743	2.07	0.554	1.97
268.8	15000	0.709	1.90	0.537	2.13
273	12000	0.656	1.85	0.516	1.80
279	6260	0.598	1.69	0.482	1.66
288	2330	0.464	1.60	0.395	1.36
293	1490	0.312	1.39	0.334	1.12
298	954	0.206	1.10	0.271	1.04

^a viscosity of glycerol at various temperatures⁵⁸; ^b quantum yield of fluorescence (error limit $\pm 5\%$); ^c fluorescence lifetime (error limit $\pm 5\%$).

Table 2.10. Radiative and non-radiative rate constants of 4 and 5 in glycerol at different temperatures

Temperature (K)	4		5	
	$k_r, 10^9 \text{ s}^{-1}{}^a$	$k_{nr}, 10^9 \text{ s}^{-1}{}^b$	$k_r, 10^9 \text{ s}^{-1}{}^a$	$k_{nr}, 10^9 \text{ s}^{-1}{}^b$
268.8	0.373	0.153	0.252	0.212
273	0.354	0.186	0.286	0.269
279	0.354	0.238	0.290	0.312
288	0.29	0.335	0.290	0.445
293	0.224	0.495	0.298	0.595
298	0.187	0.722	0.261	0.701

^a rate constant for radiative decay estimated as per equation 2.5;

^b rate constant for nonradiative decay estimated as per equation 2.6.

of α were obtained from the slope as 0.46 for 4 and 0.4 for 5. These results were almost the same as found for other chromophores such as cyanines and rhodamines in alcohols.^{62,63}

Several nonradiative processes occur from the singlet excited state, which include intersystem crossing, internal conversion, isomerization, bond twisting etc. The k_{nr}^{tot} value, estimated using equation 2.6, is the sum of the rate constants of all the nonradiative processes from the singlet excited state. The k_{nr}^{tot} were broadly divided into two components (i) the temperature dependent or activated component ($k_{nr}(T)$) and (ii) the temperature independent or nonactivated component (k'_{nr}), as shown in equation 2.8⁶⁴

$$k_{nr}^{tot} = k'_{nr} + k_{nr}(T) \quad (2.8)$$

One of the major channels for nonactivated decay from the singlet excited state is through intersystem crossing to the triplet state. Attempts were made to investigate the excited state properties of hemicyanines in polar solvents such as methanol, using nanosecond laser flash photolysis techniques and no transients were observed. These results indicate that the intersystem crossing is of minor importance for hemicyanines, **4** and **5** in methanol. The activated components of the nonradiative rate constants were further evaluated from the lifetimes of **4** (or **5**) in glycerol at various temperatures (Table 2.10) using equation 2.9⁶⁴

$$k_{nr}(T) = \tau_T^{-1} - \tau_{max}^{-1} \quad (2.9)$$

where τ_{max} is the limiting fluorescence lifetime. The activation energies $E_{obs}^{\#}$ for the nonradiative process were estimated using the Arrhenius equation by plotting the logarithm of the temperature dependent nonradiative rate constant ($\log k_{nr}(T)$) versus $1/T$ (Figures 2.19 and 2.20). The $E_{obs}^{\#}$ for **4** and **5** were evaluated from the slopes of the plots as 42 kJ/mol and 50.6 kJ/mol, respectively. The activation energy $E_{obs}^{\#}$ is the barrier of the reaction which has to be crossed. For an adiabatic photoreaction the main factors influencing the processes are diffusive effects and intrinsic thermal barrier⁶⁵, as illustrated in Scheme 2.4. The diffusive effects mainly depend on (i) the viscosity of the medium and its temperature and (ii) on the size of the reaction volume.⁶⁶ The

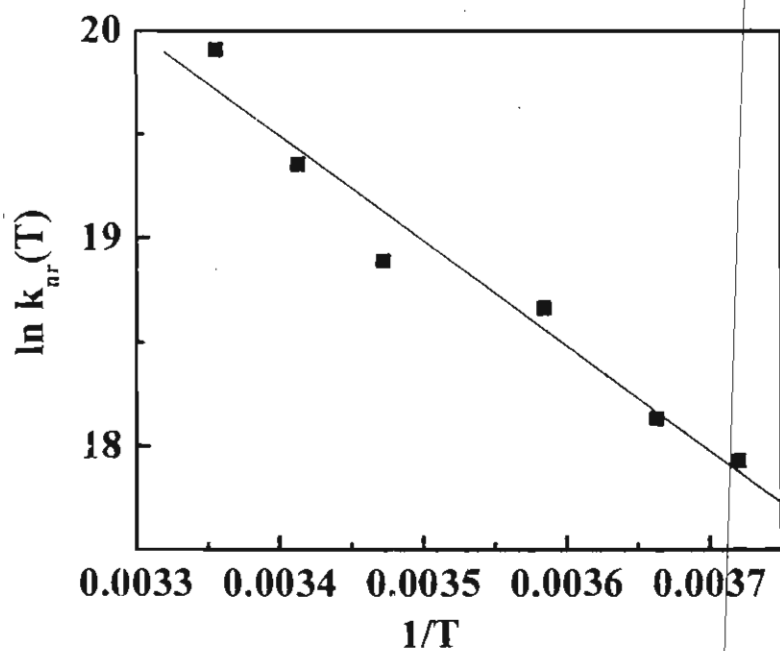


Figure 2.19. Plot of $\log k_{nr}$ vs $1/T$ for 4 in glycerol at different temperatures.

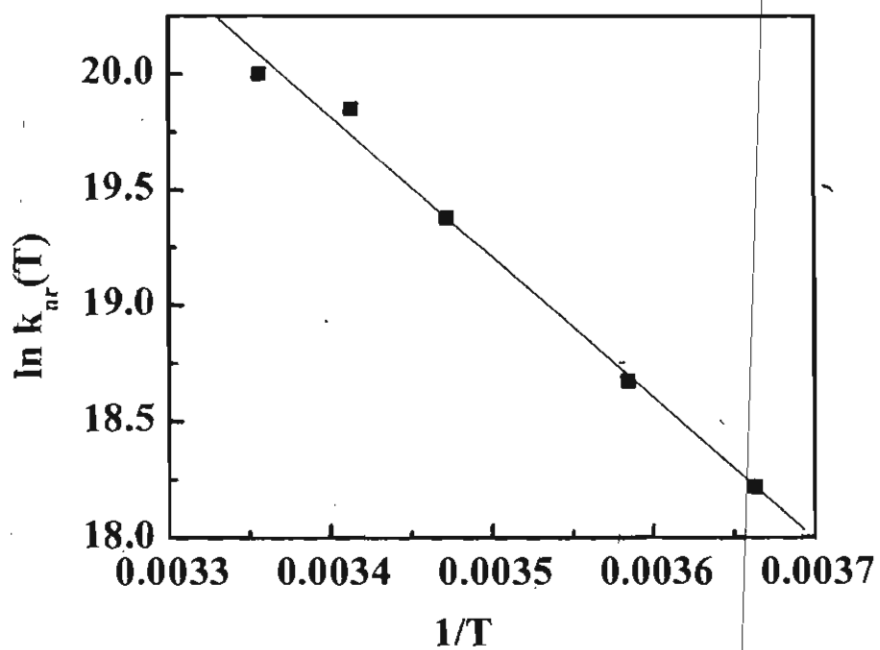
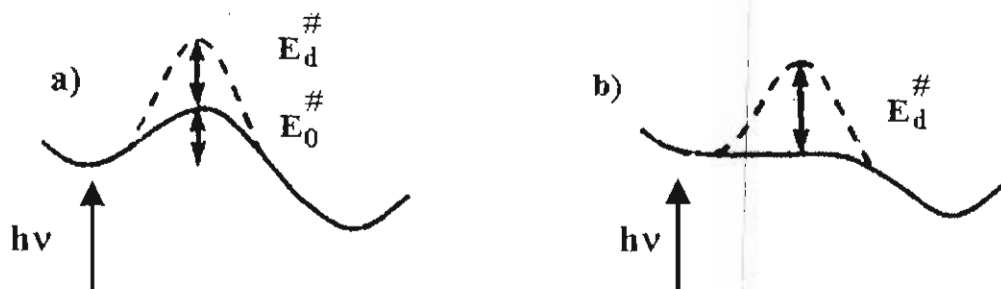


Figure 2.20. Plot of $\log k_{nr}$ vs $1/T$ for 5 in glycerol at different temperatures.

viscosity dependent photophysical studies of 4-6 in glycerol have shown that the diffusive effects play a significant role in slowing down the bond twisting. This is often described by a hydrodynamic model using the Debye-Stoke-Einstein relation.



Scheme 2.4. Schematic representation of an adiabatic photoreaction involving two states separated by an intrinsic barrier $E_0^{\#}$ and diffusive one $E_d^{\#}$; a) and b) denote cases with and without intrinsic barrier.⁶⁵

The intrinsic thermal height is derived from the relative population of the transition and depend on the polarity and temperature of the medium. Thus, the observable activation energy $E_{\text{obs}}^{\#}$ of hemicyanines 4 and 5 in glycerol were related to the diffusive activation energy (E_{η}) and to the intrinsic barrier height $E_0(P)$ using equation 2.10⁶⁵

$$E_{\text{obs}}^{\#} = \alpha E_{\eta} + E_0(P) \quad 2.10$$

The diffusive activation energy of a particular solvent can be estimated using the Andrade equation,⁶⁵ which relates the temperature dependence of solvent viscosity (equation 2.11),

$$\ln \eta = \frac{E_{\eta}}{R} \times \frac{1}{T} + \ln A_{\eta} \quad 2.11$$

where, A_η is the preexponential factor and R is the Universal gas constant. The viscosity of glycerol at different temperatures⁵⁸ are summarized in Table 2.9 and the E_η was estimated as 67.3 kJ/ mol for glycerol from the slope of the plot of $\ln \eta$ versus $1/T$ (Figure 2.21). The thermally activated intrinsic barriers ($E^\#_0$)

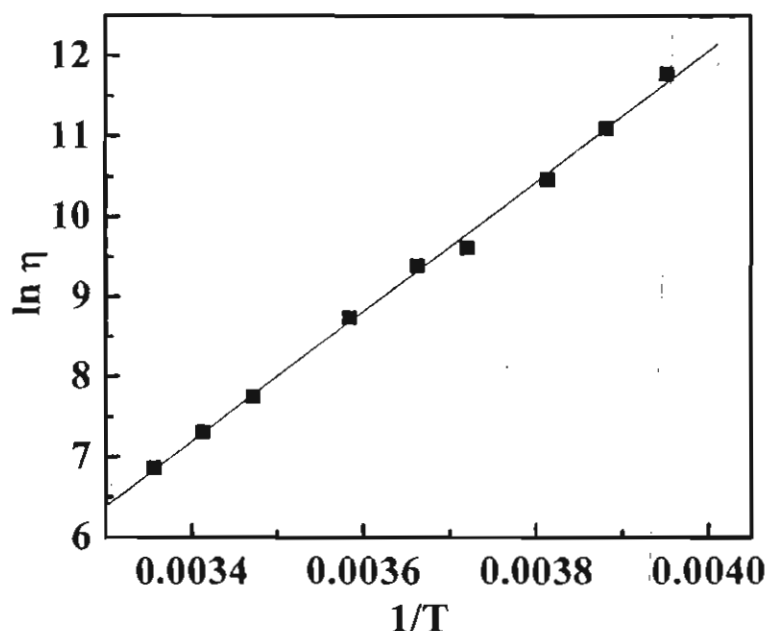


Figure 2.21. Plot of \ln viscosity vs $1/T$ for glycerol at different temperatures (viscosity values are adopted from reference 58).

were further investigated by substituting the values of $E^\#_\eta$ for glycerol and α , the viscosity dependent parameter for radiationless relaxation (Figure 2.18) in equation 2.8. The polarity dependent activation energy ($E^\#_0$) for **4** was estimated as 11.0 kcal/mol. These results indicate that the viscosity dependent factors play a dominant role in the singlet excited state photophysics of hemicyanines.

2.4. Conclusions

A systematic study of the effect of polarity and viscosity of the environment on the excited state properties of hemicyanines was carried out. A substantial increase in the fluorescence quantum yield as well as the singlet lifetime, observed with increase in viscosity of the medium is suggestive of a restricted bond twisting. The activation energy ($E_{\text{obs}}^{\#}$) for the singlet state nonradiative deactivation was estimated and separated into diffusive barrier ($E_{\text{d}}^{\#}$) and a thermally activated intrinsic barrier ($E_{\text{o}}^{\#}$). In hemicyanines, the diffusive barrier was found to have a substantial contribution in the observable activation energy $E_{\text{obs}}^{\#}$ and is attributed to the bond twisting in the singlet excited state.

2.5. Experimental Section

General method for the preparation of hemicyanines (4 and 5)

A mixture of the quaternary salt of the chromophore (1 mmol) and N,N-dimethyl-4-aminobenzaldehyde (1 mmol) was refluxed in dry methanol (15 mL) in the presence of piperidine (2 drops) for 48 h under argon atmosphere. The solvent was removed under reduced pressure and the crude product obtained was purified.

Hemicyanine 4. The crude product obtained was recrystallized from a mixture of chloroform and hexane to give 72 % of 4, m.p. 259-260 °C (decomp.); IR

(KBr) ν_{\max} 1571, 1531, 1487, 1442, 1381, 1343, 1265, 1125, 924 cm^{-1} ; ^1H NMR ($\text{CDCl}_3 + \text{DMSO-}d_6$) δ 8.2- 6.7 (m, 10H), 4.3 (s, 3H), 3.0 (s, 6H); HRMS calculated for $\text{C}_{18}\text{H}_{19}\text{N}_2\text{SI}$ $[\text{M}-1]^+$ 295.1269 found 295.1259 (FAB high resolution mass spectroscopy).

Hemicyanine 5. The crude product was recrystallized from a mixture of chloroform and hexane to give 60 % of **5**, m.p. 249-250 $^{\circ}\text{C}$ (decomp.); IR (KBr) ν_{\max} 1588, 1466, 1381, 1287, 1179, 935, 812, 755, 680, 573 cm^{-1} ; ^1H NMR (CD_3OD) δ 8.2-6.7 (m, 10H), 4.06 (s, 3H), 3.09 (s, 6H); HRMS calculated for $\text{C}_{18}\text{H}_{19}\text{N}_2\text{OI}$ $[\text{M}-1]^+$ 279.1497 found 279.1509 (FAB high resolution mass spectroscopy).

Hemicyanine 6 was prepared as per a reported procedure.⁶⁷ The crude product was chromatographed over silica gel (100-200 mesh) using a mixture (1:4) of methanol and chloroform to give 84% of **6**, mp 254-256 $^{\circ}\text{C}$ (decomp.).

Instrumental Techniques

All melting points are uncorrected and were determined on an Aldrich melting point apparatus. IR spectra were recorded on a Perkin-Elmer Model 882 IR Spectrometer and the UV-Visible spectra on a Shimadzu UV-3101PC UV-VIS-NIR Scanning Spectrophotometer. ^1H and ^{13}C NMR spectra were recorded on a Bruker DPX-300 MHz spectrometer. Emission spectra were recorded on a SPECTRACQ spectrofluorimeter and corrected using the program supplied by the manufacturer. Quantum yield of fluorescence was

determined by a relative method using optically dilute solutions of the dyes (OD of 0.1 at the excitation wavelength) using Rhodamine 6G in ethanol ($\Phi_f=0.9$) as standard. Fluorescence lifetimes were measured using a Tsunami Spectra Physics or Edinburgh FL900CD single photon counting system. The viscosity of different compositions of glycerol/methanol mixtures were determined using a Brookefield Viscometer.

2.6. References

- (1) Ogoshi, K.; Matsui, F.; Yamamoto, T. in *Technical Digest of Tropical Meeting on Optical Data Storage WDD2*, Washington, D.C., **1985**.
- (2) Ohba, H.; Abe, M.; Umehara, M.; Satoh, T.; Ueda, Y.; Kunikane, M. *Appl. Opt.* **1986**, *25*, 4023.
- (3) Matsui, F.; Yanagisawa, S.; Miyadera, T.; Namba, K.; Aoi, T. *Shingakugihou* **1988**, *87*, 387.
- (4) Nagae, Y. in *Thermal Writing Displays*, (Ed.:M. Matsuoka), Plenum Press, New York and London, **1990**.
- (5) Kakuta, A. in *Laser Printer Application*, (Ed.:M. Matsuoka), Plenum Press, New York and London, **1990**.
- (6) Loew, L. M.; Simpson, L. L. *Biophys. J.* **1981**, *34*, 353.
- (7) Fromherz, P.; Dambacher, K. H.; Ephardt, H.; Lambacher, A.; Muller, C. O.; Neigl, R.; Schaden, H.; Schenk, O.; Vetter, T. *Ber. Bunsenges. Phys. Chem.* **1991**, *45*, 1333.
- (8) Haugland, R. P. in *Handbook of Fluorescent Probes and Research Chemicals, Molecular Probes*, Eugene, **1996**.
- (9) Dougherty, T. J. *Photochem. Photobiol.* **1987**, *46*, 569.
- (10) Seis, H. *Angew. Chem. Int. Ed. Engl.* **1986**, *25*, 1058.
- (11) Mathews, J. L.; Newman, J. T.; Sogundares-Bernal, F.; Judy, M. M.; Skiles, H.; Levison, J. E.; Marengo-Rowe, A. J.; Chan, T. C. *Transfusions* **1988**, *28*, 81.
- (12) McCullough, J. L.; Wanstein, G. D.; Douglas, J. L.; Berns, M. W. *Photochem. Photobiol.* **1987**, *46*, 77.
- (13) Wat, C. K.; Mew, D.; Levy, J. G.; Towers, G. H. in *Progress in Clinical and Biological Research*, (Ed.:D. R. Doiron, C. J. Gomer), Vol. 170, Alan R. Liss, New York, **1984**, 351.
- (14) Zollinger, H. in *Color Chemistry*, VCH, Weinheim, **1991**.

- (15) Fromherz, P.; Danbacher, K. H.; Ephardt, H.; Lambacher, A.; Muller, C. O.; Neigl, R.; Schaden, H.; Schenk, O.; Vetter, T. *Ber. Bunsen-Ges-Phys. Chem.* **1991**, *95*, 1333.
- (16) Cohen, L. B.; Salzberg, B. M.; Davila, H. V.; Ross, W. N.; Landowne, D.; Waggoner, A. S.; Wang, C. H. *J. Membr. Biol.* **1974**, *19*, 1.
- (17) Grinvald, A.; Hidesheim, R.; Farber, I. C.; Anglister, L. *Biophys. J.* **1982**, *39*, 301.
- (18) Orbach, H. S.; Cohen, L. B. *J. Neurosci.* **1983**, *3*, 2251.
- (19) Grinvald, A.; Salzberg, B. M.; Lev-Ram, V.; Hidesheim, R. *Biophys. J.* **1987**, *51*, 643.
- (20) Fromherz, P.; Schenk, O. *Biochim. Biophys. Acta* **1994**, *299*, 1191.
- (21) Ephardt, H.; Fromherz, P. *J. Phys. Chem* **1989**, *93*, 7717.
- (22) Gorman, C. B.; Marder, S. R. *Proc. Natl. Acad. Sci.* **1993**, 11297.
- (23) Blanchard-Desce, M.; Wortmann, R.; Lebus, S.; Lehn, J. M.; Kramer, P. *Chem. Phys. Lett.* **1995**, *245*, 526.
- (24) Roberts, G. B. in *Langmuir-Blodgett Films*, Plenum Press, New York, **1990**.
- (25) Chemla, D. S.; Zyss, J. in *Nonlinear Optical Properties of Organic Molecules and Crystals*, Academic, Orlando, **1987**.
- (26) Messier, J.; Kajzar, F.; Prasad, P. in *Organic Molecules for Nonlinear Optics and Photonics*, Klumer Academic, **1991**.
- (27) Alfimov, M. V.; Churakov, A. V.; Federov, Y. V.; Federova, O. A.; Gromov, P.; Hester, R. E.; Howard, J. A. K.; Kuzmina, L. G.; Lednev, K.; Moore, J. N. *J. Chem. Soc. Perkin. Trans. 2* **1997**, 2249.
- (28) Thomas, K. J.; Thomas, K. G.; Manojkumar, T. K.; Das, S.; George, M. V. *Proc. Ind. Acad. Sci. (Chem. Sci.)* **1994**, *106*, 1375.
- (29) Gorner, H.; Gruen, H. *J. Photochem.* **1985**, *28*, 329.
- (30) Fromherz, P.; Heilemann, A. *J. Phys. Chem* **1992**, *96*, 6864.
- (31) Strehmel, B.; Seifert, H.; Rettig, W. *J. Phys. Chem. B* **1997**, *101*, 2232.

- (32) Cao, X.; Mc Hale, J. L. *J. Chem. Phys.* **1998**, *109*, 1901.
- (33) Kim, J.; Lee, M. *J. Phys. Chem. A* **1999**, *103*, 3378.
- (34) Gorner, H.; Schulte-Forhlinde, D. *Chem. Phys. Lett.* **1983**, *101*, 79.
- (35) Gorner, H.; Forhlinde, D. S. *J. Phys. Chem.* **1985**, *89*, 525.
- (36) Gusten, H.; Schulte-Forhlinde, D. *Chem. Ber.* **1971**, *104*, 402.
- (37) Schulte-Forhlinde, D.; Gusten, H. *Justus Liebigs Ann. Chem.* **1971**, *749*, 49.
- (38) Williams, J. L. R.; Carlson, J. M.; Adel, R. E.; Reynolds, G. A. *Can. J. Chem.* **1965**, *43*, 1345.
- (39) Takagi, K.; Ogata, Y. *J. Org. Chem.* **1982**, *47*, 1409.
- (40) Abdel-Mottaleb, M. S. A. *Laser Chem.* **1984**, *4*, 305.
- (41) Gusten, H.; Schulte-Forhlinde, D. *Z. Naturforsch* **1979**, *34b*, 1556.
- (42) Gorner, H.; Fojtik, A.; Wroblewski, J.; Currell, L. J. *Z. Naturforsch* **1985**, *40a*.
- (43) Cao, X.; Tolbert, R. W.; McHale, J. L.; Edwards, W. D. *J. Phys. Chem. A* **1998**, *102*, 2739.
- (44) Hall, R. A.; Thistlewaite, P. J.; Greiser, F.; Kimizuka, N.; Kunitake, T. *J. Phys. Chem.* **1993**, *97*, 11974.
- (45) Fromherz, P. *J. Phys. Chem.* **1995**, *99*, 7188.
- (46) Xu, Z.; Lu, W.; Bohn, P. *J. Phys. Chem.* **1995**, *99*, 7154.
- (47) Kim, O.-K.; Choi, L.-S.; Zhang, H.-Y.; He, X.-H.; Shih, Y.-H. *J. Am. Chem. Soc.* **1996**, *118*, 12220.
- (48) Ogawa, M. *Chem. Mater.* **1996**, *8*, 1347.
- (49) Lang, A.-D.; Zhai, J.; Huang, C.-H.; Gan, L.-B.; Zhao, Y.-L.; Zhou, D.-L.; Chen, Z.-D. *J. Phys. Chem.* **1998**, *102*, 1424.
- (50) Lee, M.; Kim, J.; Yang, J.-H.; Choy, J.-H. *J. Phys. Chem. A* **2000**, *104*, 1388.
- (51) Hamer, F. M. *J. Chem. Soc.* **1956**, 1480.

- (52) Zheng, J.; Li, F.; Huang, C.-H.; Liu, T.; Zhao, X.; Yu, X.; Wu, N. *J. Phys. Chem. B* **2001**, *105*, 3229.
- (53) Shibasaki, K.; Itoh, K. *J. Raman. Spectrosc.* **1991**, *28*, 329.
- (54) Reichardt, C. *Chem. Rev.* **1994**, *94*, 2319.
- (55) Meyer, M.; Mialocq, J. C. *Opt. Commun.* **1987**, *64*, 264.
- (56) Lippert, E. *Z. Naturforsch.* **1955**, *10a*, 541.
- (57) Mataga, N.; Kaifu, Y.; Koizumi, M. *Bull. Chem. Soc. Jpn.* **1956**, *29*, 465.
- (58) Weast, R. C. in *CRC Handbook of Chemistry and Physics*, CRC Press, Boca Raton, Florida, **1979**.
- (59) Simon, J. D.; Su, S.-G. *J. Phys. Chem.* **1990**, *94*, 3656.
- (60) Tredwell, C. J.; Keary, C. M. *Chem. Phys.* **1979**, *43*, 307.
- (61) Sundstrom, V.; Gillbro, T. *Chem. Phys.* **1981**, *61*, 257.
- (62) Casey, K. G.; Quitivis, E. L. *J. Phys. Chem.* **1988**, *92*, 6590.
- (63) Chang, T. L.; Cheung, H. C. *J. Phys. Chem.* **1992**, *96*, 4874.
- (64) Grude, C.; Rettig, W. *J. Phys. Chem. A* **2000**, *104*, 8050.
- (65) Rettig, W.; Fritz, R.; Braun, D. *J. Phys. Chem. A* **1997**, *101*, 6830.
- (66) Alwatter, A. H.; Lumb, M. D.; Birks, J. B. in *Organic Molecular Photophysics, Vol. 1*, Wiley, New York.
- (67) Dix, J. P.; Vogtle, F. *Chem. Ber.* **1980**, *113*, 457.

CHAPTER 3

Conformational Switching and Exciton Interactions in Hemicyanine Based Bichromophores

3.1. Abstract

Two novel hemicyanine based bichromophores, **1** and **2** have been synthesized and characterized. The photophysical properties of these dyes have been studied in detail. Both the bichromophores exist in an extended conformation in polar medium and undergoes an intramolecular folding to a well ordered, parallel stacked conformation, on decreasing the polarity as well as temperature of the medium. The polarity dependent conformational changes of the bridging unit and the solvophobicity of the dye in nonpolar medium drive the folding of the bichromophores. Dramatic changes in the ground and excited singlet state properties, observed upon folding are attributed to the formation of intramolecular aggregates of H-type. Folding-unfolding processes in these molecular systems were completely reversible and studied, in detail, using steady state absorption and time resolved fluorescence spectroscopy. The equilibrium constant as well as the free energy of formation of intramolecular aggregates are reported. Based on the steady state emission and excitation studies it is suggested that the weak emission observed in the case of the folded form originates from a forbidden state. Time resolved fluorescence studies indicate that both the bichromophores exhibit monoexponential decay, with a short lifetime, in dichloromethane solutions

containing $\leq 50\%$ toluene. Interestingly, a biexponential decay with a short and long lived species was observed at a higher toluene concentration, due to the presence of unfolded and folded forms. Folding results in the intramolecular stacking of chromophores which restrict their torsional dynamics, leading to a longer lifetime. Laser excitation of the folded form results in a temporal conformational switching, to the unfolded form of the bichromophore, due to light induced temperature jump.

3.2. Introduction

Design and study of molecular as well as supramolecular photoactive systems have been actively pursued in recent years, due to their potential applications in optoelectronic devices¹⁻⁶ (for e.g., molecular switches,²⁻⁴ sensors,³ transducers,⁵ information processing and storage devices⁶). Synthetic molecular systems and polymers, which can adopt well-defined conformations in solution, analogous to the folded state of proteins, are of particular interest. Spectroscopic investigations of these systems, by various groups have provided reasonable understanding on the interactions such as hydrogen bonding and solvophobic forces.⁷ These studies also provided insight into the manner in which conformational ordering develops in molecular systems to helical, pleated and foldameric structures.⁸

3.2.1. Conformational Ordering of Molecules

Several types of synthetic foldamers have been explored in recent years, among which the β -peptides are the most thoroughly characterized in terms of folding properties.⁹ Oligomeric systems which can adopt secondary structures through hydrogen bonding have also been examined.¹⁰ Another class of molecular system, based on oligomeric donor-acceptors (Chart 3.1), was reported to fold into pleated secondary structures, resulting from the interaction between alternating electron-rich donor and electron-deficient acceptor groups.¹¹

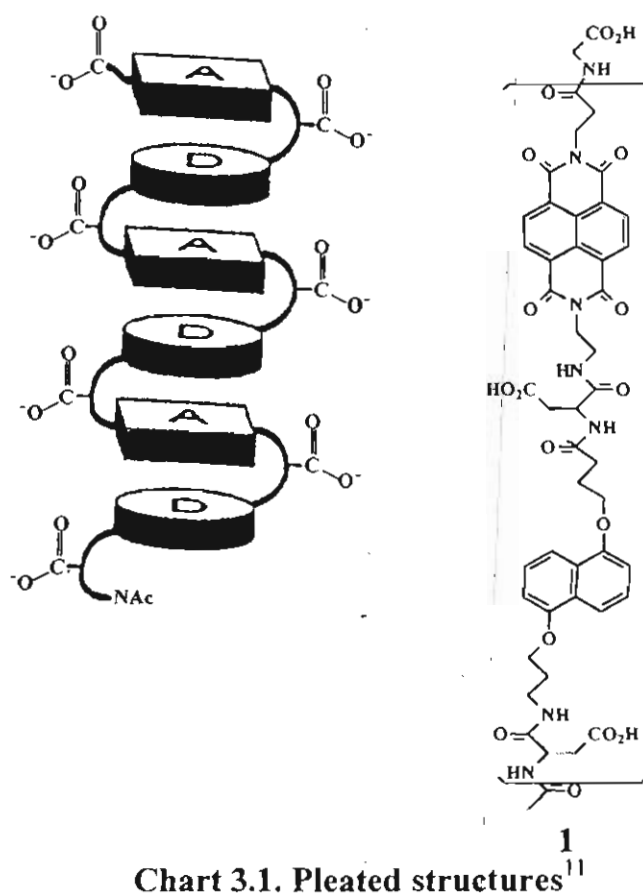


Chart 3.1. Pleated structures¹¹

Solvophobic driven folding of phenylene-ethynylene oligomers (for e.g., compound 2) to helical conformation (Chart 3.2) has been recently demonstrated

by Prince *et al.*¹² This putative helical conformation creates a barrel-like cavity that may function as a molecular container for specific recognition and complexation.

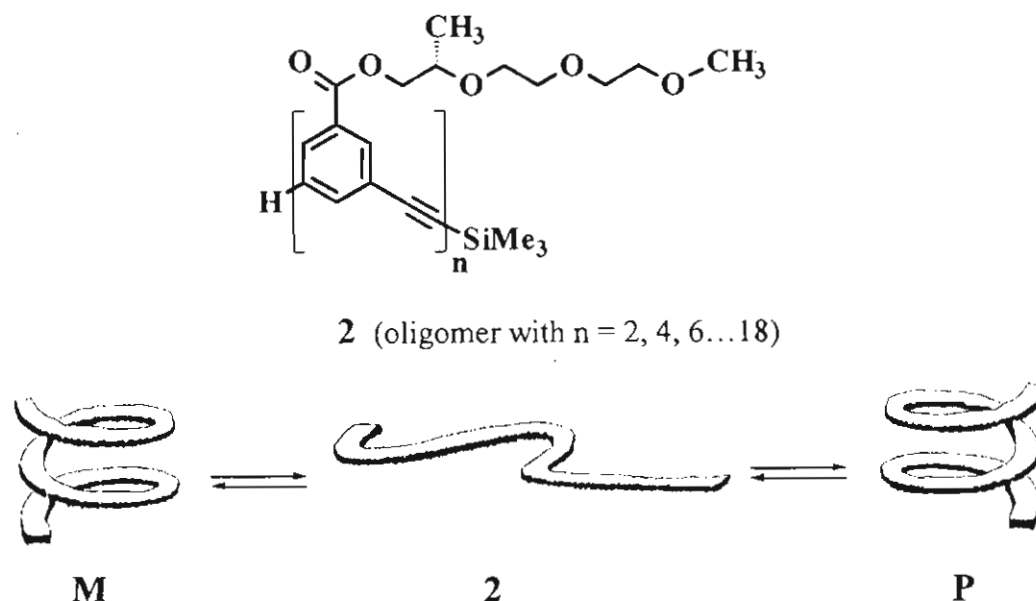


Chart 3.2. Solvophobic driven folding¹²

Conformational changes in molecular and supramolecular systems can, in principle, be modulated by chemical, photochemical or electrochemical methods.^{1,2} Such changes when translated to optical as well as electronic properties form the basis of switching devices.¹ Most of the above mentioned systems are either oligomeric or polymeric in nature and it is difficult to understand the dynamics of the conformational changes in these complex molecular structures. Another class of molecular systems which can form well ordered structures in solution are bichromophores and a few representative examples are summarized below.

3.2.2. Bichromophores

Bichromophores are molecular systems consisting of two chromophoric units linked together by a bridging unit. Conformational changes in such systems can be modulated by varying the nature of the bridging (rigid or flexible) and the chromophoric units (charge density, hydrophobicity/hydrophilicity etc.). Conformational changes in bichromophores can affect the interchromophoric separation and their close proximity results in coupling. This can induce changes in their ground and excited state properties, for e.g., unsymmetric bichromophores containing chromophoric units with properly tuned optical and redox properties, can induce energy or electron transfer. Photoinduced energy transfer studies in coumarin based unsymmetric bichromophores, linked together by penta(ethylene oxide) spacer, have been reported by Valeur and coworkers¹³ (Chart 3.3).

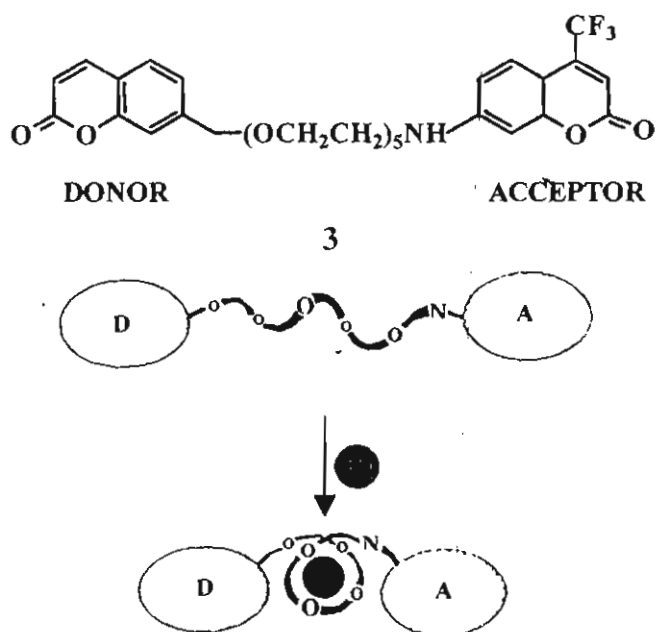


Chart 3.3. Photoinduced energy transfer in bichromophores¹³

A significant increase in efficiency and rate of energy transfer was observed upon complexing with Pb^{2+} . More recently solvent dependent conformational changes in a poly(oxoethylene) linked binuclear complex were investigated by probing the photoinduced energy transfer.¹⁴

Conformational changes in symmetric bichromophores can lead to the formation of either ground state aggregates or excimers. Aromatic compounds (for e.g., pyrene¹⁵) form molecular associates in their excited states (excimers), whereas the interaction between the chromophoric dyes in their ground state leads to the formation of aggregates and is explained on the basis of the theory of exciton coupling.¹⁶

3.2.3. Exciton Coupling in Chromophoric Dyes

The self-association of dyes in solution (or at the solid-liquid interface) is referred to as aggregation and its importance has been widely recognized in photographic sciences, tunable lasers and photomedicine.¹⁷ Aggregation leads to spectroscopic changes in molecules such as spectral shifts, nonconformity with Beer-Lambert law and fluorescence quenching. The most widely used techniques to study aggregation are absorption and emission spectroscopy. The ability of chromophoric dye molecules to aggregate depends on (i) the structure of the dye, (ii) solvent medium, (iii) temperature and (iv) the presence of electrolytes. The various driving forces of aggregation are electrostatic dipole-dipole interactions, solvophobic interactions and intermolecular hydrogen bonding.¹⁸ In the case of

ionic dyes, aggregation results from the strong hydrophobic interactions, which first overcomes the coulombic repulsion between the chromophores and then brings them to a reasonable distance to form dimers (and subsequently higher oligomers). There have been different approaches to explain the phenomenon of aggregation, the simplest of which is the theory of exciton coupling put forward by Mc Rae and Kasha.¹⁶

According to exciton theory,¹⁶ the dye molecule is considered as a point dipole. Strong dipole-dipole interactions in the excited state lead to the formation of an exciton band. Dye aggregation splits its singlet state into two levels; one lower in energy and the other higher in energy, than the excited state of the corresponding monomer (Chart 3.4).

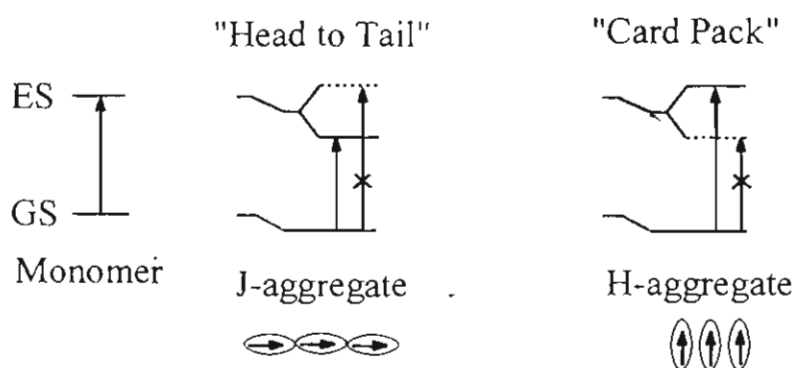


Chart 3.4. Exciton splitting in dye aggregates¹⁶

The allowed transitions are governed by the tilt angle, α (often referred as angle of slippage) as shown in Chart 3.5. When the slippage angle is less than approximately 54° , the transition to the lower energy level is allowed. This leads to a narrow red shifted absorption, relative to that of the monomer absorption and

is often referred as J-aggregates. In contrast, transition to the higher level is allowed, when the slippage angle is more than 54° resulting in a hypsochromically shifted absorption band (H-aggregates). In the case of H-aggregates, the molecules get packed in a plane to plane manner, and in an ideal situation it forms a sandwich type arrangement. For any intermediate geometry, both the blue shifted as well as the red shifted peaks may appear. The oscillator strengths of the

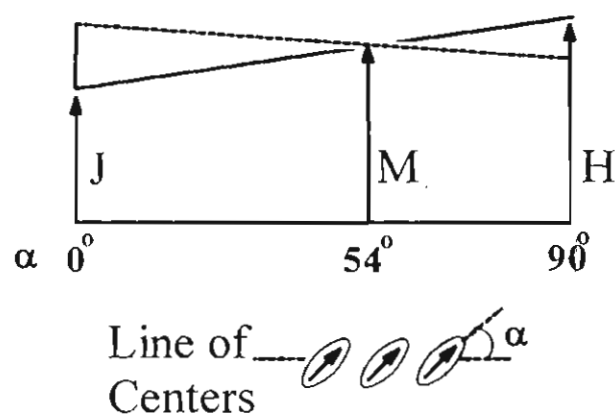


Chart 3.5. Angle of slippage in dye aggregates

short wavelength (f_1) as well as long wavelength bands (f_2) and the slippage angle (α) can be correlated by the equation (3.1).¹⁹

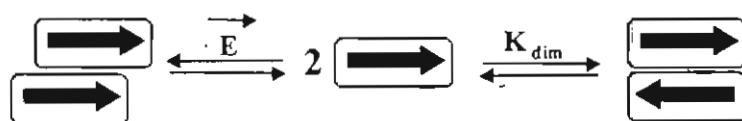
$$f_1/f_2 = \tan^2 \{(180-\alpha)/2\} \quad (3.1)$$

The extent of splitting depends on the magnitude of interaction between the oscillating dipoles of the two molecules and in the case of coulombic interactions, only the dipole-dipole term is considered.²⁰ In such cases, the interaction energy, ΔE (equation (3.2)) is related to the transition moment integral,

$$\Delta E = [2M^2/R^3] G \quad (3.2)$$

$|M|$ and d , the distance of separation between the centers of gravity of the component molecules in the dimer (G is the geometry factor).

Earlier studies were focused on the spectroscopic characterization of the ground state of aggregates. The most notable investigations on their photophysical properties are by Rohatgi and Singhal²¹ on ionic dyes and by Neckers and coworkers¹⁹ on Rose Bengal based systems. Polymethine dyes such as cyanines and squaraines have a strong tendency to form aggregates and are widely used as photosensitizers in optoelectronic devices and as fluorescent probes in biomedical field²² (details on the applications are presented in Chapter 1). An understanding of the intermolecular interactions such as aggregation, in these chromophoric systems, can help in tuning their photophysical properties (by structural modifications). These aspects have been investigated in great detail by several groups of workers. For example, Wurthner and Yao,²³ in a recent report, have related the low nonlinear optical susceptibilities of merocyanine dyes in polymeric materials to an aggregation mechanism (Scheme 3.1). Merocyanine dyes are



Scheme 3.1. Dipole-dipole interactions and electric-field-induced orientation (model for the competition between internal organization of dipolar dyes by dipole-dipole interactions (right) and external organization by electric-field-induced orientation leading to a noncentro-symmetric metastable dye arrangement as desired for nonlinear optical applications).²³

considered as the most suitable candidate for photorefractive applications on the basis of their molecular properties.²⁴ However, such dipolar dye molecules aggregate in an antiparallel fashion as a result of internal electrostatic forces (Scheme 3.1, right) which counteract the external forces imparted by the electric field during poling and thus fail in providing the expected electro-optic responses.

Advances in the ultrafast spectroscopic methods (nanosecond as well as picosecond time resolved absorption and emission techniques) have widened the scope of our understanding of the excited state properties of dye aggregates. Excited state properties of an aggregated cyanine were investigated in detail by Khairutdinov and Serpone²⁵ and found that these aggregates have longer singlet lifetime, though their fluorescence quantum yield are lower than that of the monomeric analogue. Another class of chromophoric aggregates, which received attention in recent years, are systems based on squaraines.²⁶ More recently, Das and coworkers²⁷ have extensively investigated, both the singlet as well as triplet excited state properties of J- and H-aggregates of squaraine dyes.

In all the above-mentioned cases, the intermolecular association of two chromophoric units results in the formation of the dimer. Further addition of monomers can lead to the formation of higher order aggregates and it is difficult to control their spatial dimension. A better control on the spatial disposition of the interacting chromophores in aggregates is possible through a rational design and bichromophores are a group of molecular systems, which have gained attention in this regard.

In an earlier work, Nakanishi and coworkers²⁸ have linked cyanine chromophores to the 1,2-positions of cyclohexane as in **4** (Chart 3.6) and have related the circular dichroism observed in **4**, to exciton coupling.

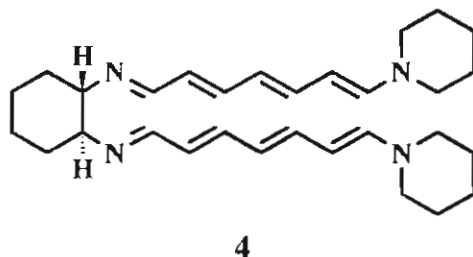


Chart 3.6. Biscyanine (Nakanishi, Harada and coworkers²⁸)

Effect of the relative orientation of the chromophores on the spectral shift in biscyanines, linked through a rigid 1,8-naphthylene skeleton as in **5** (Chart 3.7), was investigated by Kato *et al.*²⁹

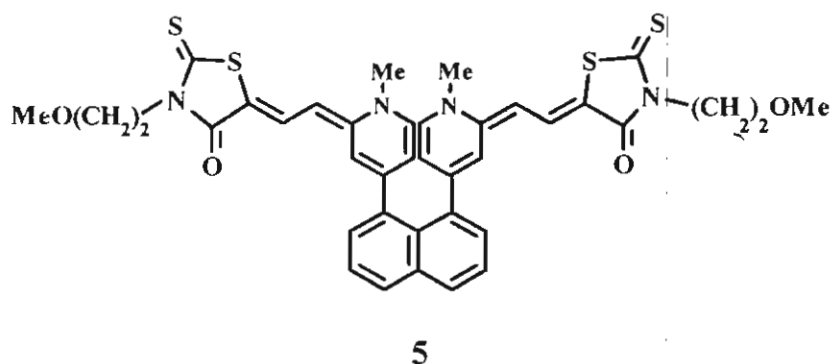


Chart 3.7. Biscyanine (Kato *et al.*²⁹)

More recently, Whitten and coworkers have investigated the aggregation properties of bichromophores based on squaraines³⁰ (**6** in Chart 3.8a) and merocyanines³¹ (**7-10** in Chart 3.8b) tethered by methylene chain.

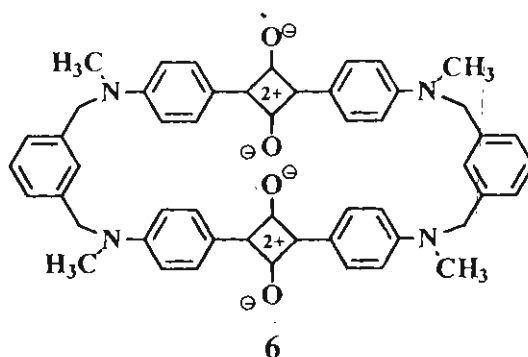


Chart 3.8a. Squaraine bichromophores (Whitten and coworkers³⁰)

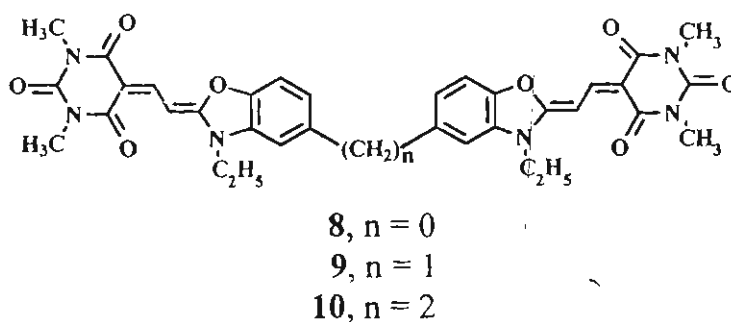
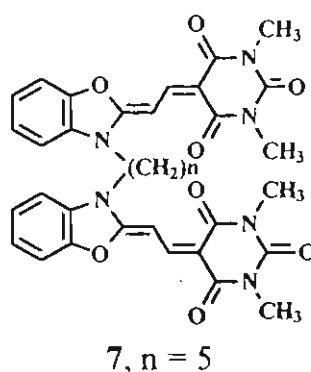


Chart 3.8b. Merocyanine bichromophores (Whitten and coworkers³¹)

For both these systems, an extended conformation is preferred in nonpolar solvents and a folded one in polar solvents leading to J- and H-aggregates, respectively. In contrast to the squaraine dimers, which do not fluoresce, excimer type fluorescence was observed from the folded form of merocyanine dimers. The studies on bichromophores reported so far, deal mainly with the chromophoric

interactions and it is possible to design optoelectronic devices by modulating their optical properties. This Chapter mainly focuses on the design of bistable molecular systems based on bichromophores, taking advantage of the chromophoric interaction and exciton coupling. In Chapter 2, we have investigated the detailed photophysical and excited state properties of a few of the hemicyanine based chromophores listed in Chart 3.9.

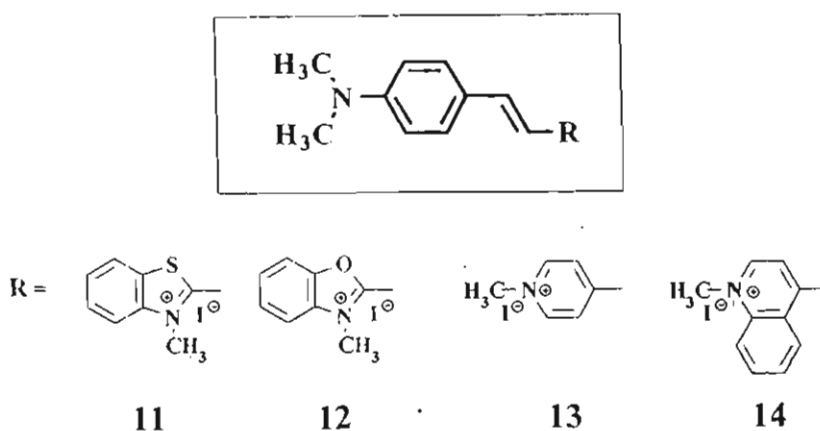


Chart 3.9

Here, we have designed a few novel bichromophores possessing the above mentioned hemicyanine units, linked together by polyethylene glycol chain (**15-19**, Chart 3.10). The detailed photophysical properties of two of these bichromophoric systems (**15** and **16**), having benzothiazolium acceptor groups, were investigated by varying the solvent polarity or by the application of an external stimulus such as heat or light. The conformational changes of the polyoxoethylene chain in nonpolar solvents bring about the folding of the bichromophore, leading to the formation of intramolecular homoaggregates.

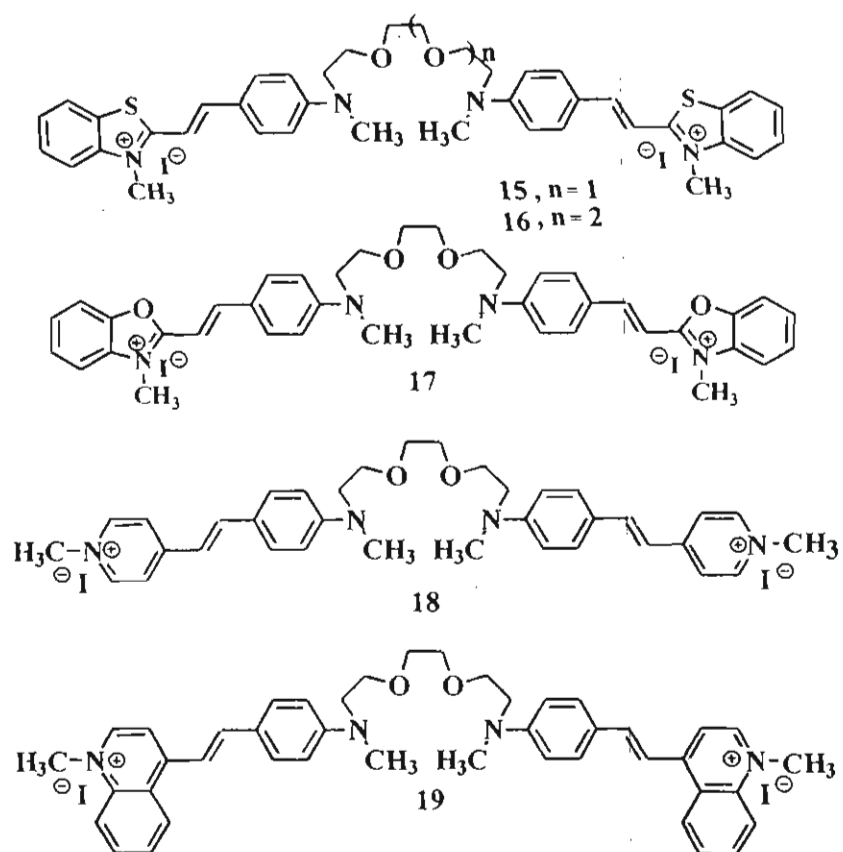


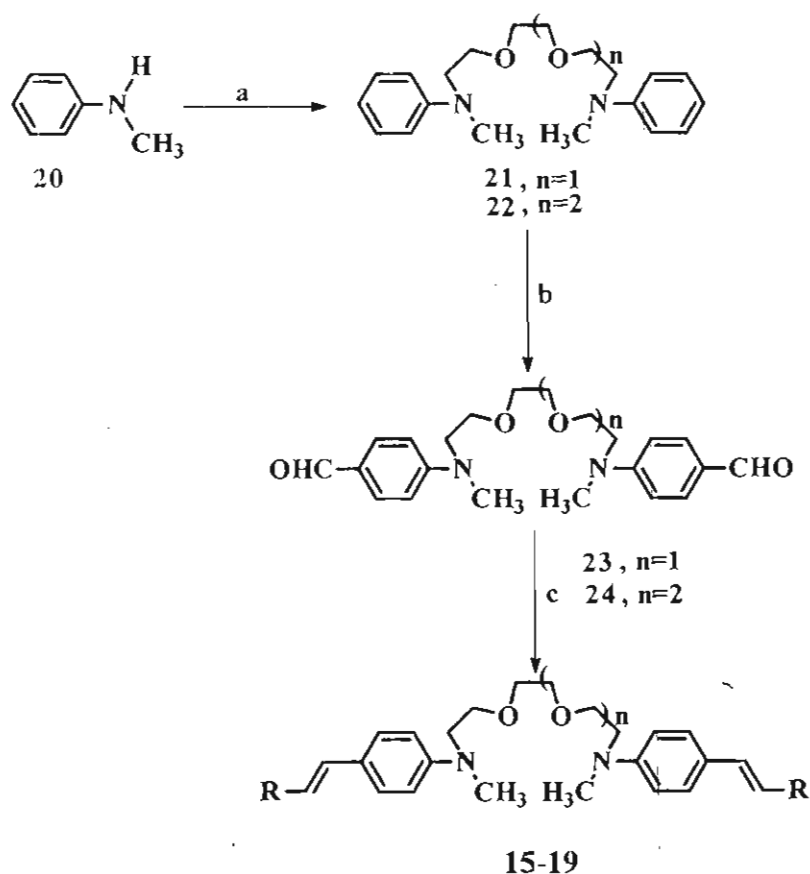
Chart 3.10

3.3. Results and Discussion

3.3.1. Synthesis and characterization of bichromophores

Syntheses of the hemicyanine based bichromophores, **15-19** (Chart 3.10), were achieved through the sequence of reactions shown in Scheme 3.2. N-methylaniline tethered glycols (**21**, **22**) were prepared through reported procedures,³² which were further subjected to Vilsmeier formylation to obtain the bisaldehydes (**23**, **24**). These bisaldehydes were the key intermediates in the syntheses of the bichromophores, **15-19** and were achieved by the condensation of the corresponding aldehydes with the appropriate quaternary salt of the

chromophore.³³ The crude product, in each case, was purified by chromatography over alumina to give the appropriate bichromophores in 40-50 % yield. All new compounds were fully characterized on the basis of analytical results and spectral data. Detailed experimental procedures for the synthesis, purification and characterization of the bichromophores and the precursors are given in Section 3.5.



Scheme 3.2. Synthesis of bichromophores a) $\text{ClCH}_2\text{-}[\text{CH}_2\text{O-CH}_2]_n\text{-CH}_2\text{Cl}$ ($n = 1, 2$), K_2CO_3 , KI, *n*-butanol; b) DMF, POCl_3 ; c) quaternary salt of the corresponding heteroaromatic compound, piperidine, dry methanol; in step (c) the salts used for **15** and **16**, 2-methylbenzothiazolium methiodide; **17**, 2-methylbenzoxazolium methiodide; **18**, 4-methyl picolinium methiodide; **19**, 4-methylquinolinium methiodide.

3.3.2. Steady State Absorption

Hemicyanine based bichromophoric systems (**15 -19**) absorb in the 450-600 nm spectral region. The structureless absorption bands observed in these bichromophores were attributed to a donor-acceptor charge-transfer (CT) transition. We have confirmed this by investigating the effect of perchloric acid on the absorption spectra of model compounds and these results are summarized in Chapter 2. Recent X-ray diffraction studies³⁴ as well as absorption spectral studies³⁵ have also suggested the involvement of an intramolecular charge transfer resonance between the nitrogen atoms in hemicyanine dyes.

The absorption spectra of the bichromophores (**15** and **16**) were compared with a corresponding model compound (**11** in Chart 3.9) and their spectral properties are summarized in Table 3.1. Comparative plots of the absorption spectra of the bichromophore **15** ($\lambda_{\text{max}} = 540$ nm) and model compound **11** ($\lambda_{\text{max}} = 553$ nm) in dichloromethane are shown in Figure 3.1. Both the bichromophores exhibit a broad band centered around 540 nm in CH_2Cl_2 . The absorbance of this band follows Beer-Lambert law and the spectral shape remains unaffected with concentration, ruling out the possibility of a strong intra- or intermolecular interactions. Thus, the broad band, absorbing around 540 nm may correspond to monomeric form of the bichromophores. Similar results were obtained for model compound **11** and bichromophores, in polar solvents such as CHCl_3 , CH_3CN ,

CH₃OH etc. The origin of this structureless absorption band is attributed to a donor-acceptor charge-transfer (CT) transition. The half width of the absorption

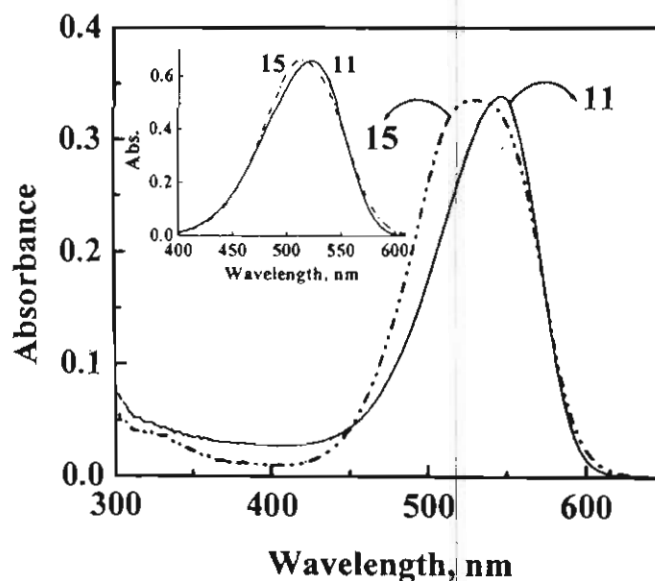


Figure 3.1. Normalized absorption spectrum of the bichromophore **15** and model compound **11** in CH₂Cl₂: (a) **15**, (b) **11**. Inset shows the absorption spectra of **15** and **11** in CH₃OH.

band ($\nu_{1/2}$) of **11** in CH₂Cl₂ is 2283 cm⁻¹ and a spectral broadening was observed with increase in polarity of the solvent. There are several bonds in hemicyanines, which may undergo torsional motions. It is suggested that the torsional motions, coupled with solvent reorganization may lead to spectral broadening of hemicyanines, in polar solvents. Compared to **11**, both the bichromophores **15** and **16** exhibit a broad absorption band and $\nu_{1/2}$ is not influenced by solvent polarity ($\nu_{1/2} \sim 3000$ cm⁻¹). The chromophoric units in **15** and **16** are linked together by a flexible poly(oxoethylene) chain. Depending on the nature of the solvent, the poly(oxoethylene) bridging unit can adopt various conformations, which may

result in weak through-space interactions between the two hemicyanine units, in **15** and **16**. These factors along with the torsional motions of the hemicyanines, may lead to the broadening of the absorption spectrum. For detailed photophysical investigations, we have selected the benzothiazolium based bichromophoric systems **15** and **16** and the results are compared with the model compound **11** (Chart 3.11).

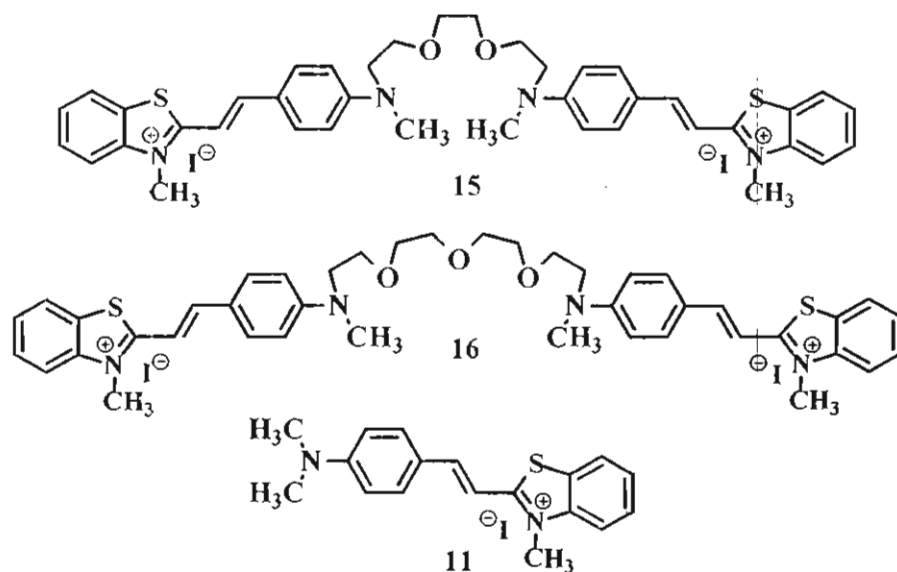


Chart 3.11

Addition of varying amounts of toluene to a solution of **15** and **16** in CH_2Cl_2 led to a gradual hypsochromic shift in its absorption band (Figures 3.2 and 3.3, respectively). Interestingly, on increasing the toluene content ($> 70\%$ (v/v) toluene/ CH_2Cl_2 at 25°C), a decrease in the intensity of the monomer band was observed, accompanied by the formation of a sharp band at 420 nm. The effect of temperature on the absorption spectrum of **15** was investigated in a mixture of 80% toluene/ CH_2Cl_2 (Figure 3.4).

Table 3.1. Absorption and emission properties of bichromophores and model compounds in dichloromethane

Compound	Absorption		Fluorescence	
	λ_{\max} (abs) (ϵ , $M^{-1}cm^{-1}$)	$\Delta\nu_{1/2}$ (cm^{-1})	λ_{\max} (em.)	Φ_f^a
15	540 (104940)	2979	600	0.01
16	540 (107000)	2979	600	0.0098
11	553 (89563)	2283	597	0.018
17	519 (85021)	2860	558	0.012
12	524 (86141)	2143	559	0.028
18	519 (62600)	3271	614	0.095
13	513 (46606)	2826	614	0.122
19	551 (22631)	3555	682	0.007
14	572 (28350)	2620	682	0.013

a) error limit $\pm 5\%$.

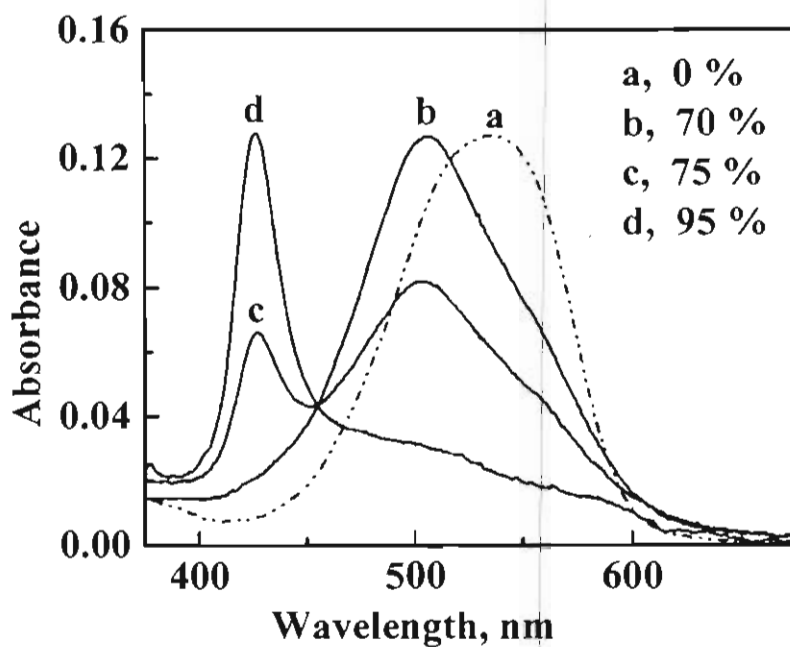


Figure 3.2. Visible absorption spectra of 15 in different compositions of toluene/ CH_2Cl_2 at 25 °C.

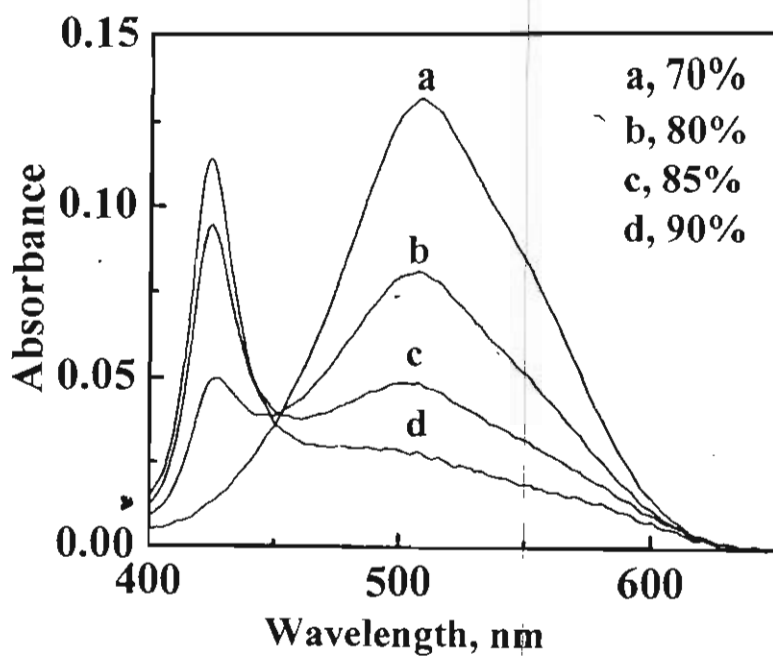
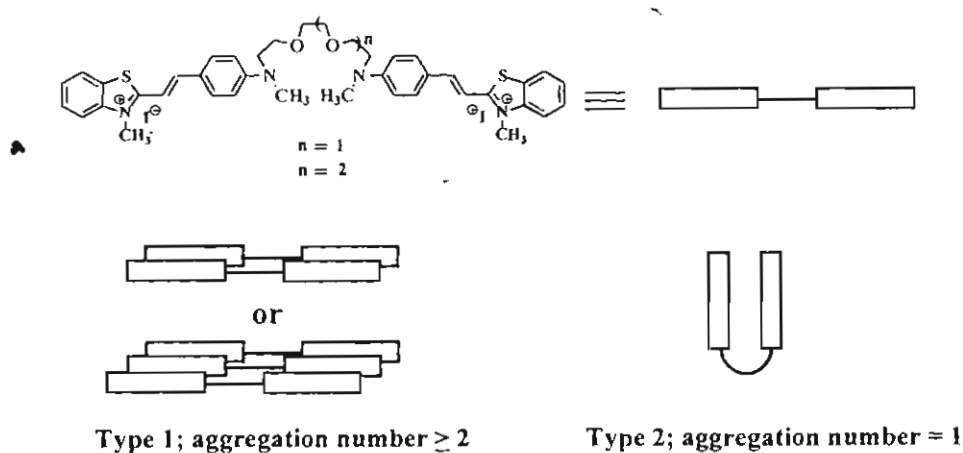


Figure 3.3. Visible absorption spectra of 16 in different compositions of toluene/ CH_2Cl_2 at 25 °C.

The intensity of the 420 nm band is markedly higher at lower temperatures. A complete reversal to the monomeric form was observed with increase in temperature, indicating that an equilibrium process is involved. Similar results were observed for the bichromophore **16** (Figure 3.5).

Cyanines and squaraines derived from benzothiazolium units are known to form face to face or parallel dimers (H-aggregates), characterized by the appearance of a blue-shifted absorption band.^{36,37} The new high-energy band, observed at 420 nm is due an H-aggregate, arising from the parallel stacking of the hemicyanine chromophores. In the present case, parallel stacking of the chromophores is possible in two different ways: (i) through an intermolecular interaction between two or more bichromophores (aggregation number ≥ 2) in a card pack arrangement or (ii) through an intramolecular interaction between two hemicyanine units of the bichromophore, as a result of the folding of the molecule (aggregation number one). Both these possibilities are illustrated in Scheme 3.3.



Scheme 3.3: Pictorial representation of the aggregation of bichromophore (Type 1-card pack arrangement; Type 2- intramolecular folding).

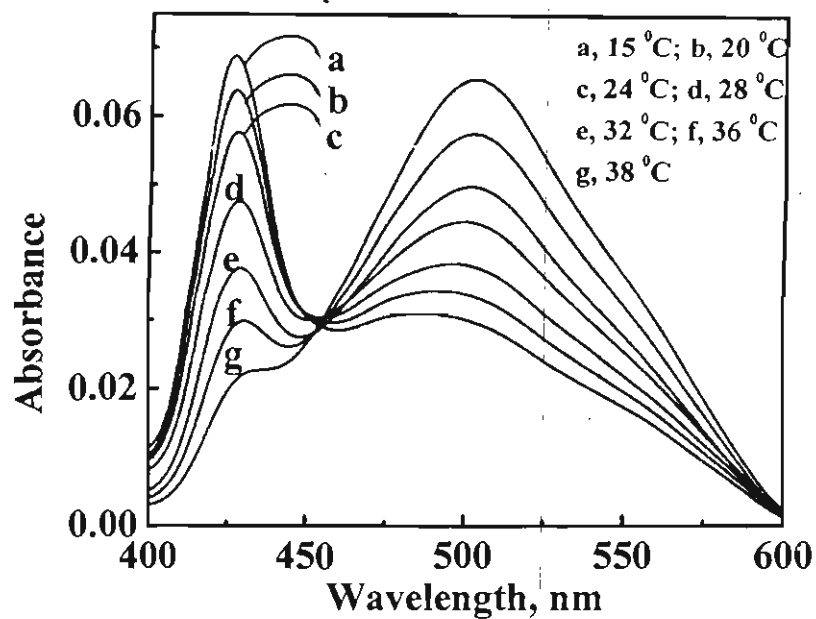


Figure 3.4. Visible absorption spectra of 15 at various temperatures in 80 % (v/v) toluene/CH₂Cl₂.

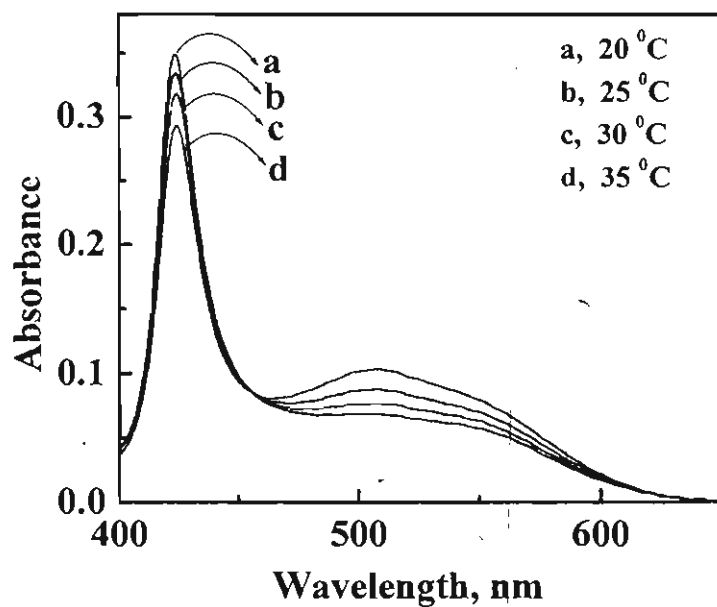


Figure 3.5. Visible absorption spectra of 16 at various temperatures in 80 % (v/v) toluene/CH₂Cl₂.

In order to understand the nature of stacking, aggregation properties of the bichromophores were investigated in detail. The aggregation numbers of **15** (Figure 3.6) and **16** (Figure 3.7) were determined by studying the effect of concentration of bichromophore on the absorption spectra. The absorption bands of the monomer and aggregate were well separated and the spectral overlap at their absorption maxima were negligible (Figure 3.2-3.7). The extinction coefficient of the monomer of both the bichromophore were estimated (for **15**, ϵ (500 nm) = 74300 M⁻¹cm⁻¹ and **16**, ϵ (500 nm) = 58300 M⁻¹cm⁻¹) at their peak maxima in 70 % toluene/ dichloromethane at 25 °C (aggregation was not observed when the toluene content was below 70 %, refer Figures 3.2 and 3.3). The concentration of the monomer ([M] = absorbance of M/ ϵ of M) and aggregate ([A] = total concentration - [M]) were estimated and they followed a linear dependence ([M] \propto [A]) for both the bichromophores. The equilibrium constants (K) for the bichromophores were estimated from the concentrations of the monomer and aggregate (equation 3.3) and the plots of the

$$K = [A]/[M] \quad (3.3)$$

log [M] versus log [A] were found to be linear. The aggregation number was estimated as one, in both the cases, indicating the formation of homoaggregates of Type II (Scheme 3.3). The equilibrium constants (K (24 °C)) for the formation of homoaggregates of **15** and **16**, through the folding of bichromophore, were estimated as 2.2 and 5.2, respectively. Based on these results it is concluded that

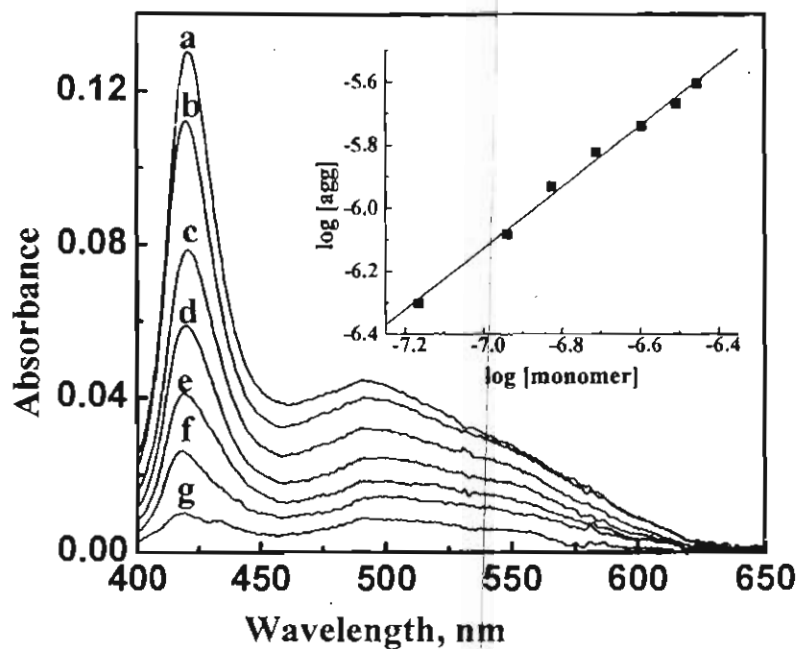


Figure 3.6. Visible absorption spectra of 15 at different concentrations (0.56-2.84 μM) in 85 % (v/v) toluene/ CH_2Cl_2 at 25 $^\circ\text{C}$.

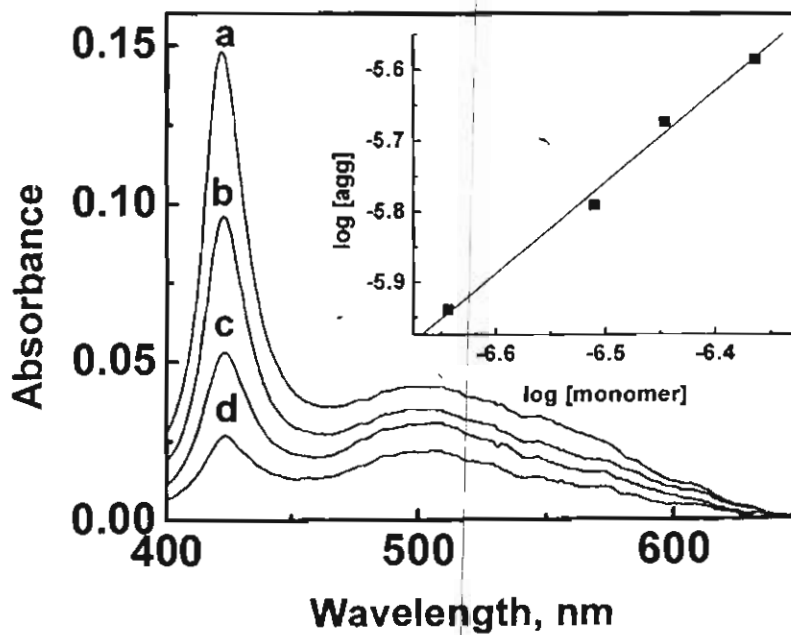
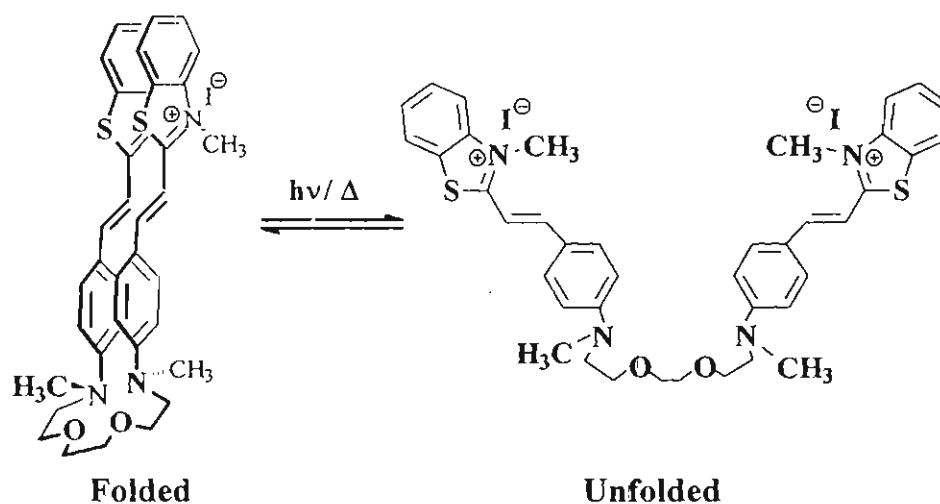


Figure 3.7. Visible absorption spectra of 16 at different concentrations (1.38-3.03 μM) in 85 % (v/v) toluene/ CH_2Cl_2 at 25 $^\circ\text{C}$.

both the bichromophores exist in equilibrium conformations, folded and unfolded (a pictorial presentation is shown in Scheme 3.4), depending on the polarity and temperature.

The sharp band with absorption at 420 nm corresponds to a well-defined folded conformation. The long wavelength band, observed in the 450-600 nm



Scheme 3.4. An illustration of the folding-unfolding process of bichromophores, based on the photophysical studies.

region corresponds to a unfolded geometry. In the unfolded geometry bichromophoric systems can exist in several conformations, which are more disordered since they are linked together by a flexible poly(oxoethylene) chain. Poly(oxoethylene) linkers exhibit solvent dependent conformational changes and have been studied by theoretical as well as experimental investigations.³⁸ It is reported that the carbon-carbon bond of $-OCH_2CH_2O-$ unit exists predominantly in the *gauche*- conformation in a highly polar medium, but shifts to the *trans*-

conformation in a low polar medium.³⁸ In **15** and **16**, the unfolded conformation may be more stable in polar solvents due to the presence of *gauche* configuration. The polarity dependent conformational changes of the bridging unit and solvophobicity of the dye in nonpolar medium, enables the folding of **15** and **16**, overcoming the coulombic repulsion between the chromophores. Solvophobicity driven folding processes were recently reported in merocyanine dimers³¹ (Chart 3.8b) and substituted phenylacetylene oligomers¹² (Chart 3.2). In the present case, the molecular systems **15** and **16** prefer a well ordered folded conformation in nonpolar medium with parallel stacking of the chromophores (Schemes 3.3 and 3.4), since such an arrangement can minimize the polar chromophoric surface exposed to the nonpolar solvent.

One of the interesting features of **15** and **16** is their ability to undergo temperature dependent conformational changes. The folding-unfolding processes were completely reversible and highly sensitive to the temperature of the medium (for e.g., Figure 3.4). In the present case, the interconversions between the two forms of the bichromophores are possible in a small temperature range. The equilibrium constants for the formation of intramolecular aggregates of bichromophores ($K_{(24)^0\text{C}}$ of **15** and **16** are 2.2 and 5.2, respectively) are orders of magnitude lower than the intermolecular dimerization constants for merocyanines.²³ In the case of hemicyanine based bichromophores, the main driving force for aggregation is the solvophobicity, whereas the latter ones are driven by electrostatic dipole-dipole interaction. The equilibrium constants for the

formation of the intramolecular aggregates of **15** and **16** were obtained at different temperatures. The free energy for the formation ($-\Delta G_{(24^{\circ}\text{C})}^{\circ}$) of the homoaggregates of **15** and **16** were estimated as 2.0 and 3.7 kJ mol⁻¹, respectively using the equation 3.4. These low energies suggest that the folded forms are not energetically

$$\Delta G = -2.303 RT \log K \quad (3.4)$$

favoured. Indeed, the low equilibrium constant and free energy of formation of intramolecular aggregates are advantageous in the present case, since they permit the interconversion in a smaller temperature range (15-35 °C). In summary, both the bichromophores undergo folding from an extended conformation to a well ordered, parallel stacked conformation, on decreasing the polarity as well as temperature of the medium.

3.3.3. Steady State Emission Properties

Recent investigations^{39,40} on the excited state properties of hemicyanine dyes suggest that (i) the singlet excited state of the chromophore deactivate mainly through bond twisting (rotamerism)³⁹ and rigidization by structural modifications^{40a} prevent nonradiative deactivation; (ii) the substitution of dialkylamino- group in hemicyanines markedly reduces the *trans-cis* isomerization.^{40b} Viscosity and polarity dependent studies of **11** indicate that the singlet excited state of the chromophore deactivates through competing radiative and nonradiative channels. The rigidization of **11** in viscous medium, prevents the

excited state bond twisting, leading to a dramatic enhancement of fluorescence quantum yield (Φ_f) and lifetime (τ_s) and these results are summarized in Chapter 2.

In this Chapter, the conformational switching of **15** as well as **16** were studied by steady state and time resolved fluorescence techniques. The unfolded form of both the bichromophores in CH_2Cl_2 emits around 600 nm (Table 3.1), with almost identical quantum yields ($\Phi_f \sim 0.01$). A substantial lowering of the emission yield was observed for both the bichromophores on increasing the toluene content. The relative emission intensities of **15** (excited at the isosbestic point), in mixtures of dichloromethane and toluene are shown in Figure 3.8. Lowering of the emission yield is attributed to the formation of intramolecular aggregates, resulting from the folding of the bichromophores. The folded form of the bichromophores (in 95 % toluene/ CH_2Cl_2) was further selectively excited at 420 nm, where the unfolded form does not absorb. Emission spectra having almost similar spectral shapes as those of the unfolded forms, with extremely low yields ($\Phi_f < 10^{-4}$) were observed in the case of the folded forms of **15** and **16**. A representative example is shown in the inset of Figure 3.8. It has been reported that intermolecular aggregates of cyanine dyes possess lower fluorescence yields and longer singlet lifetimes, than those of their corresponding monomers.^{36a} Based on the exciton theory, the transition to the upper energy level is allowed for the H-aggregates, which rapidly deactivate to the lower energy level *via* internal

conversion. The emission from the lower energy level is theoretically forbidden¹⁹ and hence the singlet excited state

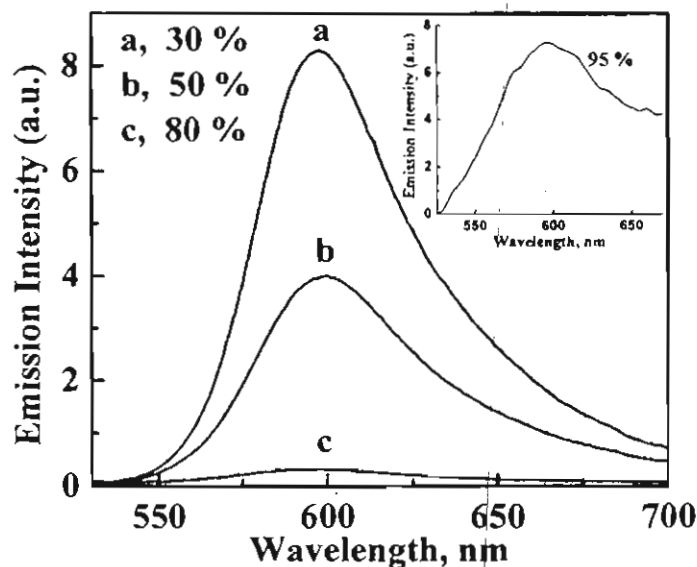
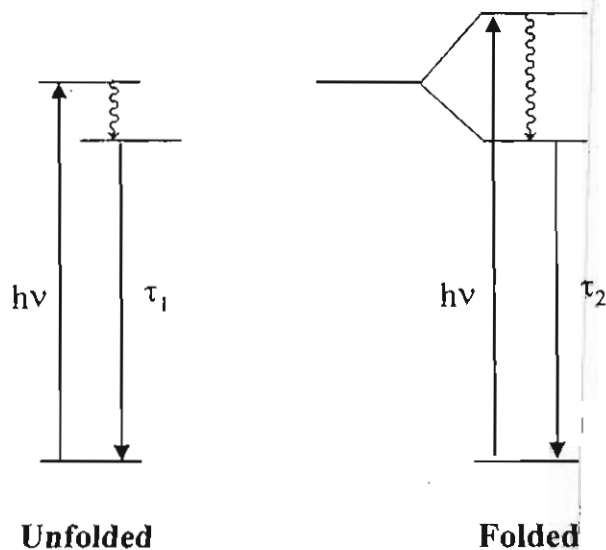


Figure 3.8. Emission spectra of **15** in different compositions of toluene/ CH_2Cl_2 at 25 °C (excitation wavelength, 450 nm). Inset shows the emission spectrum of the folded form of **15** in 95 % toluene/ CH_2Cl_2 mixture (excitation wavelength, 420 nm).

of the bichromophoric aggregates get trapped in a low emissive state. Based on the absorption and emission maxima of the folded as well as unfolded forms, an energy diagram of the Davydov splitting in the bichromophores is proposed in Scheme 3.5.

The effect of addition of toluene on the quantum yield of fluorescence of **11** in CH_2Cl_2 was studied. A slight increase in ϕ_f was observed for **11**, on increasing the proportions of toluene and is attributed to the decrease in polarity of the medium. The lack of strong ϕ_f dependency of **11**, in mixtures of toluene- CH_2Cl_2 , further supports the formation of intramolecular H-aggregates of the bichromophores. The origin of the emission of the folded and unfolded forms was confirmed by recording the

excitation spectra of the bichromophores as a function of solvent composition (Figure 3.9). The excitation spectrum of **15**, recorded in 50 % (v/v) toluene/ CH_2Cl_2 at 25 $^\circ\text{C}$,



Scheme 3.5. Schematic representation of the energy levels of the unfolded and the folded forms of **15**.

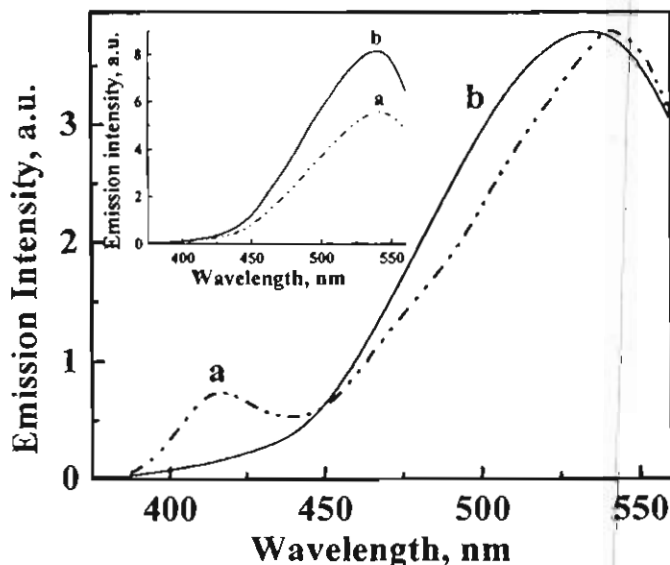


Figure 3.9. Excitation spectra of **15** in toluene/ CH_2Cl_2 mixtures ; (a) 85 %, (b) 50 %. Inset shows the excitation spectra of **11** in same solvent mixtures (emission monitored at 580 nm for **15** and **11**).

possesses a broad band around 540 nm, which closely matches the absorption characteristics of the unfolded bichromophore (Figure 3.2). In 85 % (v/v) toluene/CH₂Cl₂, the excitation spectrum of **15** (trace a) exhibits a band at 420 nm, apart from the long wavelength band and matches with the corresponding absorption spectrum in spectral shape (Figures 3.2 and 3.4). The intensity of the long wavelength band is higher in the excitation spectrum due to the higher emission yield of the monomer, compared to the aggregated form. These results further confirm that the emission of the folded form originates from the 420 nm band and the unfolded form, from the 540 nm band. The excitation spectrum of **11**, in both the solvent mixtures, is shown in the inset of Figure 3.9 for comparison and the 420 nm band is absent.

3.3.4. Fluorescence Lifetimes

Characterization of the singlet excited state properties of the folded form as well as the unfolded forms of **15** and **16** was achieved by investigating the singlet lifetimes as a function of solvent composition and temperature. Samples were excited at 440 nm and the fluorescence lifetime measurements were followed at 600 nm. Both the bichromophores exhibited monoexponential decay with a short lifetime (~ 350 ps) in 0-50 % (v/v) toluene/CH₂Cl₂ mixtures at 20 °C. Interestingly, both the bichromophores exhibited biexponential decay in 70-95 % (v/v) toluene/CH₂Cl₂ mixtures at 20 °C, with a short-lived (τ_1) and long-lived (τ_2) component. Representative fluorescence decay profiles of **15** and **16** in 30 % and 95 % (v/v)

toluene/ CH_2Cl_2 at 20°C are illustrated in Figures 3.10 and 3.11. The fluorescence lifetimes of **16** in various compositions of toluene/ CH_2Cl_2 are presented in Table 3.2. The interconversion between folded and unfolded forms was further investigated by plotting their fractional contribution of lifetimes, as a function of solvent polarity (Figure 3.12) and temperature. The population of the long-lived species increased substantially for both the bichromophores on (i) increasing the toluene content (Figure 3.10) and (ii) decreasing the temperature of the medium (Table 3.3). A complete reversal in the fractional contribution of lifetimes was observed on increasing the temperature of the medium.

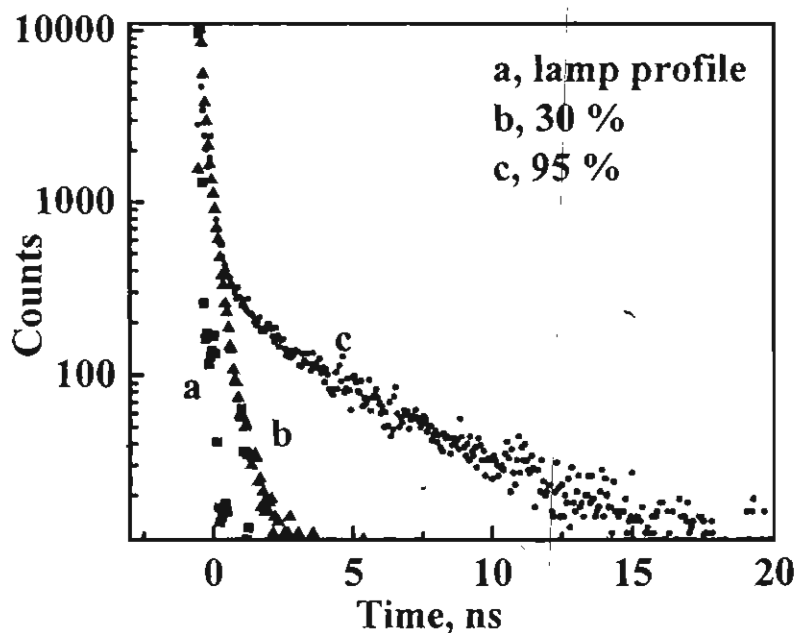


Figure 3.10. Fluorescence decay profiles of **15** in toluene/ CH_2Cl_2 mixtures at 20°C . A third component (with a longer lifetime) is not analyzed since its relative distribution is only around 1.5 %.

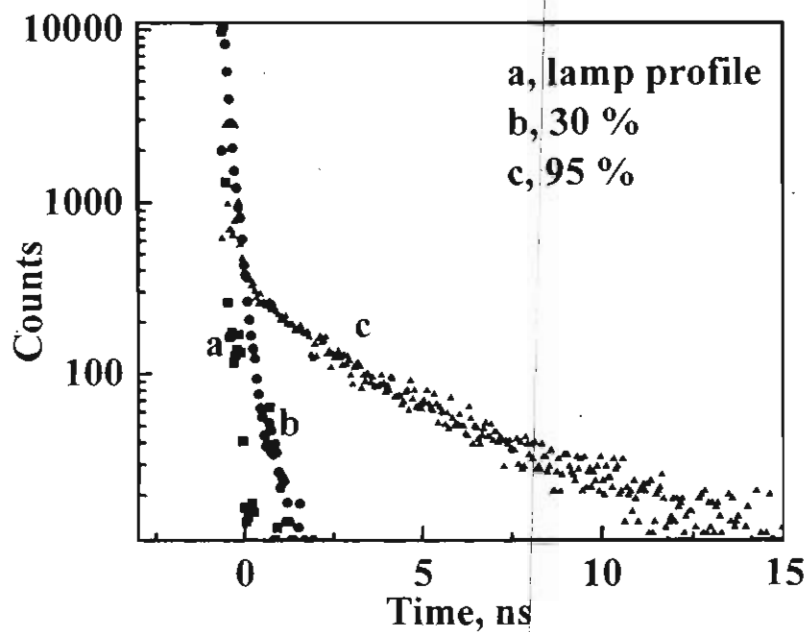


Figure 3.11. Fluorescence decay profiles of 16 in toluene/ CH_2Cl_2 mixtures at 20 °C. A third component (with a longer lifetime) is not analyzed since its relative distribution is only around 1.5 %.

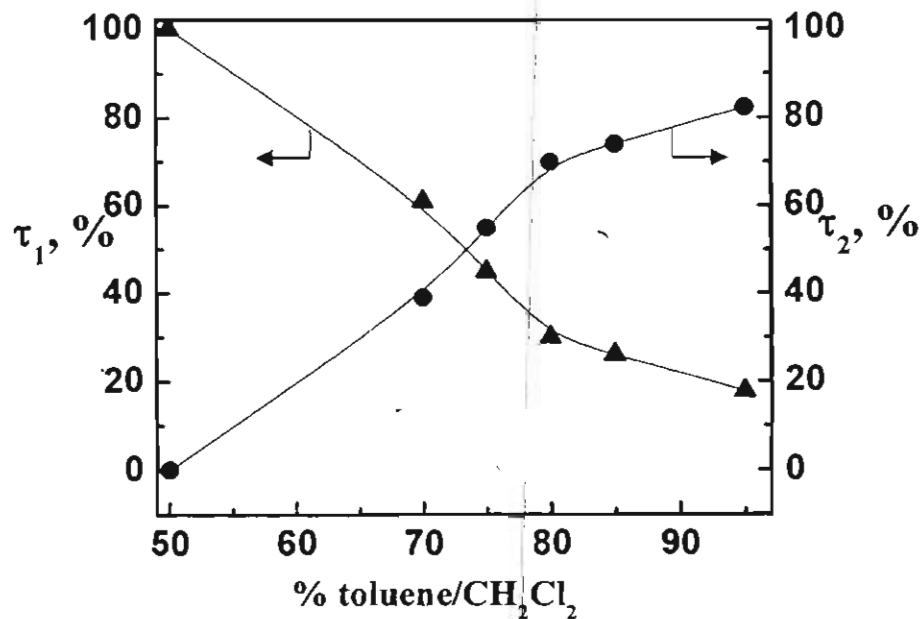


Figure 3.12. Relative distribution of folded and unfolded forms of 15 in mixtures of toluene/ CH_2Cl_2 at 20 °C.

Table 3.2. Fluorescence lifetimes^{a-c} and fractional contributions^{d,e} of 16 in toluene/CH₂Cl₂ mixtures at 20 °C

% toluene/ CH ₂ Cl ₂	τ_1 ($\chi_1\%$)	τ_2 ($\chi_2\%$)	χ^2
50	0.37 (100)		1.13
75	0.33 (56)	3.08 (44)	1.16
85	0.33 (35)	3.76 (65)	1.29
95	0.76 (21)	4.2 (79)	1.10

a) τ_1 and τ_2 ; b) error limit $\pm 5\%$; c) excited at 440 nm and emission followed at 600 nm; d) χ_1 and χ_2 ; e) fractional contributions of 15 is presented as Figure 3.12.

Table 3.3. Fluorescence lifetimes^{a-c} and fractional contributions^d of 15^e as a function of temperature

Temp. (°C)	τ_1 ($\chi_1\%$)	τ_2 ($\chi_2\%$)	χ^2
17.5	0.51 (25)	4.23 (75)	1.14
21	0.41 (38)	3.69 (62)	0.879
25	0.42 (49)	3.72 (51)	1.14
27	0.33 (51)	3.15 (49)	0.98
33	0.27 (72)	3.06 (28)	1.17

a) τ_1 and τ_2 ; b) error limit $\pm 5\%$; c) excited at 440 nm and emission followed at 600 nm; d) χ_1 and χ_2 ; e) 75 % (v/v) toluene/CH₂Cl₂.

3.3.5. Laser Flash Photolysis Studies

We have further demonstrated the laser-induced processes in the folded and unfolded forms of bichromophores using laser flash photolysis experiments. The folded form was excited using an excimer pumped dye laser (420 nm) and the unfolded form using ND-YAG laser (532 nm).

In polar solvents, such as methanol, both the bichromophores exist in the unfolded form and no transient was observed in the nanosecond time scale. Interestingly, an intense transient absorption was observed for **15** in 50% (v/v) toluene/CH₂Cl₂ (Figure 3.13). The transient decay at 420 nm (inset of Figure 3.13) consist of a major short lived ($k_1 = 1.07 \times 10^4 \text{ s}^{-1}$) and a minor long-lived component ($k_2 = 6.32 \times 10^3 \text{ s}^{-1}$). The major component is quenched by O₂, ferrocene and β -carotene.⁴¹ Based on these results and the similarity of spectral behaviour to those reported for other hemicyanines,^{40d} the major transient species is assigned as triplet. In less polar solvents, the bichromophores may exist as a contact ion pair and the heavy atom induced intersystem crossing leads to the formation of the triplet. A transient species with similar properties observed on addition of I⁻ to a methanolic solution of the bichromophore, further confirmed the heavy atom induced triplet formation. The yield of the minor component (k_2) is less than 10 % and hence no attempt was made to establish its identity.

Laser pulse excitation of the folded form of bichromophores results in their unfolding. Figure 3.14 shows the transient spectrum of the folded form of the

bichromophore **15** (90% (v/v) toluene/dichloromethane), observed immediately after the laser pulse excitation. The unfolding process is prompt and we could not observe it in the nanosecond time scale. The transient formed was not quenched by O_2 . The negative absorbance observed in the spectral region of 375-450 nm is due to the laser-induced depletion of the ground state of the folded form. The band observed at 450-600 nm corresponds to the ground state absorption of the unfolded form and it does not decay up to 100 μs (100 μs is the highest detection

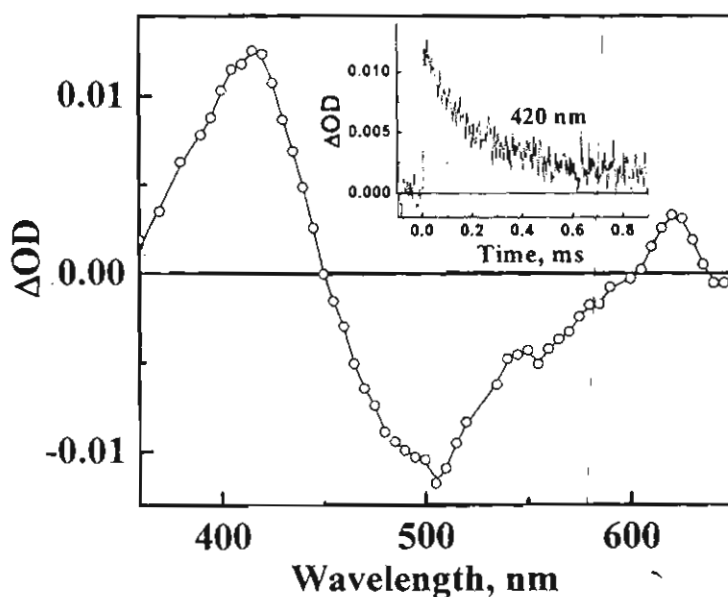


Figure 3.13. Transient absorption spectrum measured following laser pulse excitation (532 nm, ~ 120 mJ/pulse) of the unfolded form of **15**. Inset shows the transient decay at 420 nm.

limit of our equipment). The ground state absorption spectra recorded before and after the laser flash photolysis remained unchanged, indicating that the refolding process is completely reversible and occurs in the time

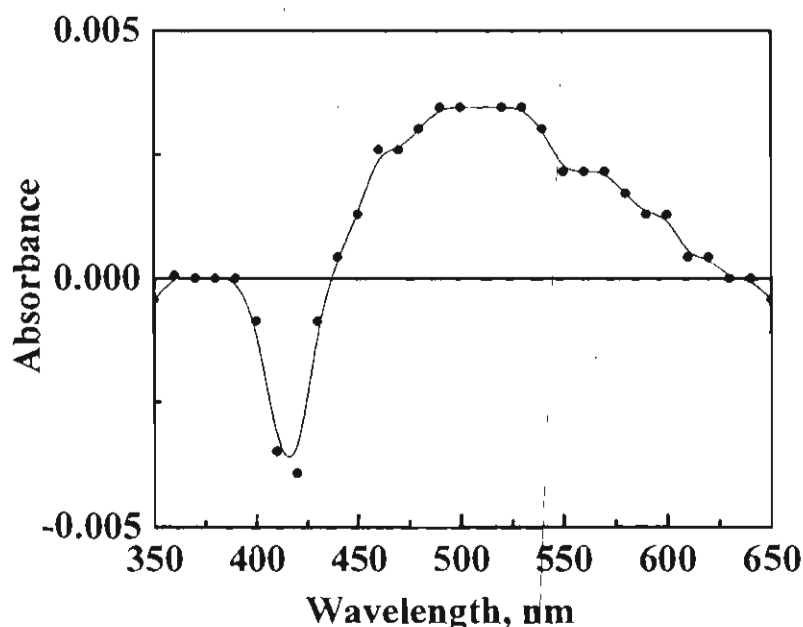


Figure 3.14. Transient absorption spectrum measured following laser pulse excitation (420 nm, ~ 10 mJ/pulse) of the folded form of **15**.

scale longer than $100 \mu\text{s}$. Intermolecular aggregates of cyanines were reported to disrupt under laser excitation through photoinduced thermal dissociation,^{36b} whereas in the case of squaraine a photodissociation mechanism^{36c} has been suggested. Results presented in Section 3.3.2 have proved that the interconversion between the two forms is possible in a small temperature range and the low equilibrium constant and free energy of formation of intramolecular aggregates indicate that the folded form is not thermodynamically stable. In the present case, the laser excitation of the folded forms of **15** as well as **16** may cause a local temperature jump, leading to the folding of bichromophores.

3.4. Conclusions

The newly designed hemicyanine based bichromophores **15** and **16** possess a unique property of folding-unfolding and their interconversion was achieved by varying the polarity of the medium or temperature. Both the bichromophores prefer a well-defined folded conformation in nonpolar medium and the solvent dependent conformational changes of the poly(oxoethylene) linker group as well as the solvophobicity of the chromophores in nonpolar solvents drive the folding process, overcoming the coulombic repulsion. The laser flash excitation of the folded forms result in fast conformational changes due to photoinduced thermal dissociation. The conformational switching in such bichromophores could lead to the design of novel type of molecular switching devices. Also, similar strategies of chromophoric interactions can be employed for probing conformational changes in macromolecular systems.

3.5. Experimental Section

General method for the preparation of N-methylaniline tethered glycols (21 and 22)

A mixture of N-methylaniline (100 mmol), potassium carbonate (100 mmol), potassium iodide (500 mg) and the appropriate polyethylene glycol dichloride (50 mmol) was refluxed in *n*-butanol (30 mL) for 90 h. On cooling, the solvent was removed under reduced pressure and the crude product was chromatographed over silica gel (100-200 mesh).

Compound 21. Elution of the column using a mixture (1:5) of ethyl acetate and hexane gave 70 % of **21** as a viscous liquid. IR (neat) ν_{\max} 2891, 1604, 1501, 1352, 906 cm^{-1} ; ^1H NMR (CDCl_3) δ 7.22-7.14 (m, 4H), 6.70–6.56 (m, 6H), 3.62–3.49 (m, 12H), 3.0 (s, 6H); ^{13}C NMR (CDCl_3) δ 149.19, 129.16, 116.23, 112.38, 112.10, 70.72, 68.61, 52.33, 38.88; exact mass calcd. for $\text{C}_{20}\text{H}_{28}\text{N}_2\text{O}_2$ [MH^+] 329.2229, found 329.2232 (FAB, high resolution mass spectroscopy).

Compound 22. Elution of the column using a mixture (1:9) of ethyl acetate and hexane gave 67 % of **22** as a viscous liquid. IR (neat) ν_{\max} 2890, 1602, 1495, 1350, 906 cm^{-1} ; ^1H NMR (CDCl_3) δ 7.14-7.09 (m, 4H), 6.63–6.57 (m, 6H), 3.54–3.40 (m, 16H), 2.86 (s, 6H); ^{13}C NMR (CDCl_3) δ 149.08, 129.06, 116.19, 112.34, 112.06, 70.60, 68.45, 52.28, 38.8; exact mass calcd. for $\text{C}_{22}\text{H}_{32}\text{N}_2\text{O}_3$ [MH^+] 373.2491, found 373.2506 (FAB, high resolution mass spectroscopy).

General method for the preparation of N-methyl (*p*-formyl)aniline tethered glycols (23 and 24)

To an ice-cold solution of N, N-dimethylformamide (30 mmol), phosphorous oxychloride (20 mmol) was added dropwise over a period of 30 min. To this mixture the appropriate N-methylaniline tethered glycol (10 mmol) was added dropwise over a period of 1 h. The reaction mixture was further heated for 1 h at 80 °C. The pH was adjusted to 7-8 and the organic portion was extracted with dichloromethane. The

solvent was removed under reduced pressure and the crude product was chromatographed over neutral alumina.

Compound 23. Elution of the column using a mixture (1:1) of chloroform and hexane gave 45 % of **23** as a viscous liquid. IR (neat) ν_{\max} 2898, 2738, 1673, 1597, 1560, 1462, 1373, 1241, 1149, 1004, 823, 726, 601, 520 cm^{-1} ; ^1H NMR (CDCl_3) δ 9.71 (s, 2H), 7.69 (d, 4H), 6.69 (d, 4H), 3.63–3.56 (m, 12H), 3.05 (s, 6H); ^{13}C NMR (CDCl_3) δ 190.14, 153.48, 131.96, 125.14, 110.97, 70.78, 68.47, 51.89, 39.08; exact mass calcd. for $\text{C}_{22}\text{H}_{28}\text{N}_2\text{O}_4$ [MH^+] 385.2127, found 385.2142 (FAB, high resolution mass spectroscopy).

Compound 24. Elution of the column using a mixture (1:1) of chloroform and hexane gave 46 % of **24** as a viscous liquid. IR (neat) ν_{\max} 2897, 2743, 1676, 1603, 1538, 1445, 1388, 1244, 1169, 822, 725, 601, 518 cm^{-1} ; ^1H NMR (CDCl_3) δ 9.71 (s, 2H), 7.7 (d, 4H), 6.7 (d, 4H), 3.7–3.4 (m, 16H), 3.0 (s, 6H); ^{13}C NMR (CDCl_3) δ 190.29, 153.72, 132.15, 125.33, 112.55, 70.97, 68.68, 52.09, 39.25; exact mass calcd. for $\text{C}_{24}\text{H}_{32}\text{N}_2\text{O}_5$ [MH^+] 429.2389, found 429.2382 (FAB, high resolution mass spectroscopy).

General method for synthesis of bichromophores (15, 16, 18 and 19)

A mixture of quarternary salt of the heteroaromatic compound (1 mmol) and the appropriate N-methyl (p-formyl)aniline-tethered glycol (0.5 mmol) was refluxed in methanol (50 mL) in presence of piperidine (2 drops) for 72 h under

argon atmosphere. The solvent was removed under reduced pressure and the crude product was chromatographed over neutral alumina.

Bichromophore 15. Elution of the column using a mixture (2:5) of methanol and chloroform gave 43 % of **15** as a solid, mp 217-218 °C (decomp.); IR (KBr) ν_{\max} 1776, 1739, 1668, 1534, 1457, 1392, 1273, 1183, 815, 758 cm^{-1} ; ^1H NMR ($\text{CDCl}_3 + \text{DMSO-d}_6$) δ 8.23 (d, $J = 7.75$ Hz, 2H), 8.03 (d, $J = 8.28$ Hz, 2H), 7.94 (d, $J = 15.2$ Hz, 2H), 7.83 (d, $J = 8.54$ Hz, 4H), 7.71 (t, $J = 7.67$ Hz, 2H), 7.61 (t, $J = 7.52$ Hz, 2H), 7.49 (d, $J = 15.33$ Hz, 2H), 6.79 (d, $J = 8.6$ Hz, 4H), 4.17 (s, 6H), 3.2–3.9 (m, 12H), 3.04 (s, 6H); ^{13}C NMR ($\text{CDCl}_3 + \text{DMSO-d}_6$) δ 153.62, 151.23, 141.44, 133.99, 128.84, 127.15, 126.84, 123.98, 121.85, 114.87, 112.25, 107.55, 105.22, 98.27, 96.09, 71.07, 68.53, 52.13, 29.65; HRMS calcd. for $\text{C}_{40}\text{H}_{44}\text{N}_4\text{O}_2\text{S}_2\text{I}_2$ $[\text{M-I}]^+$ 803.1950, found 803.1964 (FAB high resolution mass spectroscopy).

Bichromophore 16. Elution of the column using a mixture (1:9) of methanol and chloroform gave 45 % of **16** as a solid, mp 143-145 °C (decomp.). IR (KBr) ν_{\max} 1587, 1534, 1519, 1435, 1389, 1343, 1268, 1183, 1116, 1031, 985, 813, 758, 717, 638, 519 cm^{-1} ; ^1H NMR ($\text{CDCl}_3 + \text{DMSO-d}_6$) δ 8.27 (d, $J = 7.83$ Hz, 2H), 8.07 (d, $J = 8.37$ Hz, 2H), 7.96 (d, $J = 15.26$ Hz, 2H), 7.85 (d, $J = 8.54$ Hz, 4H), 7.74 (t, $J = 7.77$ Hz, 2H), 7.64 (t, $J = 7.61$ Hz, 2H), 7.54 (d, $J = 15.32$ Hz, 2H), 6.83 (d, $J = 8.73$ Hz, 4H), 4.20 (s, 6H), 3.2–3.9 (m, 16H), 3.07 (s, 6H); ^{13}C NMR ($\text{CDCl}_3 + \text{DMSO-d}_6$)

d_6) δ 171.65, 153.29, 150.38, 142.33, 133.33, 129.29, 127.85, 127.22, 124.22, 121.93, 116.36, 112.45, 106.55, 104.79, 70.48, 70.39, 68.36, 51.68, 36.08; HRMS calcd. for $C_{42}H_{48}N_4O_3S_2I_2$ $[M-I]^+$ 847.2213, found 847.2186 (FAB high resolution mass spectroscopy).

Bichromophore 18. Elution of the column using a mixture (1:1) of methanol and chloroform gave 50 % of **18** as a solid, mp 168-170 °C (decomp.). IR (KBr) ν_{\max} 1651, 1583, 1548, 1479, 1432, 1388, 1335, 1175, 1136, 1039, 986, 935, 884, 824, 7215, 660, 594, 534, 498 cm^{-1} ; 1H NMR ($CDCl_3+CD_3OD$) δ 8.46 (d, $J = 6.5$ Hz, 4H), 7.73 (d, $J = 6.65$ Hz, 4H), 7.53 (d, $J = 15.87$ Hz, 2H), 7.43 (d, $J = 8.78$ Hz, 4H), 6.72 (d, $J = 18.42$ Hz, 2H), 6.68 (d, $J = 8.95$ Hz, 4H), 4.19 (s, 6H), 3.64–3.55 (m, 12H), 3.04 (s, 6H); ^{13}C NMR ($CDCl_3+CD_3OD$) δ 154.30, 151.73, 143.05, 130.78, 128.77, 122.58, 122.49, 116.29, 112.08, 70.99, 68.65, 52.10, 38.85; HRMS calcd. for $C_{36}H_{44}N_4O_2I_2$ $[M-I]^+$ 691.2509, found 691.2496 (FAB high resolution mass spectroscopy).

Bichromophore 19. Elution of the column using a mixture (1:9) of methanol and chloroform gave **19** as a solid, mp 298-300 °C (decomp.). IR (KBr) ν_{\max} 2356, 1653, 1586, 1540, 1524, 1484, 1438, 1382, 1331, 1235, 1185, 1118, 1068, 828, 754, 658, 618, 560, 519 cm^{-1} ; 1H NMR ($DMSO-d_6$) δ 9.01(d, $J = 6.54$ Hz, 2H), 8.90 (d, $J = 8.68$ Hz, 2H), 8.27-7.86 (m, 14H), 7.78 (d, $J = 8.54$ Hz, 2H), 6.78 (d, $J = 8.84$ Hz, 4H), 4.38 (s, 6H), 3.58–3.51 (m, 12H), 3.03 (s, 6H); ^{13}C NMR ($DMSO-d_6$) δ 153.67,

152.06, 147.24, 145.15, 139.26, 131.98, 129.12, 126.24, 123.54, 119.49, 114.42, 113.50, 112.44, 104.90, 70.64, 68.53, 51.75, 33.91; HRMS calcd. for $C_{44}H_{48}N_4O_2I_2$ $[M-I]^+$ 791.2822, found 791.2866 (FAB high resolution mass spectroscopy).

Synthesis of Bichromophore 17. A mixture of 2-methylbenzoxazolium methiodide (1 mmol) and the bisaldehyde (0.5 mmol) was refluxed in acetic anhydride (5 mL) for 45 min. The solvent was removed under reduced pressure and the resultant solid was recrystallized from a mixture of chloroform and hexane to give 40 % of 17 as a solid, mp 219-220 °C (decomp.). IR (KBr) ν_{max} 1588, 1533, 1456, 1390, 1284, 1184, 1121, 928, 811, 751, 694, 586 cm^{-1} ; 1H NMR ($CDCl_3 + DMSO-d_6$) δ 8.18 (d, $J = 15.23$ Hz, 2H), 7.96–7.93 (m, 6H), 7.87 (d, $J = 8.65$ Hz, 2H), 7.65 (t, $J = 7.3$ Hz, 4H), 7.31 (d, $J = 15.3$ Hz, 2H), 6.86 (d, $J = 8.5$ Hz, 4H), 4.06 (s, 6H), 3.6 – 3.2 (m, 12H), 3.08 (s, 6H); ^{13}C NMR ($CDCl_3 + DMSO-d_6$) δ 153.18, 150.95, 149.70, 146.78, 140.59, 133.05, 128.84, 127.01, 121.02, 113.39, 112.06, 111.82, 96.39, 69.98, 67.95, 67.63, 51.18, 31.70; HRMS calcd. for $C_{40}H_{44}N_4O_4I_2$ $[M-I]^+$ 771.240, found 771.2434 (FAB high resolution mass spectroscopy).

Instrumental Techniques

All melting points are uncorrected and were determined on an Aldrich melting point apparatus. IR spectra were recorded on a Perkin-Elmer Model 882 IR Spectrometer and the UV-Visible spectra on a Shimadzu UV-3101PC UV-VIS-NIR Scanning Spectrophotometer. 1H and ^{13}C NMR spectra were recorded on a

Bruker DPX-300 MHz spectrometer. Emission spectra were recorded on a SPECTRACQ spectrofluorimeter and corrected using the program supplied by the manufacturer. Quantum yield of fluorescence was determined by a relative method using optically dilute solutions of the dyes (OD of 0.1 at the excitation wavelength) using Rhodamine 6G in ethanol ($\Phi_f = 0.9$) as standard. Fluorescence lifetimes were measured using a Tsunami Spectra Physics single photon counting system. Ti Sapphire laser, having a fundamental wavelength of 880 nm, was used as an excitation source. The average output power is 680 mW with a pump power of 4.5W. The pulsewidth of the laser is <2 ps. The flexible harmonic generator (FHG) gives the second harmonic (440 nm) output from the Tsunami laser system. The fluorescence was detected using two-stage microchannel plate photomultiplier (MCP-PMT R38094). The fluorescence decay measurements were further analyzed using the IBH software library, which includes an iterative shift of the fitted function as part of χ^2 goodness of the fit criterion. Laser flash photolysis of the unfolded form was carried out in an Applied Photophysics model LKS-20 Laser Kinetic Spectrometer using the second harmonic (532 nm) of a Quanta Ray GCR-12 series pulsed Nd:YAG laser with a pulse duration of 10 ns and energy of 120 mJ/pulse. Laser flash photolysis experiments of the folded form were carried out using a Lambda Physik Lextra 50 excimer laser pumped scanmate 2-dye laser. The excitation wavelength was 420 nm. All solutions for laser flash photolysis were deaerated by bubbling argon for 15 minutes unless otherwise indicated.

3.6. References

- (1) a) Lehn, J.-M. *Supramolecular Photochemistry: Concepts and Perspectives*, VCH, Weinheim, 1995. b) Balzani, V.; Moggi, L.; Scandola, F. in *Supramolecular Photochemistry*, (Ed.: V. Balzani), Reidel, Holland, 1987, pp 1-28. c) Jortner, J., Ratner, M., *Molecular Electronics*, Blackwell: Oxford, 1997.
- (2) a) Irie, M. *Chem. Rev.* **2000**, *100*, 1685. b) Credi, A.; Raymo, F. M.; Stoddart, J. F. *Angew. Chem. Int. Ed.* **2000**, *39*, 3348.
- (3) a) de Silva, A. P.; Gunaratne, H. Q. N.; Gunnlaugsson, T.; Huxley, A. J. M.; McCoy, C. P.; Rademacher, J. T.; Rice, T. E. *Chem. Rev.* **1997**, *97*, 1515. b) Fabbrizzi, L.; Poggi, A. *Chem. Soc. Rev.* **1995**, *24*, 197.
- (4) a) de Silva, A. P. ; Mc Clenaghan, N. D. *J. Am. Chem. Soc.* **2000**, *122*, 3965. b) de Silva, A. P. ; Dixon, I. M. ; Gunaratne, H. Q. N. ; Gunnlaugsson, T. ; Maxwell, P. R. S. ; Rice, T. E. *J. Am. Chem. Soc.* **1999**, *121*, 1393. c) Rathore, R.; Magueres, P. L.; Lindeman, S. V.; Kochi, J. K. *Angew. Chem. Int. Ed.* **2000**, *39*, 809. d) Ashton, P. R.; Balzani, V.; Becher, J.; Credi, A.; Fyfe, M. C. T.; Matternsteig, G.; Menzer, S.; Nielsen, M. B.; Raymo, F. M.; Stoddart, J. F.; Venturi, M.; Williams, D. J. *J. Am. Chem. Soc.* **1999**, *121*, 3951. e) Fernandez-Acebes, A.; Lehn, J. M. *Chem. Eur. J.* **1999**, *5*, 3285. f) Zahn, S.; Canary, J. W. *Angew. Chem. Int. Ed.* **1998**, *37*, 305.
- (5) Krauss, R.; Weinig, H.; Seydack, M.; Bendig, J.; Koert, U. *Angew. Chem. Int. Ed.* **2000**, *39*, 1835.
- (6) a) Kawata, S.; Kawata, Y. *Chem. Rev.* **2000**, *100*, 1777. b) Gryko, D. T.; Clausen, C.; Roth, K. M.; Dontha, N.; Bocian, D. F.; Kuhr, W. G.; Lindsey, J. S. *J. Org. Chem.* **2000**, *65*, 7345. c) Li, J.; Gryko, D.; Dabke, R. B.; Diers, J. R.; Bocian, D. F. ; Kuhr, W. G.; Lindsey, J. S. *J. Org. Chem.* **2000**,

- 65, 7379. d) Brown, C. L.; Jonas, U.; Preece, J. A.; Ringsdorf, H.; Seitz, M.; Stoddart, J. F. *Langmuir* **2000**, *16*, 1924.
- (7) Rowan, A. E.; Nolte, R. J. M. *Angew. Chem. Int. Ed.* **1998**, *110*, 65
- (8) a) Lokey, R. S.; Iverson, B. L. *Nature* **1995**, *375*, 303.
- (9) Iverson, B. L. *Nature* **1997**, *385*, 113.
- (10) a) Kilbinger, A. F. M.; Schenning, A. P. H. J.; Goldoni, F.; Feast, W. J.; Meijer, E. W. *J. Am. Chem. Soc.* **2000**, *122*, 1820. b) Gin, M. S.; Yokozawa, T.; Prince, R. B.; Moore, J. S. *J. Am. Chem. Soc.* **1999**, *121*, 2643. c) Prince, R. B.; Brunsveld, L.; Meijer, E. W.; Moore, J. S. *Angew. Chem. Int. Ed.* **2000**, *39*, 228. d) Nelson, J. C.; Saven, J. G.; Moore, J. S.; Wolynes, P. G. *Science* **1997**, *277*, 1793.
- (11) Zych, A. J.; Iverson, B. L. *J. Am. Chem. Soc.* **2000**, *122*, 889.
- (12) Prince, R. B.; Brunsveld, L.; Meijer, E. W.; Moore, J. S. *Angew. Chem. Int. Ed.* **2000**, *39*, 228.
- (13) Valeur, B.; Pouget, J.; Bourson, J.; Kaschke, M.; Ernsting, N. P. *J. Phys. Chem.* **1992**, *96*, 6545.
- (14) Fletcher, N. C.; Ward, M. D.; Encinas, S.; Armaroli, N.; Flamigni, L.; Barigelletti, F. *Chem. Commun.* **1999**, 2089.
- (15) Forster, T. *Angew. Chem. Int. Ed. Engl.* **1969**, *8*, 333.
- (16) Rae, E. G. M.; Kasha, M. in *The Molecular Exciton Model, in Physical Processes in Radiation Biology*, (Eds: Augenstein, L.; R. Mason, Rosenberg, B.), Academic Press, New York, **1964**, pp 23-42.
- (17) Blum, A.; Grossweiner, L. I. *Photochem. Photobiol.* **1971**, *14*, 551.
- (18) a) E. Rabinowitch; Epstein, L. F. *J. Am. Chem. Soc.* **1941**, *63*, 69. b) Forster, T.; Konig, E. *J. Am. Chem. Soc.* **1957**, *79*, 344. c) Sheppard, S. E., *Proc. Roy. Soc. (London)* **1909**, *A82*, 256. d) Sheppard, S. E.; Geddes, A. L. *J. Am. Chem. Soc.* **1944**, *66*, 2003. e) Leyschin, V. L.; Krotova, L. V. *Opt. Spectry. (U.S.S.R)* **1962**, *13*, 457.
- (19) Valdes-Agulera, O.; Neckers, D. C. *Acc. Chem. Res.* **1989**, *22*, 171

- (20) Rohatgi, K. K.; Mukhopadhyay, A. K. *J. Phys. Chem.* **1972**, *76*, 3970.
- (21) Rohatgi, K. K.; Singhal, G. S. *J. Phys. Chem.* **1966**, *70*, 1695.
- (22) a) Yuzhakov, V. I. *Russ. Chem. Rev.* **1979**, *48*, 1076. b) Herz, A. H. *Photogr. Sci. Eng.* **1974**, *18*, 323. c) Blum, A.; Grossweiner, I. I. *Photochem. Photobiol.* **1985**, *41*, 27.
- (23) Wurthner, F.; Yao, S. *Angew. Chem. Int. Ed.* **2000**, *39*, 1978.
- (24) a) Beckmann, S.; Etzbach, K.-H.; Lukaszuk, K.; Matschiner, R.; Schmidt, A. J.; Schihmacher, P.; Sens, R.; Seybold, G.; Wortmann, R.; Wurthner, F. *Adv. Mater.* **1999**, *11*, 536. b) Wortmann, R.; Wurthner, F.; Sautter, A.; Lukaszuk, K.; Matschiner, R.; Meerholz, K. *Proc. SPIE* **1998**, 3471, 41.
- (25) Khairutdinov, R. F.; Serpone, N. *J. Phys. Chem. B* **1997**, *101*, 2602.
- (26) Das, S.; Thomas, K. G.; George, M. V. in (Eds.: V. Ramamurthy, K. S. Shanze), *Vol. 1*, **1997**.
- (27) a) Santhosh, U. ; Das, S., *J. Phys. Chem. A.* **2000**,*104*, 1842 b) Das, S.; Thomas, K. G.; Thomas, K. J.; Madhavan, V.; Liu, D.; Kamat, P. V.; George, M. V. *J. Phys. Chem.* **1996**, *100*, 17310 c) Sauve, G.; Kamat, P. V.; Thomas, K. G.; Thomas, K. J.; Das, S.; George, M. V. *J. Phys. Chem.* **1996**, *100*, 2117.
- (28) Gargiulo, D.; Derguini, F.; Berova, N.; Nakanishi, K.; Harada, N. *J. Am. Chem. Soc.* **1991**, *113*, 7046.
- (29) Katoh, T.; Inagaki, Y.; Okazaki, R. *J. Am. Chem. Soc.* **1998**, *120*, 3623.
- (30) Liang, K.; Frahat, M. S.; Perlstein, J.; Law, K. Y.; Whitten, D. G. *J. Am. Chem. Soc.* **1997**, *119*, 830.
- (31) Lu, L.; Lachicotte, R. J.; Penner, T. L.; Peristein, J.; Whitten, D. G. *J. Am. Chem. Soc.* **1999**, *121*, 8146.
- (32) Robello, D. R. *J. Polym. Sci. A: Polym. Chem.* **1990**, *28*, 1.
- (33) Hamer, F. M. *J. Chem. Soc.* **1956**, 1480.

- (34) Alfimov, M. V.; Churakov, A. V.; Federov, Y. V.; Federova, O. A.; Gromov, P.; Hester, R. E.; Howard, J. A. K.; Kuzmina, L. G.; Lednev, K.; Moore, J. N. *J. Chem. Soc. Perkin. Trans. 2*, **1997**, 2249.
- (35) Thomas, K. J.; Thomas, K. G.; Manojkumar, T. K.; Das, S.; George, M. V. *Proc. Ind. Acad. Sci.(Chem. Sci)* **1994**, *106*, 1375.
- (36) a) Seifert, J. L.; Corner, R. E.; Kushon, S. A.; Wang, M.; Armitage, B. A. *J. Am. Chem. Soc.* **1999**, *121*, 2987. b) Khairutdinov, R. F.; Serpone, N. *J. Phys. Chem. B* **1997**, *101*, 2602.
- (37) Das, S.; Thanulingam, T. L.; Thomas, K. G.; Kamat, P. V.; George, M. V. *J. Phys. Chem.* **1993**, *97*, 13620.
- (38) Bjorling, M.; Karlstrom, G.; Linse, P. *J. Phys. Chem.* **1991**, *95*, 6706.
- (39) a) Ephardt, H.; Fromherz, P. *J. Phys. Chem.* **1989**, *93*, 7717. b) Kim, J.; Lee, M. *J. Phys. Chem.* **1999**, *103*, 3378.
- (40) a) Rucker, C.; Heilemann, A.; Fromherz, P. *J. Phys. Chem.* **1996**, *100*, 12172. b) Gerner, H.; Gruen, H. *J. Photochem.* **1985**, *28*, 329.
- (41) Carmichael, I.; Hug, G. L. *J. Phys. Chem. Ref. Data* **1986**, *15*, 1.

Chapter 4

Photophysical Processes in Pyrene Based Conjugated Donor-Acceptor Systems

4.1. Abstract

The synthesis and photophysical properties of a conjugated donor-acceptor system, containing *p*-(dimethylaminostyryl) group linked to pyrene (**1** in Chart 4.1), and the corresponding bichromophore (**2**), were carried out. Photophysical properties of these compounds are compared with a model compound **3**, which does not possess a donor group. The absorption spectra of **1-3** were broad and not influenced by varying the polarity of the solvent. The emission spectrum of **3** in toluene possesses structured bands. Peak position and the spectral shape of **3** remain more or less unaffected, by varying the solvent polarity. Interestingly, a substantial shift in emission band was observed for **1** and **2** with increase in polarity, indicating the possibility of a charge transfer (CT) in the excited singlet state. Also, an enhancement in the fluorescence lifetime was observed, for both **1** and **2**, with increase in polarity of the solvent. Complexation properties of **1** and **2** with copper perchlorate were investigated using absorption as well as steady state and time resolved fluorescence techniques. Dramatic changes in the photophysical properties were observed, in CH₂Cl₂, on addition of micromolar quantities of Cu²⁺. Uncomplexed and complexed forms were characterized and the latter one

possesses a longer lifetime compared to the free ligand. The reduction of complex on addition of sodium dithionate, led to the decomplexation.

4.2. Introduction

The photoinduced electron transfer (PET) processes in fluorescent molecules, through host-guest interaction (for example, ligand-metal ion interaction), possess extensive application in sensing of ions and organic molecules.¹⁻⁴ The supramolecular aspects of these systems arise from the interaction between the ligand and guest molecules.⁵⁻⁸ Such supramolecular systems containing redox-active guest can be extended as fluorescent 'on-off' switches.^{9,10} Most of the chromophoric ligands employed for such applications are based on electron donor-acceptor systems, which exhibit charge-transfer absorption or emission in the visible and near-infrared region.^{11,12} Co-ordination with ions can affect the intensity as well as position of the absorption and emission bands of the chromophore. The direction of shift of the bands depends on the coordination site, relative to the electron donor and acceptor site, in the chromophore. Also, the extent of shift depends on the charge density of the metal ion, nature of solvent etc. Principles involved in the design of such molecular devices and the details of the photophysical effects arising from the host-guest interaction were presented, with numerous examples, by de Silva et al.¹³

The excimer-monomer formation in pyrene based molecular and supramolecular systems have been extensively utilized for sensing and switching.¹⁴⁻²⁶ Guest-induced switching of excimer emission with corresponding

changes in monomer emission form the basis of the design strategy adopted, in these systems.

In this Chapter, the molecular bistability was demonstrated by varying the redox properties of the metal ion in a ligand-metal ion complex. Molecular systems containing dimethylamino styryl group linked to pyrene (**1** and **2** in Chart 4.1) were synthesized for this purpose. These chromophoric systems form complexes with metal cations such as Cu^{2+} . The redox interconversion of metal ions between their various oxidation states were found to modulate the photophysical properties (absorption as well as steady state and time resolved emission) of the chromophore and also their binding properties.

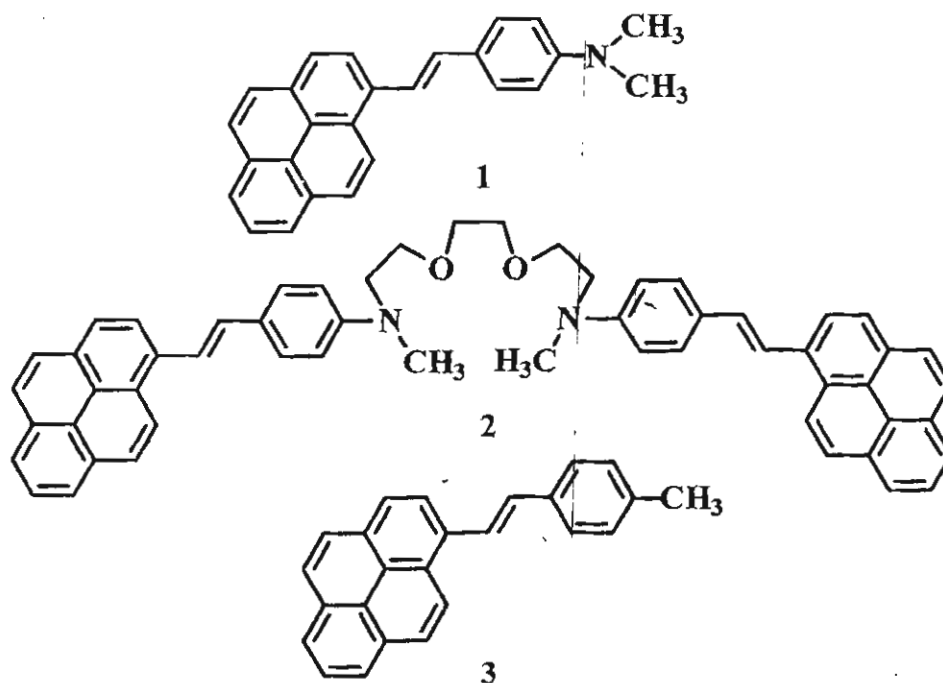
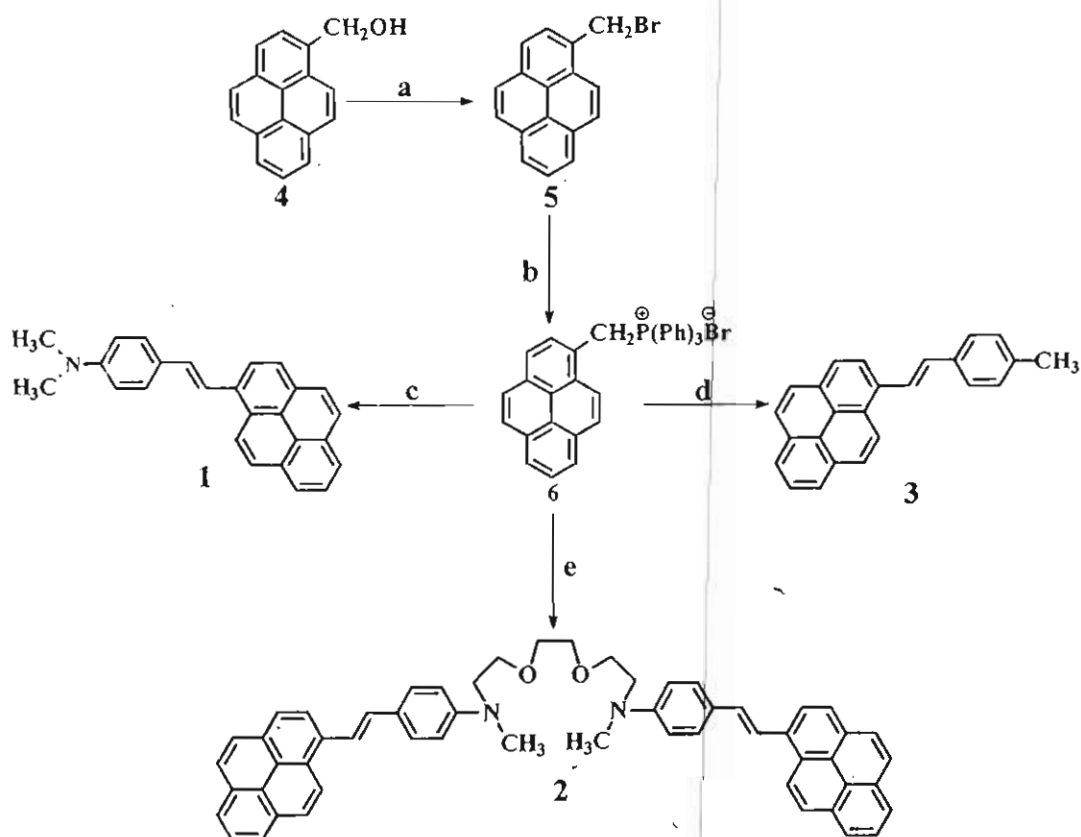


Chart 4.1. Compounds under investigation

4.3 Results and Discussion

4.3.1 Synthesis and Characterization

Syntheses of the compounds **1-3** were carried out as shown in Scheme 4.1. The compounds were fully characterized on the basis of analytical results and spectral data. The experimental procedures for the synthesis, purification and characterization of the hemicyanines are given in Section 4.5.



Scheme 4.1. Scheme for the synthesis of **1-3**; a) PBr_3 , dry chloroform; b) triphenylphosphine, dry benzene; c) *N,N*-dimethyl(*p*-amino)benzaldehyde, sodium hydride, dry THF; d) *p*-tolualdehyde, sodium hydride, dry THF; e) 2-*N*-methyl(*p*-formyl)anilinoethoxy ethane, sodium hydride, dry THF.

4.3.2. Absorption and Emission Properties

The absorption and emission properties of **1-3** were studied in solvents of varying polarity. The absorption spectrum of **1** in toluene ($\epsilon_T^N = 0.099$) showed a maximum around 386 nm and emits around 486 nm (trace a, Figure 4.1). With increase in solvent polarity, the absorption maximum remains more or less unaffected, whereas a large bathochromic shift in the emission band was observed. The spectral shape of the emission band remains unaffected with solvent polarity. Similar results were observed for bichromophore **2** (Figure 4.2). The absorption and emission maxima as well as the Stokes shift of both the compounds, in solvents of varying polarity are summarized in Table 4.1.

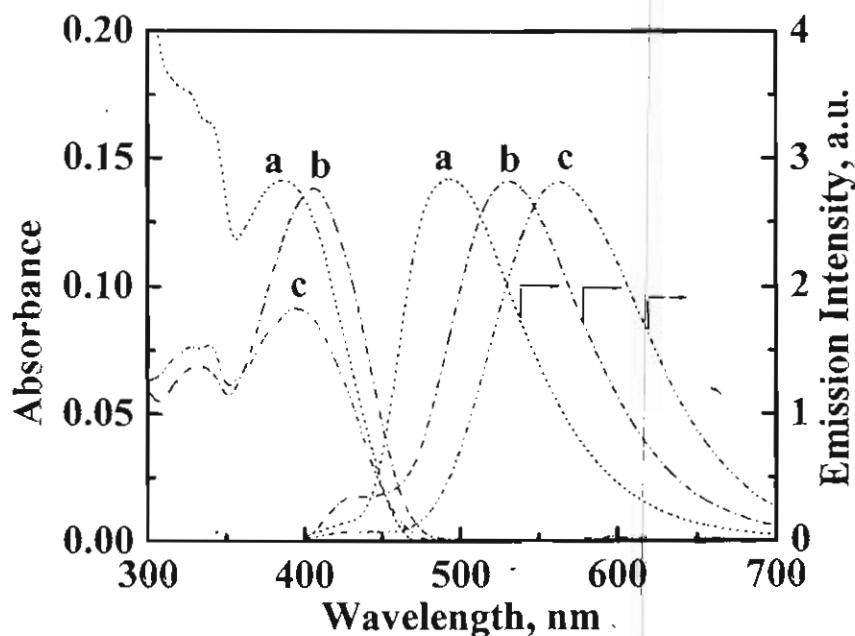


Figure 4.1. Absorption and emission spectra of **1** in solvents of varying polarity: (a) $C_6H_5CH_3$, (b) CH_2Cl_2 , (c) CH_3CN .

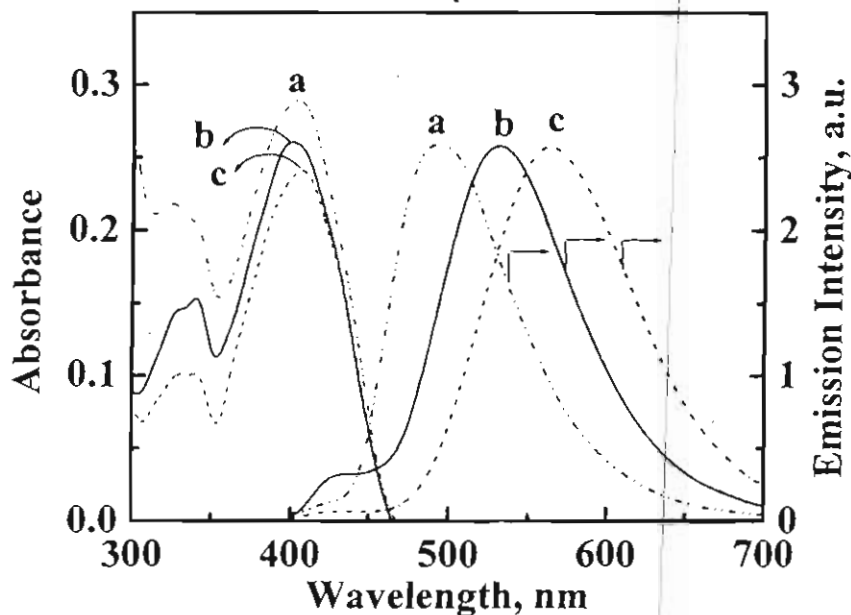


Figure 4.2. Absorption and emission spectra of **2** in solvents of varying polarity: (a) $C_6H_5CH_3$, (b) CH_3CN , (c) CH_2Cl_2 .

The donor-acceptor interactions between pyrene and the donor moiety (4-(N,N-dimethyl)aminostyryl group) were compared to that of hemicyanines in Chapter 2. The ground as well as Franck-Condon excited state of **1** and **2** were not influenced by solvent polarity. An excited state charge transfer is thermodynamically possible in these systems, from anilinic donor to pyrene moiety. The emission of both the compounds may be originating from a charge transfer (CT) state, which exhibits a bathochromic shift with increase in the solvent polarity. The charge transfer state may be more stabilized in a polar solvent, leading to a red shift in the emission band (Figures 4.1- 4.2). It can also be seen from Table 4.1, that with increase in solvent polarity the Stokes shift increases for both the compounds. For example, the Stokes shift of **1** in toluene is

5330 cm^{-1} whereas in a polar solvent such as acetonitrile it is around 7679 cm^{-1} . These results further support the view that CT state of **1** and **2**, are more stabilized in polar solvents. Thus, the excited singlet state properties of these compounds are quite different from that of hemicyanines reported in Chapter 2. The charge transfer nature is further confirmed by investigating the absorption and emission properties of a model compound **3**, which does not possess a donor group (Figure 4.3). The emission spectrum of **3** possesses structured bands and the shape as well as peak positions were not influenced by varying the solvent polarity. These studies indicate that the charge transfer occurs in the excited singlet state, from the anilinic donor group.

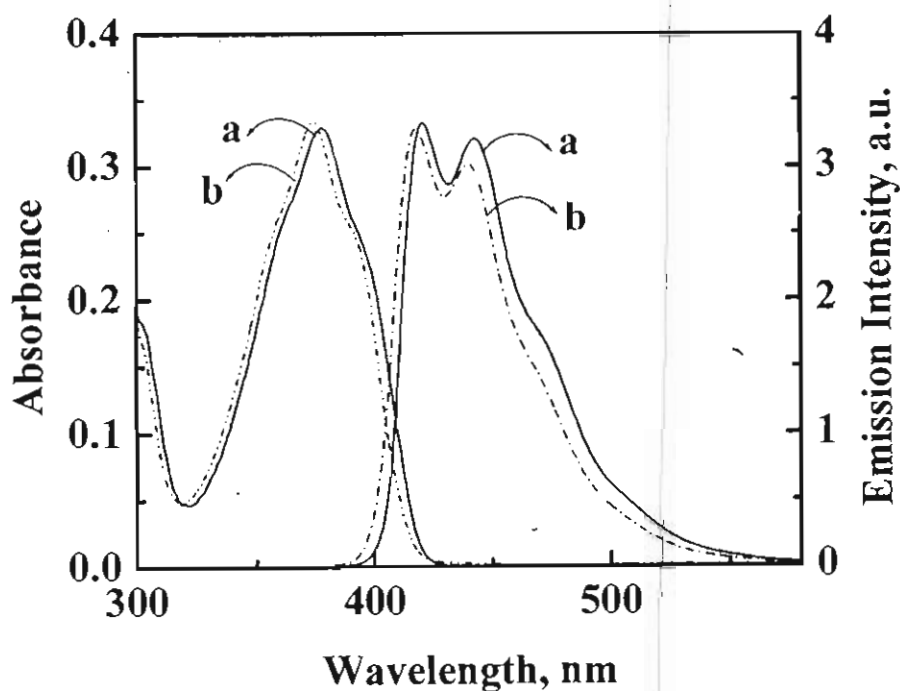


Figure 4.3. Absorption and emission spectra of **3** in solvents of varying polarity: (a) CH_2Cl_2 , (b) CH_3CN .

Table 4.1. Absorption and emission properties of **1** and **2**

Solvent	ϵ_T^N	1			2		
		$\lambda_{\max}(\text{abs})$ nm	$\lambda_{\max}(\text{em.})$ nm	$(\nu_a-\nu_f)$ cm^{-1}	$\lambda_{\max}(\text{abs})$ nm	$\lambda_{\max}(\text{em.})$ nm	$(\nu_a-\nu_f)$ cm^{-1}
$\text{C}_6\text{H}_5\text{CH}_3$	0.099	386	486	5330	402	492	4550
CH_2Cl_2	0.309	406	527	5655	406	531	5798
CH_3CN	0.460	395	567	7679	400	564	7269

The fluorescence decay profile of **1** and **2** in different solvents were measured by using the time correlated single-photon counting (TCSPC) system. The samples were excited at 366 nm. Emission spectra of both the compounds shift to red with increase in polarity and hence the fluorescence decay was followed at the maximum (Table 4.1). Lifetime measurements were carried out at 293 K. The decay profiles of **2**, in different solvents, are shown in Figure 4.4 and fitted to a monoexponential decay. The lifetimes were extracted from the measured decay curve, by deconvolution of instrument response function and are summarized in Table 4.2. An enhancement in lifetime was observed with increase in polarity. For example, the lifetime of **1** in toluene and acetonitrile are 0.72 and 1.6 ns, respectively. These results indicate that the emission in a polar solvent may be originating from a more stabilized state. The emission decay profiles of **2** in solvents of varying polarity were fitted to a biexponential decay and the lifetimes

extracted, are summarized in Table 4.2. The biexponential behavior may be due to the presence of different conformations of the bichromophore, depending upon the solvent polarity.

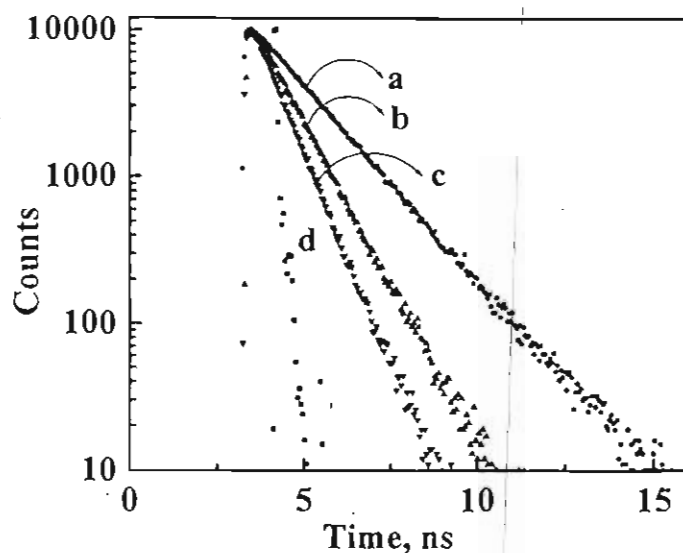


Figure 4.4. Fluorescence decay profiles of **1** in solvents of varying polarity: (a) CH_3CN , (b) CH_2Cl_2 , (c) $\text{C}_6\text{H}_5\text{CH}_3$ (the lamp profile is shown in trace d).

Table 4.2. Emission properties of **1** and **2**

Solvent	ϵ_T^N	1		2		
		Φ_f	τ_b , ns	Φ_f	τ_1^{a-c} , ns ($\chi_1\%$) ^d	τ_2^{a-c} , ns ($\chi_2\%$) ^d
$\text{C}_6\text{H}_5\text{CH}_3$	0.099	0.26	0.72	0.34	0.68 (93%)	3.32 (7%)
CH_2Cl_2	0.309	0.19	0.94	0.24	0.62 (57%)	2.12 (43%)
CH_3CN	0.46	0.24	1.6	0.24	0.69 (70%)	3.61(30%)

a) τ_1 and τ_2 are lifetimes of the short- and long-lived species; b) the quality of the fit is judged by means of usual statistical parameters such as χ^2 (1.04-1.20); c) excited at 366 nm and emission followed at the maxima; d) χ_1 and χ_2 are the relative distributions.

4.3.3. Complexation Studies with Metal Ions

Complexation of **1** with copper perchlorate in CH_2Cl_2 was investigated using absorption as well as steady state and time resolved emission studies. The absorption spectrum of **1** in CH_2Cl_2 possesses a broad band centered around 386 nm. Absorption spectral changes on addition of Cu^{2+} to a solution of **1**, in CH_2Cl_2 , are presented in Figures 4.5-4.7. A decrease in the absorption of the 386 nm band, accompanied by the formation of a long wavelength band, was observed on addition of low amounts of Cu^{2+} ($< 5 \mu\text{M}$). These changes were marked by the presence of a clear isosbestic point at 480 nm. The spectral changes were reversed on addition of a methanolic solution of sodium dithionate ($\sim 4 \mu\text{M}$) to the above solution. These results indicate that the long wavelength band is due to a dye-copper

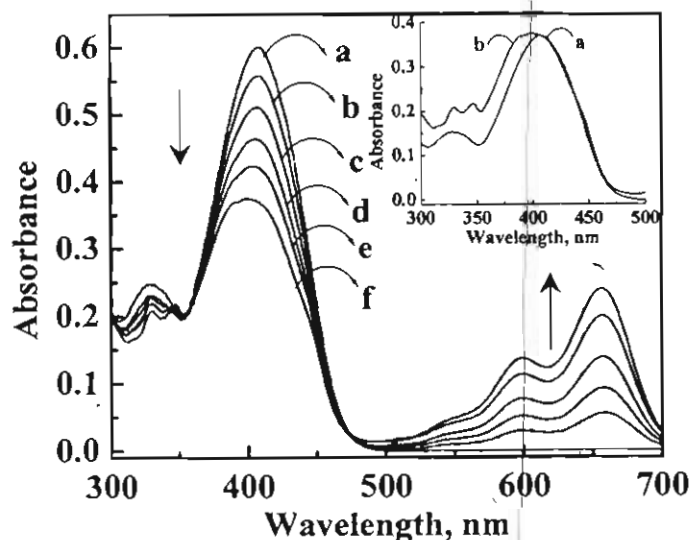


Figure 4.5. Effect of Cu^{2+} on the absorption spectrum of **1** in CH_2Cl_2 : $[\text{Cu}^{2+}]$ (a) 0, (b) 1, (c) 2, (d) 3, (e) 4 and (f) $5 \mu\text{M}$. Inset shows the normalised absorption spectra (300-500 nm) of **1** in presence of Cu^{2+} : $[\text{Cu}^{2+}]$ (a) 0, (b) $5 \mu\text{M}$.

ion complex and the reduction of Cu^{2+} led to the disruption of the complex. The stability constant for the complex formation of **1** with Cu^{2+} was estimated as $8.33 \times 10^4 \text{ M}^{-1}$ using Benesi-Hildebrand equation,

$$\frac{1}{A-A_0} = \frac{\epsilon_L}{\epsilon_L - \epsilon_{ML}} \left\{ \frac{1}{K_s[M]} + 1 \right\} \quad (4.1)$$

where A is the absorbance (followed at 650 nm) of the solution containing different concentrations of Cu^{2+} , A_0 is the absorbance of the free ligand (**1** does not have any absorption at 650 nm), K_s is the stability constant, $[M]$ is the concentration of Cu^{2+} , ϵ_L and ϵ_{ML} are the molar extinction coefficients of the free ligand and complexed ligand, respectively. A plot of $1/(A-A_0)$ versus $1/[M]$ was linear (Figure 4.6) in the case of **1**, indicating a 1:1 stoichiometry of the dye-metal complex at concentrations $< 5 \mu\text{M}$.

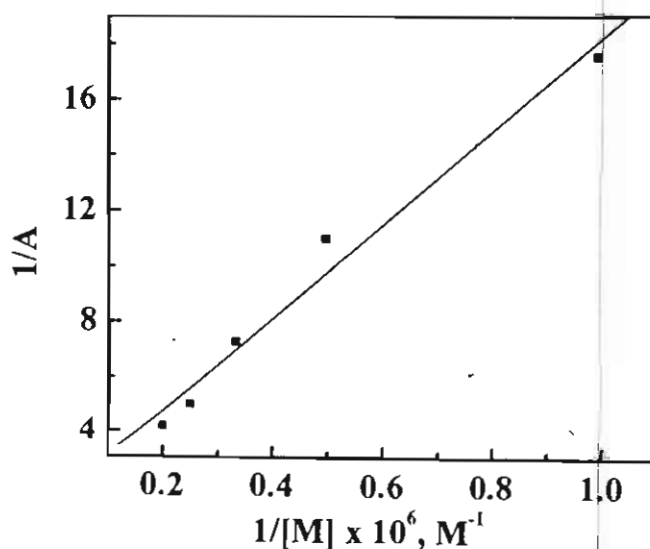


Figure 4.6. Plot of $1/A$ vs the reciprocal of concentration of Cu^{2+} for a solution of **1** in CH_2Cl_2 .

The normalized absorption spectrum of **1**, in the absence and presence of Cu^{2+} ($5 \mu\text{M}$) is shown in the inset of Figure 4.5. From this it is clear that a new band is also formed at the shorter wavelength, on addition of Cu^{2+} . This band became dominant and spectral changes were more significant on further addition of copper perchlorate ($5\text{-}9 \mu\text{M}$) to a solution of **1** (Figure 4.7). Spectral features were reversed on addition of a methanolic solution of sodium dithionate ($\sim 4 \mu\text{M}$), indicating the formation of a copper complex. The new band formed is buried in the absorption of **1** and hence difficult to investigate the stoichiometry of the complex, based on absorption spectral changes. The long wavelength band was more or less unaffected on addition of Cu^{2+} in the concentration range of $5\text{-}9 \mu\text{M}$. Intensity of the short wavelength band ($\lambda_{\text{max}} = 390 \text{ nm}$) as well as long wavelength band ($\lambda_{\text{max}} = 650 \text{ nm}$) decreases, on further addition of Cu^{2+} ($> 10 \mu\text{M}$). These changes were accompanied by the formation of a new structured absorption band, similar to that of pyrene and the spectral changes are shown in Figure 4.8. The new structured absorption band was unaffected by the addition of sodium dithionate, indicating the possibility of an irreversible reaction. Attempts were made to characterize the long wavelength absorption band ($\lambda_{\text{max}} = 650 \text{ nm}$) as well as the short wavelength absorption band ($\lambda_{\text{max}} = 390 \text{ nm}$), formed on addition of Cu^{2+} to **1**. Blank experiments were carried out by adding same concentrations of copper perchlorate to CH_2Cl_2 and no absorption was observed in the long

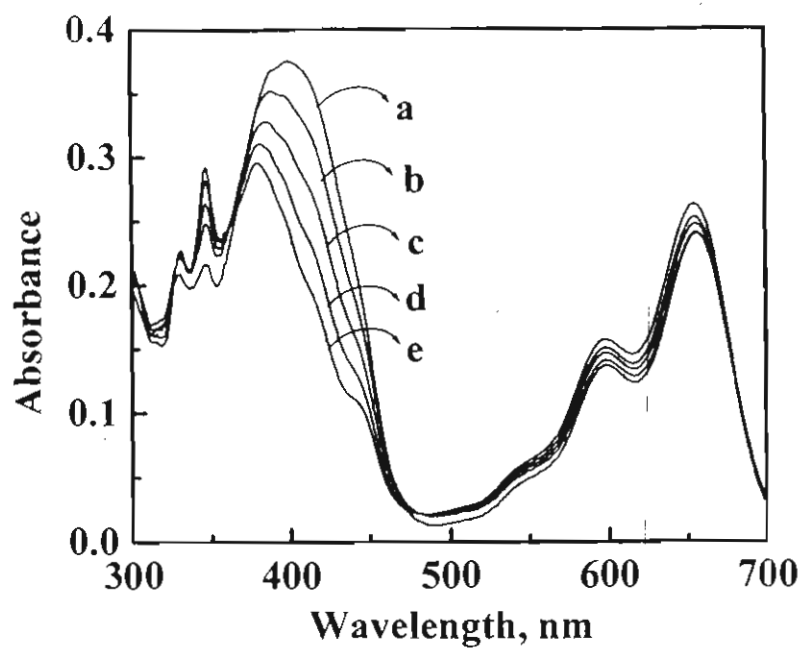


Figure 4.7. Effect of Cu²⁺ on the absorption spectrum of **1** in CH₂Cl₂: [Cu²⁺] (a) 5, (b) 6, (c) 7, (d) 8 and (e) 9 μM.

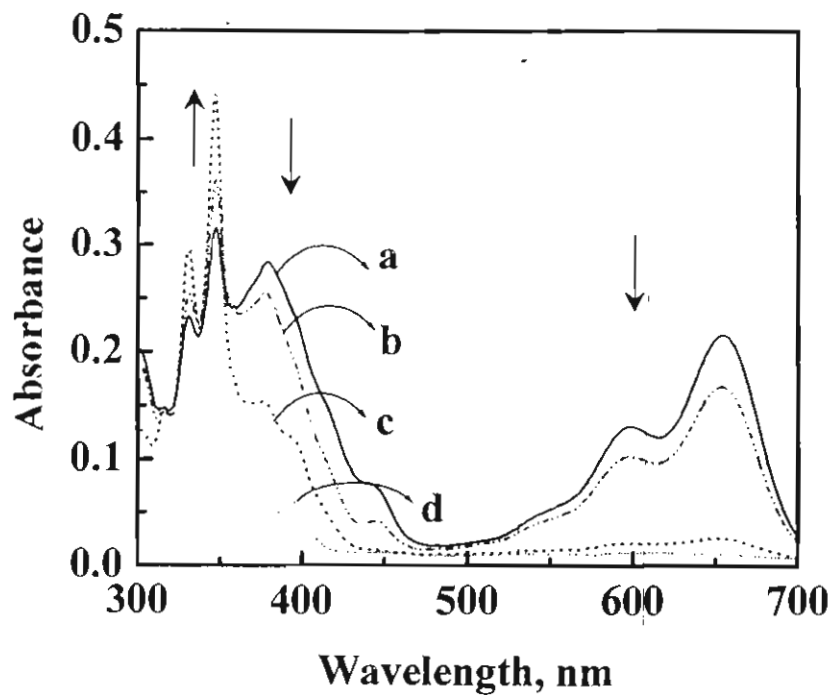


Figure 4.8. Effect of Cu²⁺ on the absorption spectrum of **1** in CH₂Cl₂: [Cu²⁺] (a) 10, (b) 11.8, (c) 16.8 and (d) 21.5 μM.

wavelength region. Interaction between pyrene and Cu^{2+} , were investigated and no spectral changes, similar to that of **1** was observed. Binding studies with Cu^{2+} were carried out using a model compound **3**, which does not possess a donor group (the dimethyl amino group is replaced by a methyl group). Interestingly, the long wavelength band was observed in compound **3** on addition of Cu^{2+} , whereas the short wavelength band is absent. These results indicate that short wavelength band may be due to the formation of a copper complex, involving the lone pair of the nitrogen atom of **1**. More detailed spectroscopic investigations were required to characterize the exact nature of the long wavelength band.

The emission spectral changes, on addition of Cu^{2+} to a solution of **1** in CH_2Cl_2 , were investigated. The long wavelength band formed was selectively excited and no emission was observed. Figures 4.9-4.10 show the emission spectra of **1**, recorded in the absence and presence of Cu^{2+} , by exciting the solutions at 355 nm (isosbestic point in Figures 4.6-4.7). In the concentrations $< 5 \mu\text{M}$ of Cu^{2+} , a decrease in the CT band was observed along with the formation of a new band at the shorter wavelength (inset of Figure 4.9). The intensity of this band became prominent at higher concentrations of Cu^{2+} ($> 5 \mu\text{M}$) and is shown in Figure 4.7. We have further investigated the complexation processes using time resolved emission studies. Solutions were excited at 366 nm and emission decay was followed at 530 nm. Compound **1** exhibits a monoexponential decay in the

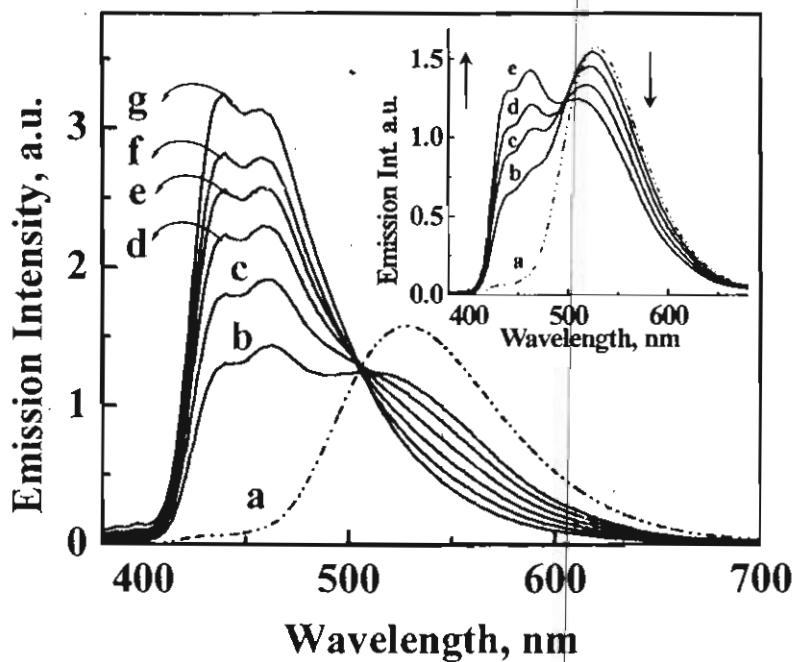


Figure 4.9. Effect of Cu^{2+} on the emission spectrum of **1** in CH_2Cl_2 : $[\text{Cu}^{2+}]$ (a) 0, (b) 5, (c) 6, (d) 7, (e) 8, (f) 9 and (g) 10 μM . Inset shows the emission spectra of **1** in presence of Cu^{2+} : $[\text{Cu}^{2+}]$ (a) 0, (b) 2, (c) 3, (d) 4 and (e) 5 μM .

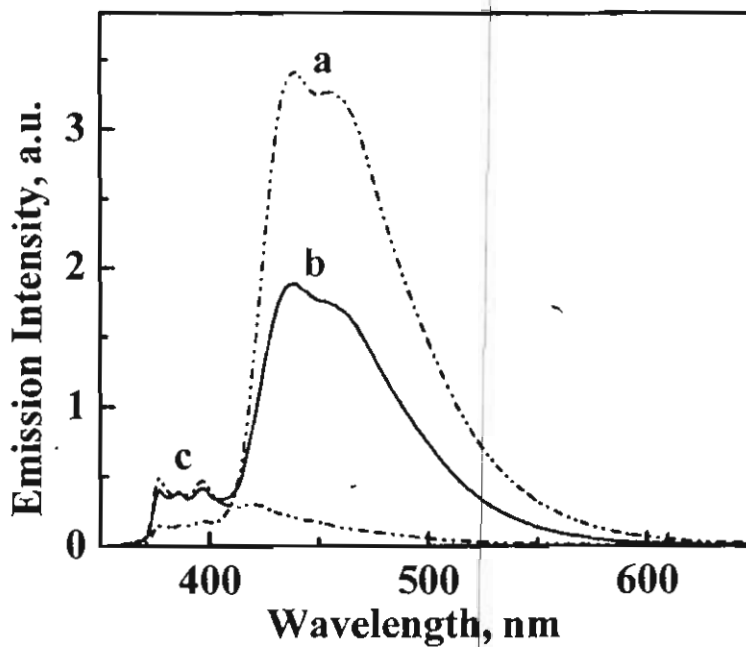


Figure 4.10. Effect of Cu^{2+} on the emission spectrum of **1** in CH_2Cl_2 : $[\text{Cu}^{2+}]$ (a) 10.8, (b) 16.8 and (c) 21.5 μM .

absence of Cu^{2+} ($\tau_1 = 0.92$ ns). A biexponential decay, with a short-lived (τ_1) and long-lived (τ_2) component, was observed in the presence of Cu^{2+} . Representative fluorescence decay profiles in the absence and presence of Cu^{2+} are shown in Figure 4.11. The lifetimes and the fractional contributions are presented in Table 4.3. The lifetimes of both the species are unaffected by metal ion concentration

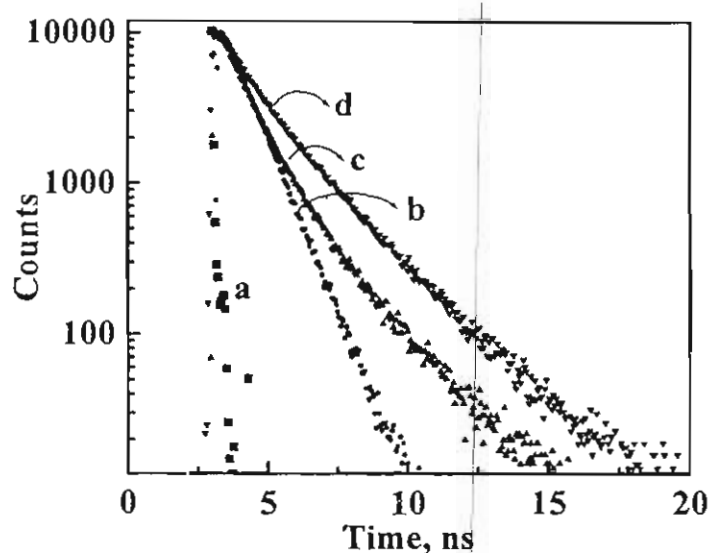


Figure 4.11. Fluorescence decay profiles of **1** monitored at 560 nm at different concentrations of Cu^{2+} : $[\text{Cu}^{2+}]$ (b) 0, (c) 4.88, (d) 16.3 μM , (lamp profile is shown as trace a).

and the relative distribution of these species as a function of Cu^{2+} concentration is presented in Figure 4.12. The population of the long-lived species increased with increase in Cu^{2+} concentration. The emission decay was selectively monitored at 420 nm and a single exponential decay, independent of the Cu^{2+} concentration was observed. Compound **1** has no absorption at 420 nm and the new short wavelength emission band with longer lifetime ($\tau_2 = 2.1$ ns), is assigned to the copper complex

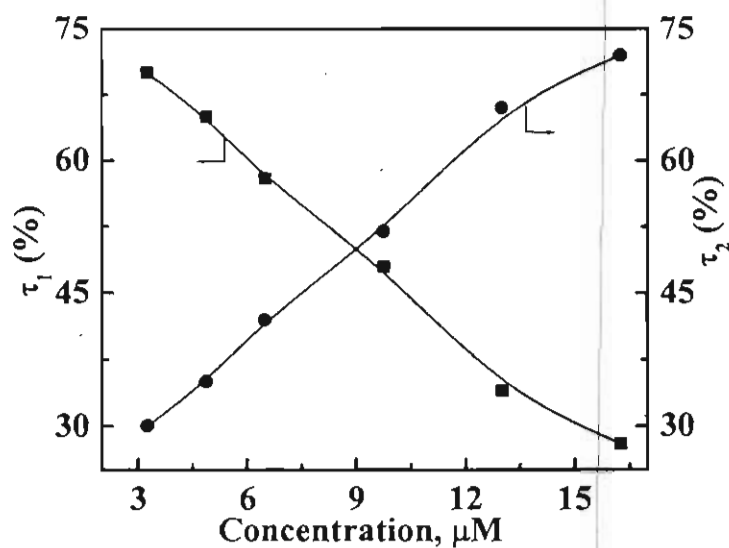


Figure 4.12. Relative distribution of the long lived and short lived species of 1 in different concentrations of Cu^{2+}

Table 4.3. Fluorescence lifetimes^{a-c} and fractional distributions^d of 1 as a function of $[\text{Cu}^{2+}]$

$[\text{Cu}]$, μM	τ_1 ($\chi_1\%$), ns	τ_2 ($\chi_2\%$), ns
0	0.92 (100)	
3.25	0.95 (70)	2.11 (30)
4.88	0.90 (65)	2.11 (35)
6.50	0.92(58)	2.16 (42)
9.75	0.98 (48)	2.34 (52)
13.0	0.93 (34)	2.27 (66)
16.25	0.88 (28)	2.25 (72)

a) τ_1 and τ_2 ; b) the quality of the fit is judged by means of usual statistical parameters such as χ^2 (1.04-1.20); c) excited at 366 nm and emission followed at 560 nm; d) χ_1 and χ_2 are the relative distributions.

of **1**. On further addition of Cu^{2+} , a decrease in the intensity of the 450 nm band was observed, followed by the formation of a structured band similar to that of pyrene (Figure 4.10). The normalized emission spectra in the absence and presence of Cu^{2+} are shown in Figure 4.13. The emission spectra are well separated and the complex absorbing around 450 nm undergoes interconversion to the uncomplexed form on addition of sodium dithionate.

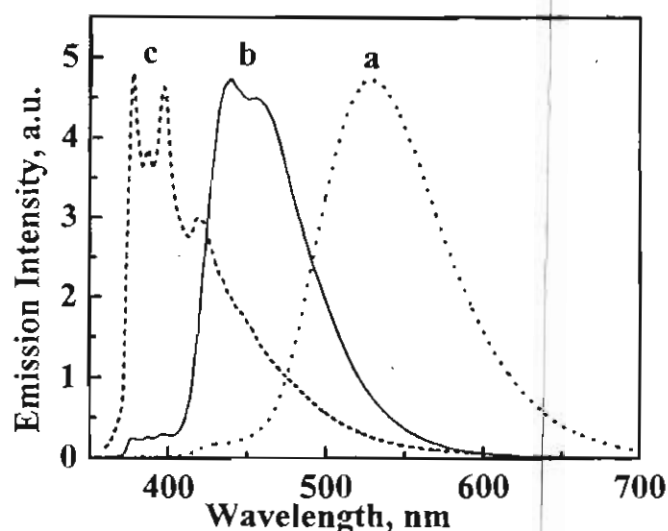


Figure 4.13. Normalised emission spectra of **1** in CH_2Cl_2 in presence of Cu^{2+} : $[\text{Cu}^{2+}]$ (a) 0, (b) 11.8 and (c) 21.5 μM

The effect of Cu^{2+} on the absorption and emission of the bichromophore was also studied. The spectral changes were more or less similar to that observed for **2**. The uncomplexed form of **2** has an emission around 530 nm (Figure 4.14). Addition of Cu^{2+} to a solution of the bichromophore in CH_2Cl_2 , led to the decrease in the intensity of the band at 530 nm, accompanied by the formation of a band with emission at 430 nm. As in the case of **1**, the band at 430 nm is more structured

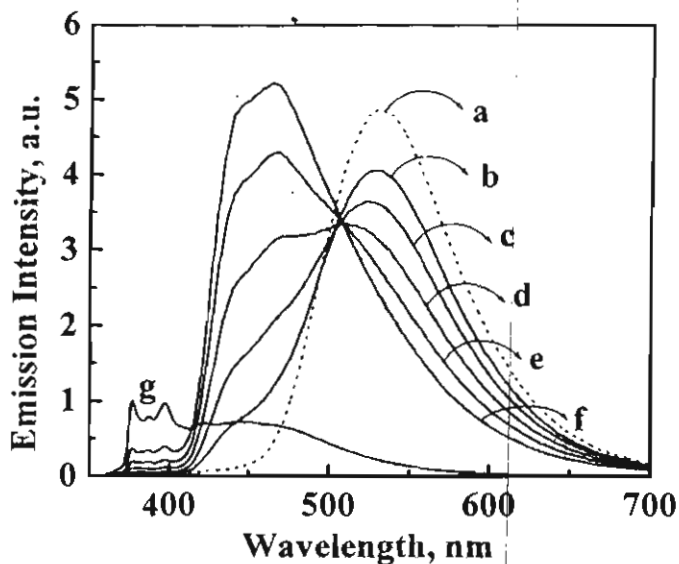


Figure 4.14. Effect of Cu^{2+} on the emission spectrum of **2** in CH_2Cl_2 : $[\text{Cu}^{2+}]$ (a) 0, (b) 4, (c) 6, (d) 8, (e) 10, (f) 11.8, and (g) 23.4 μM

compared to the uncomplexed form. Also, the emission yield of the complexed form is higher than that of **2**. Higher concentrations of Cu^{2+} led to the formation of a structured band (trace g in Figure 4.14), similar to that of pyrene.

4.4. Conclusions

Photophysical investigations of a pyrene based conjugated donor-acceptor system (**1**), the corresponding bichromophore (**2**) and a model compound (**3**) were carried out. The absorption spectra of these compounds were not influenced by solvent polarity, whereas a substantial shift in the emission band was observed with increase in polarity. Solvent sensitive emission of **1** and **2** may be originating from a charge transfer state. Complexation behavior of **1** and **2** with copper perchlorate were investigated using absorption as well as steady state and time

resolved emission studies. The complexed form emits at a shorter wavelength and its lifetime is longer than that of the uncomplexed dye and the former one can be converted into uncomplexed ligand by chemical reduction.

4.5. Experimental Section

Compound 5. To a solution of 1-pyrenemethanol (2 g, 8.6 mmol) in dichloromethane (30 mL), phosphorous tribromide (2.33 g, 8.6 mmol) was added dropwise over a period of 30 min under ice cold conditions. The reaction mixture was stirred at room temperature for 12 h and was neutralized using a saturated solution of sodium bicarbonate. The organic layer was extracted using dichloromethane and the solvent was removed under reduced pressure to give **5** (2.3 g, 90%) as a solid. m.p. 243-245 °C.

Compound 6. A mixture of 1-bromomethylpyrene (1 g, 3.4 mmol) and triphenylphosphine (0.9 g, 3.4 mmol) was refluxed in dry benzene (30 mL) for 12 h. The reaction mixture was cooled and filtered under suction to give **6** as a white solid (1.5 g, 78 %). The Wittig salt thus obtained was directly used for the subsequent reactions with out further characterization.

Compound 1. To a suspension of sodium hydride (0.12 g, 5 mmol) in dry THF, **6** (0.56 g, 1 mmol) was added and the mixture was refluxed for 30 min. To the above solution, N,N-dimethyl *p*-aminobenzaldehyde (0.15 g, 1 mmol) in dry THF (40 mL) was added dropwise over a period of 45 min. The reaction mixture was then refluxed for 24 h. On cooling, excess sodium hydride was quenched by

adding ice cold water. The organic layer was extracted using dichloromethane. The solvent was removed under reduced pressure and the residue was chromatographed over silica gel (100-200 mesh) using a mixture (3:7) of chloroform and hexane to give **1** (160 mg, 46 %). mp 188-190 °C (decomp.); IR (KBr) ν_{\max} 3035, 2893, 2723, 2612, 2494, 2370, 2323, 1668, 1604, 1451, 1346, 1223, 1180, 1066, 951, 838, 806, 751, 705, 597, 482 cm^{-1} ; ^1H NMR (CDCl_3) δ 6.7-8.5 (15H, m) 2.96 (6H, s); HRMS calculated for $\text{C}_{26}\text{H}_{21}\text{N}$ $[\text{M}]^+$ 347.1674 found 347.1688 (FAB high resolution mass spectroscopy).

Compound 2. To a suspension of sodium hydride (0.12 g, 5 mmol) in dry THF (20 mL), **6** (0.87 g, 1.6 mmol) was added and the mixture was refluxed for 30 min. To the above solution, *N*-methyl-*p*-formylanilinoethoxy ethane (0.3 g, 0.8 mmol) in dry THF (50 mL) was added dropwise over a period of 75 min and the reaction mixture was refluxed for 24 h. On cooling, excess sodium hydride was quenched by adding ice cold water. The organic layer was extracted using dichloromethane. The solvent was removed under reduced pressure and the residue was chromatographed over neutral alumina using a mixture (2:3) of chloroform and hexane to give 75 mg (12 %) of **2**, mp 138-141 °C (decomp.); IR (KBr) ν_{\max} 3747, 3614, 3554, 3472, 3051, 2883, 2346, 1810, 1711, 1605, 1515, 1450, 1359, 1207, 1122, 965, 816, 707, 611, 515 cm^{-1} ; ^1H NMR (CDCl_3) δ 6.76-8.44 (m, 30H), 3.50-3.69 (m, 12H), 3.05 (s 6H); HRMS calcd. for $\text{C}_{56}\text{H}_{48}\text{N}_2\text{O}_2$ $[\text{M}]^+$ 780.3716 found 780.3730 (FAB high resolution mass spectroscopy).

Compound 3. To a suspension of sodium hydride (0.12 g, 5 mmol) in dry THF, **6** (0.56 g, 1 mmol) was added and the mixture was refluxed for 30 min. To this *p*-tolualdehyde (0.12 g, 1 mmol) in dry THF (40 mL) was added dropwise over a period of 45 min. The reaction mixture was then refluxed for 24 h. On cooling, excess of sodium hydride was quenched by adding ice-cold water. The organic layer was extracted using dichloromethane. The solvent was removed under reduced pressure and the residue was chromatographed over silica gel (100-200 mesh) using a mixture (3:7) of chloroform and hexane to give **3** (72 mg, 60 %). mp 145-147 °C (decomp.); ¹H NMR (CDCl₃) δ 8.48-7.23 (m, 15 H), 3.00 (3H, s); ¹³C NMR (CDCl₃) δ 137.78, 134.99, 129.52, 127.47, 126.64, 124.96, 123.61, 21.32.

Instrumental Techniques

All melting points are uncorrected and were determined on an Aldrich melting point apparatus. IR spectra were recorded on a Perkin-Elmer Model 882 IR Spectrometer and the UV-Visible spectra on a Shimadzu UV-3101PC UV-VIS-NIR Scanning Spectrophotometer. ¹H and ¹³C NMR spectra were recorded on a Bruker DPX-300 MHz spectrometer. Emission spectra were recorded on a SPECTRACQ spectrofluorimeter and corrected using the program supplied by the manufacturer. Fluorescence lifetimes were measured using a Tsunami Spectra Physics single photon counting system.

4.6. References

- (1) Lakowicz, J. R. *Topics in Fluorescence Spectroscopy*, Vol.4, Plenum Press, New York and London, **1994**.
- (2) Bissell, R. A.; de Silva, A. P.; Gunaratne, H. Q. N.; Lynch, P. L. M.; Maguire, G. E. M.; Mc Coy, C. P.; Sandanayake, K. R. A. S. *Top. Curr. Chem.* **1993**, 168.
- (3) Reinhoudt, D. N.; Sudholter, E. J. R. *Adv. Mater.* **1990**, 2, 23.
- (4) Cobben, P. L. H. M.; Egberink, R. J. M.; Bomer, J. G.; Bergveld, P.; Verboom, W.; Reinhoudt, D. N. *J. Am. Chem. Soc.* **1992**, 114, 10573.
- (5) Lehn, J. M. in *Supramolecular Chemistry: Concepts and Perspectives*, VCH, Weinheim, **1995**.
- (6) Balzani, V.; Maggi, L.; Scandola, F. in *Supramolecular Photochemistry*, Reidel, Holland, **1987**, 1.
- (7) Balzani, V.; Gomez-Lopez, M.; Stoddart, J. P. *Acc. Chem. Res.* **1998**, 31, 405.
- (8) Sauvage, J. P. *Acc. Chem. Res.* **1998**, 31, 611.
- (9) de Silva, A. P.; de Silva, S. A. *J. Chem. Soc. Chem. Commun.* **1986**, 1709.
- (10) de Silva, A. P.; Gunaratne, H. Q. N.; Habib Jiwan, J. L.; McCoy, C. P.; Rice, T. E.; Soumillion, J. P. *Angew. Chem. Int. Ed. Engl.* **1995**, 34, 1728.
- (11) MacQueen, D. B.; Schanze, K. S. *J. Am. Chem. Soc.* **1991**, 113, 6108.
- (12) Yoon, D. I.; Bergbrennan, C. A.; Lu, H.; Hupp, J. J. *Inorg. Chem.* **1992**, 31, 3192.
- (13) de Silva, A. P.; Gunaratne, H. Q. N.; Gunnlaugsson, T.; Huxley, A. J. M.; McCoy, C. P.; Rademacher, J. T.; Rice, T. E. *Chem. Rev.* **1997**, 97, 1515.
- (14) Winnik, M. A. *Chem. Rev.* **1981**, 81, 491.
- (15) Winnik, F. M. *Chem. Rev.* **1993**, 93, 587.
- (16) Zachariasse, K. A.; Vaz, W. L. C.; Sotomayor, C.; Kuhnle, W. *Biophys. Biochim. Acta* **1982**, 688, 323.

- (17) Wang, Y. C.; Morawetz, H. *J. Am. Chem. Soc.* **1976**, *98*, 3611.
- (18) Morawetz, H. *J. Lumin.* **1989**, *43*, 59.
- (19) Goldenberg, M.; Emert, J.; Morawetz, H. *J. Am. Chem. Soc.* **1978**, *100*, 7171.
- (20) Wang, Y. C.; Morawetz, H. *J. Am. Chem. Soc.* **1976**, *98*, 3611.
- (21) Ueno, A.; Suzuki, I.; Osa, T. *J. Chem. Soc. Chem. Commun.* **1988**, 1373.
- (22) Ueno, A.; Suzuki, I.; Osa, T. *J. Am. Chem. Soc.* **1989**, *111*, 6391.
- (23) Sasaki, D. Y.; Shnak, D. R.; Pack, D.; Arnold, F. H. *Angew. Chem. Int. Ed. Engl.* **1995**, *34*, 905.
- (24) Emert, J.; Kodali, D.; Catena, R. *J. Chem. Soc. Chem. Commun.* **1981**, 758.
- (25) Jin, T.; Ichikawa, K.; Koyama, T. *J. Chem. Soc. Chem. Commun.* **1992**, 499.
- (26) Saika, T.; Iyoda, T.; Honda, K.; Shimidzu, T. *J. Chem. Soc. Chem. Commun.* **1992**, 591.